University of Texas at El Paso
DigitalCommons@UTEP

Open Access Theses & Dissertations

2013-01-01

Development and Validation of a Novel Framework to Map Brain Function

Cristhian Mauricio Potes
University of Texas at El Paso, cmpotes@gmail.com

Follow this and additional works at: https://digitalcommons.utep.edu/open_etd

 Part of the Biomedical Commons, and the Neuroscience and Neurobiology Commons

Recommended Citation
Potes, Cristhian Mauricio, "Development and Validation of a Novel Framework to Map Brain Function" (2013). *Open Access Theses & Dissertations*. 1705.
https://digitalcommons.utep.edu/open_etd/1705

This is brought to you for free and open access by DigitalCommons@UTEP. It has been accepted for inclusion in Open Access Theses & Dissertations by an authorized administrator of DigitalCommons@UTEP. For more information, please contact lweber@utep.edu.

Development and Validation of a Novel Framework to Map Brain Function

Cristhian Mauricio Potes Blandon

Department of Electrical and Computer Engineering

Approved:

Patricia Nava, Chair, Ph.D.

Homer Nazeran, Ph.D.

Melissa Carroll, Ph.D.

Gerwin Schalk, Ph.D.

Benjamin Flores, Ph.D.
Dean of the Graduate School

To my beautiful wife Marcela, my little prince Santiago, and to my lovely and exemplary parents Rodrigo and Luz Elena.

Development and Validation of a Novel Framework to Map Brain Function

by

Cristhian Mauricio Potes Blandon, B.S.B.E., M.S.E.E

Dissertation

Presented to the Faculty of the Graduate School of

The University of Texas at El Paso

in Partial Fulfillment

of the Requirements

for the Degree of

DOCTOR OF PHILOSOPHY

Department of Electrical and Computer Engineering
University of Texas at El Paso
December 2013

Trust in the LORD with all your heart. Do not depend on your own understanding. Seek His will in all you do, and He will show you which path to take.

Proverbs 3:5-6

Acknowledgments

Seven years ago I left Colombia to start this long journey. Completing my Ph.D. studies was a process that not only provided me with research and technical skills, but also helped me to mature in personal qualities such as patience, endurance, perseverance, and critical thinking. This process involved the direct and indirect help of people that I would like to acknowledge in this section of my dissertation.

To God. First that all, I want to profoundly thank God who gave me the guidance, physical and spiritual strength, knowledge, wisdom, and health to achieve one more goal in my life. He brought me to the United States not only to pursue my Ph.D. degree but also to start a new family with my beautiful wife Marcela and son Santiago. I am deeply grateful with what God has done in my life.

To my family. I want to greatly thank my lovely wife for her patience and support during these seven years. I want to thank her for taking care of our son while I had to write this dissertation, and for her continuous and unconditional love and support. I really enjoyed going to conferences and internships with her. I thank her for listening to me when I shared those complex and abstracts of engineering concepts. Even when she did not understand a single word of what I said, at least she made her best effort to understand me. My lovely wife and son are the fuel of my life. Also, I want to thank my lovely parents. I want to thank them for their support and guidance. I am the person who I am today because of the character they built in me. The discipline, self-confidence, and organization they instilled in me when I was a kid have been one of the reasons for

the success in my career. Also thanks to my mother and father in-law for their support and advice, and for making me feel like their son.

To my advisors and professors. Special thanks to my advisor Dr. Patricia Nava. I greatly appreciate her advice and academic, administrative, and financial support at the University of Texas at El Paso (UTEP). I also want to thank Dr. Homer Nazeran and Dr. Melissa Carroll for being part of this dissertation committee. I want to mention the great guidance and enthusiasm of my advisor and great friend, Gerwin Schalk. For the last three years in Albany, NY, I have greatly enjoyed our long scientific discussions. In particular, I will never forget the great ideas that surfaced after those discussions at the gym. His vision of science and research, his insights, and his incredible dedication and passion for research are just few of the many qualities of this ECoG evangelist. I want to express to him my deep thanks for letting me join his research team after my internship in 2009. Dr. Schalk and his family have been a great support to my family. I also want to express my sincere thanks to my friend and professor Dr. Miguel Argaez. Because of his support, I could start my Ph.D. studies at UTEP.

To administrative assistants, clinicians, laboratory personnel, and patients. I want to show my appreciation for the administrative support of Sukie Quezada and Linda Romero at UTEP. Thanks to them I could get my research and teaching assistant appointments on time. I appreciate the administrative assistance of Sophia Pallone during my stay at Wadsworth Center New York State Department of Health. My sincere appreciation to Drs. Antony Ritaccio, Timothy Lynch, Bridget Frawley, and Matthew Adamo for providing clinical support and access to clinical data. Many thanks to Dr. Jonathan Wolpaw and Ms. Theresa Vaughan for their sincere support and valuable comments during our laboratory meetings. I want to thank to my colleagues and friends Peter Brunner, Aysegul Gunduz, Jeremy Hill, William Coon, and Adriana dePesters for helping me collect data and run experiments, for their advice, and for our meaningful scientific discussions. I would also like to thank all the patients that participated in the studies related to this dissertation for their time and patience.

To my friends. While in the United States, I met wonderful people who were always willing to assist and advise me unconditionally. I enjoyed sharing with them our different cultures, in particular our exotic food. I want to thank from the bottom of my heart

to Miryam and Jaymes Picott, Javier Flores, Disha Gupta, David Vaughan, Reynaldo Sanchez, Oscar and Maria Claudia Villamarin, Xiaomei Pei, Corey and Trista Deame.

To MY SPONSORS. This work was supported by the NIH (EB006356 (GS), EB00856 (JRW and GS)) and the US Army Research Office (W911NF-07-1-0415 (GS) and W911NF-08-1-0216 (GS)).

Abstract

Neuroimaging approaches have identified multiple brain sites that are activated in music perception, including the posterior part of the superior temporal gyrus and adjacent perisylvian areas. Yet, to what extent brain signals represent the time course of specific acoustic features in natural auditory stimuli and the detailed spatial and temporal relationship of neural signals that support auditory function are largely unknown. In the two studies documented in this dissertation, a novel neuroimaging framework is applied to electrophysiological signals recorded from the surface of the brains (electrocorticography (ECoG)) of 8-10 human epileptic subjects while they were listening to a continuous piece of music. This framework allows clinicians and researchers to identify those ECoG features related to the processing of a continuous piece of music and to investigate their spatial, temporal, and causal relationships. The results presented here demonstrate robust stimulus-related modulations in the alpha (8-12 Hz) and high gamma (70-110 Hz) bands at neuroanatomical locations implicated in auditory processing. Specifically, stimulus-related ECoG modulations in the alpha band were identified in areas adjacent to primary auditory cortex, which are known to receive afferent auditory projections from the thalamus. In contrast, stimulus-related ECoG modulations in the high gamma band were identified not only in areas close to primary auditory cortex, but also in other perisylvian areas known to be involved in higher-order auditory processing, and in an unexpected and distinct area in superior premotor cortex. Moreover, ECoG activity in the high gamma band recorded from these cortical areas were observed to be highly correlated with the sound intensity of music. Across all implicated areas, modulations in the high gamma band preceded those in the alpha band by 280 ms, and activity in the high gamma band causally predicted alpha activity, but not vice versa (Granger causality, $p < 1e^{-8}$). Additionally, detailed analyses using Granger

causality identified causal relationships of high gamma activity between distinct locations in early auditory pathways within STG and posterior STG, between posterior STG and inferior frontal cortex, and between STG and the newly identified location in premotor cortex. Evidence suggests that these relationships reflect direct cortico-cortical connections rather than common driving input from subcortical structures such as the thalamus. In summary, analyses showed that ECoG signals encode information about the sound intensity of music, and define the spatial and temporal relationships between music-related brain activity in the alpha and high gamma bands. They provide experimental evidence supporting current theories about the putative mechanisms of alpha and gamma activity, i.e., reflections of thalamo-cortical interactions and local cortical neural activity, respectively. These results are also in agreement with existing functional models of auditory processing and highlight a previously largely unrecognized role of superior premotor cortex in music processing. Results documented in this study make a strong case for the use of ECoG to map brain activity and brain networks related to cognitive, sensory, and motor functions.

Keywords: electrocorticography (ECoG), alpha and high gamma activity, thalamo-cortical interactions, epilepsy, neurosurgery, brain activity and networks

Contents

1 Introduction **1**
- 1.1 Motivation . . . 1
- 1.2 Main Research Questions and Contributions . . . 4
- 1.3 Dissertation Outline . . . 7

2 Functional Neuroimaging Techniques **9**
- 2.1 Introduction . . . 9
- 2.2 Origin of Brain Electrical Activity . . . 10
- 2.3 Types of Functional Neuroimaging Techniques . . . 12
  - 2.3.1 Techniques Based on Direct Measure of Neural Activity . . . 13
  - 2.3.2 Techniques Based on Indirect Measure of Neural Activity . . . 15
- 2.4 Comparison of the Recording Techniques . . . 19
  - 2.4.1 Temporal Resolution . . . 19
  - 2.4.2 Spatial Resolution and Coverage . . . 20
  - 2.4.3 Invasiveness Degree and Risk Level . . . 20
  - 2.4.4 Implementation Cost . . . 21
- 2.5 Conclusion . . . 21

3 Electrocorticography (ECoG) **23**
- 3.1 Introduction . . . 23
- 3.2 Electrophysiological Processes Detected with ECoG . . . 25
  - 3.2.1 Thalamocortical Activity . . . 26
  - 3.2.2 Local Cortical Activity . . . 30
- 3.3 Methods for Collecting and Recording ECoG Signals . . . 33
  - 3.3.1 General Overview . . . 34
  - 3.3.2 Brain Model Generation and Electrode Localization . . . 37
  - 3.3.3 Hardware and Software . . . 39

3.3.4 Experimental Session . . . 39
3.4 Techniques to Analyze ECoG Signals . . . 41
3.4.1 Preprocessing . . . 42
3.4.2 Feature Extraction . . . 44
3.4.3 Statistical Analysis . . . 48
3.4.3.1 Measures of Dependence . . . 48
3.4.3.2 Measures of Causality . . . 50
3.5 Clinical Applications . . . 52
3.5.1 Real-Time Functional Mapping . . . 52
3.5.2 Electrical Cortical Stimulation (ECS) . . . 53
3.5.3 Brain Computer Interfaces (BCI) . . . 53
3.6 Conclusion . . . 53

4 Auditory Processing **55**
4.1 Introduction . . . 55
4.2 Sound Stimulus and Perception . . . 56
4.3 Peripheral Auditory System . . . 56
4.4 Central Auditory System . . . 58
4.5 Cortical Areas Related to Auditory Perception . . . 58
4.6 Corticocortical Pathways . . . 60
4.7 Thalamocortical and Corticothalamic Pathways . . . 62
4.8 Conclusion . . . 65

5 ECoG Activity during Listening to Music **66**
5.1 Introduction . . . 66
5.2 Materials and Methods . . . 68
5.2.1 Subjects and Data Collection . . . 68
5.2.2 Cortical Mapping . . . 70
5.2.3 Extraction of ECoG Features . . . 71
5.2.4 Extraction of Sound Intensity . . . 72
5.3 Results . . . 72
5.3.1 Relevant Cortical Locations . . . 72
5.4 Discussion . . . 76
5.4.1 The Role of ECoG Gamma Activity in Sound Processing . . . 76
5.4.2 Current Experimental Limitations . . . 77
5.4.3 Future Work . . . 79

6 Spatio-Temporal Relationship of ECoG Activity During Music Processing **83**
6.1 Introduction . . . 83
6.2 Materials and Methods . . . 85
6.2.1 Subjects and Data Collection . . . 85

6.2.2 Cortical Mapping . . . 86
6.2.3 Extraction of ECoG and Sound Features . . . 87
6.2.4 Intersubject Correlation (ISC) Analysis . . . 88
6.2.5 Intersubject Granger Causality (ISG) Analysis . . . 89
6.3 Results . . . 91
6.3.1 Spatial Relationship . . . 91
6.3.2 Temporal Relationship . . . 93
6.3.3 Relationships with Anatomical and Neurophysiological Models . . . 93
6.3.4 Causal Relationships . . . 94
6.4 Discussion . . . 95
6.4.1 The Role of Alpha and High Gamma Activity in Music Processing . . . 95
6.4.2 Implications . . . 97
6.4.3 Future Research Questions . . . 98

7 Conclusion and Future Work **103**
7.1 Limitations . . . 104
7.2 Future Work . . . 105

Curriculum Vitae **131**

List of Figures

1.1 Analogy between the desired neuroimaging technique and a spy satellite . 5

2.1 Origin of Brain Electrical Activity 12
2.2 Size and location of sensors that acquire brain signals. 16
2.3 fMRI scanner and BOLD response 17

3.1 Implantation of ECoG grid 24
3.2 Power spectrum profile during listening and silence tasks 27
3.3 Thalamic and cortical neurons involved in the thalamocortical circuit . . . 29
3.4 Thalamocortical circuit 31
3.5 A heuristic model for how broadband spectral increases might emerge from increases in presynaptic action potentials firing rate 34
3.6 ECoG procedure 36
3.7 Details of ECoG implant 37
3.8 Subject-specific brain model and electrode localization 38
3.9 Bedside monitoring systems 40
3.10 Real-time screening session 42
3.11 Preprocessing of the ECoG signal 45

4.1 Peripheral auditory system 57
4.2 Central auditory system 59
4.3 Primary and secondary auditory cortex 61
4.4 Thalamocortical connections mediating higher order auditory processing . 64

5.1 Subdural ECoG implant 70
5.2 Subject-specific brain models 71
5.3 ECoG vs sound intensity 73

5.4 Significance of cortical areas for sound intensity processing 74
5.5 Cortical locations in the posterior part of the superior temporal gyrus with the highest correlation between ECoG high gamma and sound intensity . . 80
5.6 Cortical locations in the dorsal part of the precentral gyrus with the highest correlation between ECoG high gamma and sound intensity 81
5.7 Average gamma in the superior temporal gyrus and the pre central gyrus . 81
5.8 Cortical mapping of face and handmotor areas 82

6.1 Subject-specific brain models and locations of implanted electrodes 87
6.2 Intersubject correlation analysis 92
6.3 Topographical distribution of accumulated negative log of the significance of the ISC values during the task and rest conditions 99
6.4 Temporal relationship between alpha, high gamma, and sound intensity . . 100
6.5 Relationship between anatomy of auditory processing, current understanding of ECoG physiology, and results of this study. 101
6.6 Intersubject Granger causality analysis 101
6.7 Intersubject Granger causality analysis during the task and rest periods for each frequency band 102

7.1 Hypothesis-driven analysis vs. Data-driven analysis 108

List of Tables

2.1 Comparison of functional neuroimaging techniques 22

5.1 Clinical profiles of the subjects that participated in the study 69
5.2 Correlation coefficient between ECoG features and SI 75

6.1 Clinical profiles of the subjects that participated in the study 86

1 Introduction

1.1 Motivation

The brain is the most complex organ of the human body. It consists of highly organized neuron cells essential for carrying out sensory, motor, and cognitive functions. To fully understand how the human brain performs each of these mental functions, it would be necessary to continuously monitor the individual activity of tens of millions of neurons and the constant interplay between small and large groups of neurons. This would be analogous to a spy satellite capable of tracking the continuous behavior of each human being and his relationship with other individuals (Baars and Cage, 2010). See Fig.1.1.

Before the advent of neuroimaging technology, our knowledge of human brain function came from patients with brain lesions and from animal studies. For instance, Pierre Paul Broca (Broca, 1861) and Carl Wernicke (Wernicke and Eggert, 1874) identified in post-mortem stroke patients the regions of the brain responsible for language processing . Gustav Fritsch and Eduard Hitzig demonstrated how electrical current applied to the different regions of the dog's brain caused specific muscular contractions (Fritsch and Hitzig, 1870). Although they yielded important information, these studies relied on indirect methods to identify the locations of the brain related to specific functions.

This issue was resolved with the development of modern imaging techniques to map function in the living human brain: first with the discovery of electroencephalogra-

phy (EEG) in 1929 (Tudor et al., 2005); and then with the development of magnetoencephalography (MEG) in 1972 (Cohen, 1972), positron emission tomography (PET) in 1975 (Ter-Pogossian et al., 1975), and functional magnetic resonance imaging (fMRI) in 1990 (Ogawa et al., 1990). With the growing demand for new technology for clinical diagnosis of brain disorders, these imaging techniques have rapidly advanced and become more suitable for evaluating brain function. Indeed, for the last decade, they have been extensively used for clinical and research purposes.

Despite of the great technological advances in functional brain imaging, these techniques are still limited by the physical properties of the recording system or the nature of the signal to be measured. The techniques enumerated above do not yet have the temporal resolution, spatial resolution, and spatial coverage necessary to track in time and space the high dynamics of brain function. Temporal resolution refers to how closely the measured activity corresponds to the timing of the actual neuronal activity, and spatial resolution refers to how well a recording technique can discriminate neuronal activity between two adjacent brain areas. Spatial coverage refers to how well a recording technique can measure neural activity covering all areas of the brain.

Current neuroimaging techniques can only tell us when or where a neural event occurs on the brain, but not both. For instance, fMRI detects hemodynamic changes (blood flow) to measure brain activity. It provides excellent spatial resolution and spatial coverage, so it can accurately localize neural events in the brain. However, since blood changes are slow (on the order of seconds), fMRI is not suitable for measuring the time course of those events, which occur on the order of milliseconds (Anderson, 2004). On the other hand, MEG and EEG measure the electric and magnetic fields generated by large group of neurons. This more direct approach makes these techniques better at measuring the time course of neural events but worse at measuring their location.

These three major technical drawbacks (i.e., limited temporal resolution, spatial resolution, and spatial coverage) have had a profound restrictive impact on the particular

questions addressed by neuroscientists as well as on the proposed models of brain function, in particular because such models currently emerge from meta-analysis of several functional neuroimaging studies. This relatively indirect approach has left room for subjective interpretation and controversial hypotheses. Typical neuroscience questions have been mostly confined to either determining the areas of the brain engaged in specific mental functions (Bilecen et al., 1998; Binder et al., 2000; Chen et al., 2008) or associating the time course of the regional brain activations with the dynamic aspects of the stimulus (Popescu et al., 2004). Moreover, the answer to questions regarding the dynamic interactions of brain areas operating in large-scale networks has been extremely difficult or almost impossible to ascertain. Although few fMRI or EEG studies have tried to answer these kinds of questions, their results, limited by the time resolution, spatial resolution, and spatial coverage of the techniques, have been extremely difficult to interpret (Hwang et al., 2011; Vinoo et al., 2012).

Returning to the spy satellite analogy, the satellite can either track the daily or monthly behavior of a group of individuals, but cannot monitor the constantly shifting interplay among them. Emerging neuroimaging techniques, such as electrical recordings from the surface of the brain (electrocorticography (ECoG)), aim to overcome this obstacle and thus allow scientists to answer more complex and broader neuroscientific questions. ECoG is a compromise between temporal resolution, spatial resolution, and spatial coverage. It provides high temporal resolution (on the order of milliseconds) and reasonably accurate spatial resolution (on the order of mm) and coverage (usually one brain hemisphere). ECoG signals contain valuable information in the time, frequency, and space domains to represent the underlying neurophysiological processes of the brain. ECoG has been shown to accurately encode the high dynamics of the sensory-motor tasks (Kubánek et al., 2009; Potes et al., 2012; Schalk et al., 2007) and to measure brain processes that could not be detected with other functional neuroimaging techniques (i.e., thalamocortical processes and local cortical activity) (Potes et al., 2013).

ECoG has been also used to identify large-scale brain networks engaged during mental functions (e.g., word production or sound processing) (Korzeniewska et al., 2011; Potes et al., 2013), thereby providing functional brain models driven directly from the data rather than from meta-analysis of functional neuroimaging studies. Thus, ECoG enables a data-driven approach to modeling brain function.

The spatial, spectral, and temporal integration of neural activity across multiple areas of the brain has opened new research opportunities as well as potential clinical applications. However, managing and visualizing vast amounts of information coming from high-dimensional ECoG signals is unclear. In the following chapters, a general neuroimaging framework is proposed that allows researchers and clinicians the facility to record, process, store, and visualize ECoG signals in order to answer specific research questions. Although this framework can be applied to any ECoG data set, the results presented here are specific to an experiment investigating auditory function.

1.2 Main Research Questions and Contributions

This dissertation offers contributions in the clinical and neuroscience fields. The main objective is to develop and validate a neuroimaging framework for ECoG signals that will allow researchers and clinicians to identify cortical areas and cortical networks associated with specific functions of the brain. This framework is specifically applied to, and validated on, brain signals recorded during an auditory experiment. Yet, this framework could be extended to other types of experiments.

Potential Contributions in the clinical field encompass a new technique to validate, facilitate, and complement the mapping results obtained after electrical stimulation of the brain in patients with epilepsy prior to surgery. Currently, the only alternative for treating patients with epilepsy who are resistant to medication is the resection of the brain area causing seizures (i.e., epileptogenic foci). Before resection of the epilepto-

Figure 1.1: **Analogy between the desired capabilities of a neuroimaging technique and a spy satellite.** The ideal neuroimaging technique should be capable of continuously tracking the activity of each neuron and group of neurons as well as the relationships among them. By analogy, a spy satellite should be capable of continuously tracking the behavior of each human being as well as his relationship with other individuals.

genic foci, clinicians must first identify if areas near the resection zone provide critical functions to the brain. This process is called identification of eloquent cortex. To identify these critical areas, clinicians typically deliver mild electrical currents to electrodes implanted on the surface of the patient's brain and monitor for any effect in their behavioral response (e.g., movement of the hand, sentence comprehension, word repetition.)

Mapping of the eloquent cortex is a very tedious, long (e.g., a couple of hours), and complex clinical procedure. It serves to identify the areas of the brain responsible for language, sensory, or motor functions, but neglects the underlying cortical networks engaged during the performance of these functions. This could explain the current high rate of post-operative neurological deficits currently reported (Little et al., 2008). The framework proposed in this dissertation could be added to the current electrical stimulation procedure to identify not only the eloquent cortex but also the underlying brain networks engaged in mental functions.

Potential Contributions in the neuroscience field include development of a novel approach to determine the most salient aspects of auditory processing in the human brain. Two main auditory processes were identified in this dissertation. The first is a process that modulates and facilitates transfer of auditory information from the periphery to the cortex. This process is carried out by neural interactions between the thalamus and cortex and is mainly reflected by activity changes in the low-frequency (8-12 Hz) components of the ECoG signal. The second is a process that represents the mean firing rate of neuronal populations in the cortex and that is reflected by broadband changes in the frequency components of the ECoG signal, mainly in frequencies greater than 30 Hz (Miller et al., 2007). The findings presented in this dissertation are consistent with existing functional models of auditory processing and point to an important and previously largely unrecognized role of the superior premotor cortex in processing music (Rauschecker, 1998; Zatorre et al., 2007).

To validate the proposed framework in the context of auditory processing, the analysis and experiments that were conducted tackled the following questions:

Research Question #1: Do ECoG signals encode the temporal dynamics of music?

Research Question #2: If they do, then what are the spatial, temporal, and causal relationships of ECoG features that support music processing?

To address both questions, the brain electrical activity from the surface of the brain of 8-10 epileptic patients was recorded. These patients underwent temporary implantation of subdural electrode arrays to localize eloquent cortex and the epileptogenic zone prior to surgical resection. All of the subjects gave informed consent to participate in the study, which was approved by the Institutional Review Board of the Albany Medical College. These subjects were instructed to listen to a complex natural auditory stimulus (the song "Another Brick in the Wall - Part 1" (Pink Floyd, Columbia Records, 1979)) while their brain electrical activity was recorded. ECoG recordings were made at the Epilepsy Monitoring Unit at Albany Medical Center, and data analyses were performed at the Wadsworth Center of the New York State Department of Health, Albany, NY.

1.3 Dissertation Outline

The remaining parts of this dissertation are organized as follows: First, Chapter 2 describes current techniques for imaging brain function. In this chapter, the basis of each recording technique is presented, as well as benefits and drawbacks of the associated technical properties, such as temporal and spatial resolution, spatial coverage, degree of invasiveness, implementation cost, and risk factors. Advantages of ECoG, compared to the other recording techniques, are detailed, and an explanation is presented on the reasons for selecting this method for the research described in this document.

Next, Chapter 3 explains the basis of ECoG. First, current understanding of the electrophysiological processes detected with ECoG are introduced. Second, the methods for collecting and recording ECoG signals are described. Third, the procedure for creating a model of the subject's brain is explained. Fourth, methods for projection and visualization of the implanted electrodes on the brain model are described. Fifth, the software

and hardware necessary to record ECoG signals without interfering with the clinical system, which takes priority at all times during recording, are enumerated. Sixth, the use of these signals for addressing specific neuroscientific questions is described. Finally, three potential applications of ECoG in the clinical field are briefly described.

Chapter 4 introduces the basis of auditory processing. To start, the scientific definition of sound is described, and the difference between sound stimulus and sound perception is discussed. The main pathways the auditory input takes when it passes through the ear and different subcortical and cortical structures of the brain are described. Next, the cortical areas that are engaged in the perception of the different aspects of the sound stimulus such as loudness and pitch are briefly explained. Finally, the auditory pathways from the thalamus to the cortex, and those within different areas of the cerebral cortex are described.

Chapters 2, 3, and 4 establish the theoretical framework of this dissertation and provide the basis of ECoG methodology necessary for researchers and clinicians to identify cortical areas and cortical networks associated with specific functions of the brain. Chapters 5 and 6 are dedicated to applying this framework to the analysis of ECoG signals in an auditory experiment and to answer the two research questions stated above: (1) do ECoG signals encode the temporal dynamics of music? and (2) what are the spatial, temporal, and causal relationships of ECoG features that support music processing.? These two chapters are part of two journal articles already published in Neuroimage (Potes et al., 2013, 2012). In Chapter 5, ECoG features and the cortical regions related to the sound intensity of continuous music are investigated. In Chapter 6, the spatial, temporal, and causal relationships between the ECoG features identified in the study described in Chapter 5 and their relationship to current understanding of auditory processing are investigated.

Finally, Chapter 7 describes conclusions, limitations, implications, and suggestions for future work.

2

Functional Neuroimaging Techniques

2.1 Introduction

The discovery of brain electrical activity dates back to 1875 when Richard Caton used a galvanometer to observe the electrical impulses originating from the surface of the brain of living animals (Caton, 1875). Since then, clinicians, scientists, and engineers have made enormous efforts to design and develop more sophisticated techniques to image the neural activity of the brain. Current neuroimaging techniques are based on direct or indirect measurement of brain activity. Techniques based on direct measure of brain activity detect the electrical activity originating from the ionic current flows within and outside of the neurons. In contrast, techniques based on indirect measure of brain activity detect changes in blood oxygenation and blood flow that occur as a result of neural activity.

This chapter describes current electrophysiological and neuroimaging techniques employed by clinicians and researchers to identify functional brain areas. In a typical human experiment, the patient performs a specific task (e.g., opening/closing of the hand or listening to music) while his brain activity is recorded. These recordings are then used to investigate the brain areas that are significantly active (i.e., functional activity) or interconnected (i.e., functional connectivity.)

The aims of this chapter are: (1) to introduce the reader to the existing imaging techniques that measure brain functional activity; (2) to present the benefits and drawbacks of each technique, with respect to temporal and spatial resolution, spatial coverage, degree of invasiveness, implementation cost, and risk factors; and (3) to demonstrate the reasons that electrocorticography (ECoG) may be a promising imaging technique, offering an appealing compromise between high temporal and spatial resolution and reasonable spatial coverage.

In this chapter: section 2.2 briefly describes the origin of neural signals; section 2.3 introduces current neuroimaging techniques based on direct or indirect measure of neural signals; section 2.4 compares each of the techniques based on their resolution, coverage, invasiveness, implementation cost, and risk factors; and section 2.5 concludes by highlighting the main properties that make ECoG a powerful imaging technique for research and clinical purposes.

2.2 Origin of Brain Electrical Activity

In this section, the manner in which neurons originate electrical signals during the processing and transmission of information is briefly explained. These signals can be measured from a single neuron, or an ensemble of neurons using different electrical recording techniques such as single unit recording (SUR), local field potentials (LFP), electrocorticography (ECoG), electroencephalography (EEG), and magnetoencephalography (MEG). Details of these techniques are provided in section 2.3.1.

The human brain consists of approximately 100 billion neurons capable of processing and transmitting information through electrical signals. Neurons are the basic functional units in the brain. A typical neuron has a cell body or soma, dendrites, and axons, as illustrated in Fig. 2.1b. The soma is the central part of the neuron and contains the nucleus of the cell. The dendrites are cellular extensions containing receptors that

respond to chemical signals (neurotransmitters). The axon is a projection of the neuron that typically conducts nerve signals from the soma to the axon terminal, which is the part of the neuron where neurotransmitters are released into synapses to communicate with other neurons.

The neuron releasing the neurotransmitter is called the pre-synaptic neuron, and the neuron receiving the neurotransmitter is called the post-synaptic neuron. The release of neurotransmitters to the post-synaptic neuron causes electrochemical changes in its membrane potential. The membrane potential is the difference in electric potential between the interior and the exterior of a biological cell. After bondage of the neurotransmitter to the post-synaptic cell membrane receptor, Na^+ channels in the post-synaptic cell membrane open, causing the Na^+ ions to flow into the cell. This causes the post-synaptic neuron to depolarize (i.e., the resting membrane potential becomes more positive (from -70 mV to -60 mV)). Continued depolarization of the post-synaptic neuron causes its membrane potential to exceed a threshold level (i.e., usually a depolarization beyond -55 mV) to start an action potential as shown in Fig. 2.1 a. This action potential is a short-lasting event ($\sim$ 2 milliseconds (ms)), in which the electrical membrane potential of a cell first rapidly rises. The electrical membrane potential then falls as the Na^+ channels close while K^+ channels open to allow K^+ ions to flow out of the cell membrane. This process, known as repolarization, returns the membrane potential back to the resting potential (i.e., -70 mV).

Techniques based on direct measurement of neural activity record either the action potentials of a single neuron (SUR) or the summation of actions potentials from thousands or millions of neurons that have similar spatial orientation (LFP, ECoG, EEG, MEG). The next section further explain these techniques.

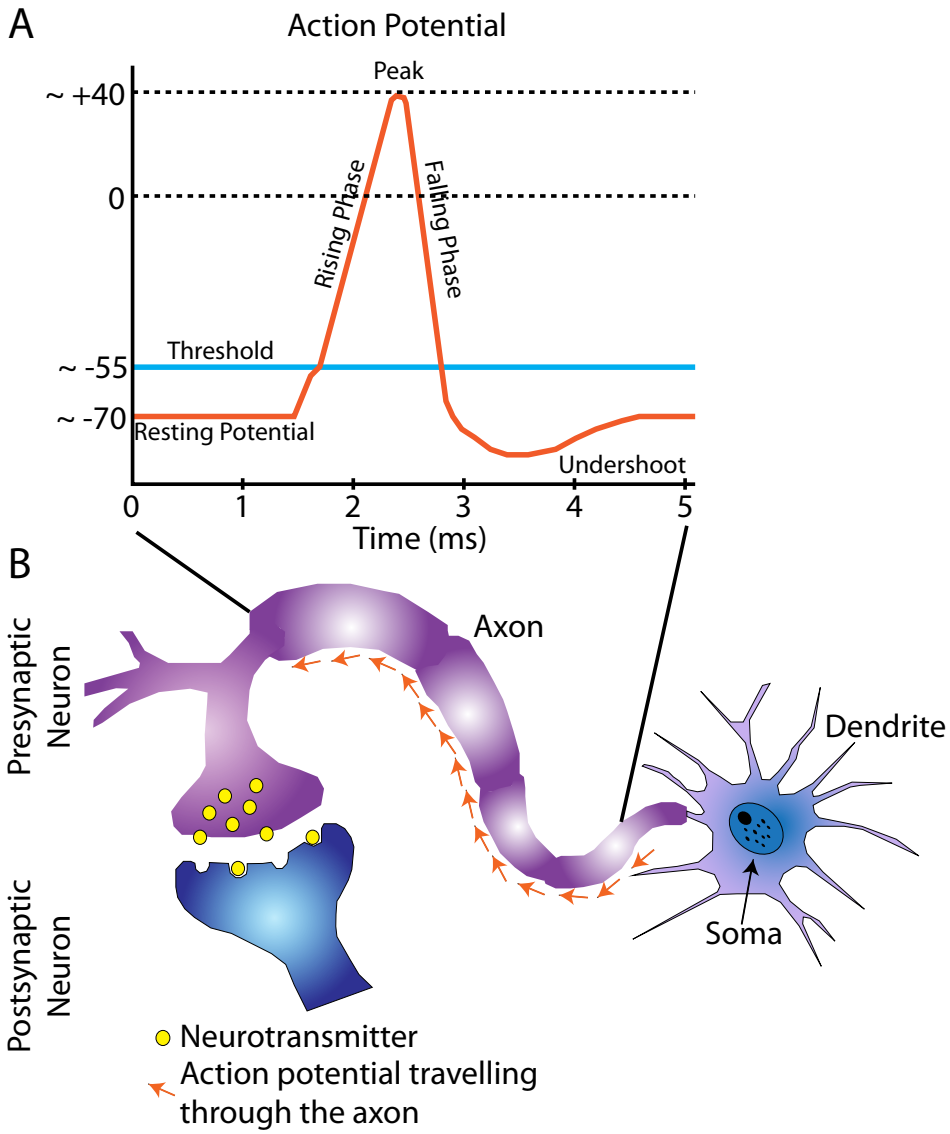

Figure 2.1: **Origin of Brain Electrical Activity.** A. Schematic of an action potential traveling through the axon. B. Neuron and its parts.

2.3 Types of Functional Neuroimaging Techniques

In this section, current neuroimaging techniques are classified as two types: (1) those that measure the brain's electrical activity directly (i.e., SUR, LFP, ECoG, EEG, MEG), and (2) those that measure indirect markers of neural activity, such as changes in the blood flow (i.e., functional magnetic resonance imaging (fMRI)) or metabolic activity (i.e., positron emission tomography (PET) and functional near-infrared spectroscopy (fNIRS)).

2.3.1 Techniques Based on Direct Measure of Neural Activity

Single-Unit Recording (SUR)

SUR measures the action potentials of a single neuron (Humphrey and Schmidt, 1991). A microelectrode is inserted in the brain to measure the current flow changes as the action potential travels down the neuron. SUR has been mostly used for research purposes (e.g., to analyze human cognition and cortical mapping). However, its clinical application is very limited due to the high risk of infection, long-term recording instability, high degree of invasiveness (Nicolelis, 2001). Like local field potentials (LFP) detailed below, SUR offers excellent temporal and spatial resolution but limited spatial coverage (Givens et al., 1998).

Local Field Potentials (LFP)

Recording of local field potentials is another invasive technique. It measures synchronized neural activity within a volume of neural tissue. The technique uses implantable extra-cellular microelectrodes to measure the electrical current flow from local population of neurons that are within approximately 250 μm of the recording electrode (Katzner et al., 2009). The signal is usually low-pass filtered to remove the spike components of individual neurons. It has been shown that population activity measured by LFP may be related to the hemodynamic changes measured with fMRI (Logothetis, 2008; Logothetis et al., 2001). LFP offers very good temporal and spatial resolution but poor spatial coverage (Ferrea et al., 2012). Extensive spatial coverage would require more microelectrodes implanted over the cortex, thus increasing the risk of infection and associated morbidity.

Electrocorticography (ECoG)

Electrocorticography, also known as intracranial EEG, is an invasive technique that measures electrical activity from the cerebral cortex using electrodes placed directly on the

surface of the brain. ECoG offers excellent temporal resolution (in the order of milliseconds), relatively high spatial resolution (0.5-1 cm), reasonable spatial coverage (most of the time electrodes cover only one brain hemisphere), high signal-to-noise ratio, and relatively inexpensive implementation cost (Ball et al., 2009; Hill et al., 2012; Leuthardt et al., 2004; Schalk et al., 2007). Although ECoG requires an invasive procedure, it does not require penetration of the cortex. Therefore, it can offer long-term stability and lower risk of infection than intra cortical methods (Margalit et al., 2003; Pilcher and Rusyniak, 1993). Thus, ECoG has recently emerged as a promising recording technique for developing potential new clinical applications (Brunner et al., 2009) and new brain-computer interfaces (BCIs) (Edwards et al., 2010; Kubánek et al., 2009; Pasley et al., 2012; Pei et al., 2011; Shenoy et al., 2008) as well as for exploring the high dynamics of many of the underlying brain processes (Shum et al., 2013). This technique is further described in Chapter 3 as it is the technique upon which the experiments in this dissertation are based.

Electroencephalography (EEG)

Electroencephalography is a non-invasive technique that uses electrodes placed over the scalp to measure the synchronized activity of large number of neurons (Berger, 1929). EEG requires a reference location whereby the electric potential is measured in reference of that point. Selection of the reference markedly affects the quality of the measured electrical signal. EEG offers excellent temporal resolution (on the order of milliseconds) but poor spatial resolution (on the order of centimeters) (Srinivasan, 1999). Unlike fMRI or PET, EEG cannot reliably detect brain activity below the surface of the cortex. This is, in part, because the original electrical activity is attenuated and distorted by the shape and layers of the cortex, the bony skull, and the conductive properties of the intervening cells (Freeman, 2004). EEG measurements must be made over multiple trials to enhance the signal-to-noise ratio. EEG has been used extensively, not only for research purposes

but also for clinical and industry purposes, mainly because of its inexpensiveness and ease of use, and the fact that it reveals clinical useful information.

Magnetoencephalography (MEG)

Magnetoencephalography is a non-invasive neuroimaging technique that measures the magnetic fields produced by the electrical activity of the brain (Ioannides, 2006). MEG measures direct brain activity with high temporal resolution (on the order milliseconds) but poor spatial resolution (on the order of centimeters) (Baars and Cage, 2010). MEG is also more sensitive to cortical activity and does not require the experimenter or physician to place electrodes on the subject's skull (Cohen and Cuffin, 1983). MEG measurements are usually taken in magnetically shielded rooms since the neuromagnetic fields produced by the brain are very weak and can be obscured by external magnetic disturbances. A major technical challenge in MEG is to estimate and localize the sources of brain electrical activity from the magnetic fields that were measured outside of the head. MEG does not provide information about the subject's brain anatomy. Therefore, it must usually be combined with other imaging techniques (e.g., magnetic resonance imaging) so that the estimated sources of brain activity are co-registered with anatomical images. In this way, brain regions related to function are integrated into a single representation.

2.3.2 Techniques Based on Indirect Measure of Neural Activity

Functional Magnetic Resonance Imaging (fMRI)

Functional magnetic resonance imaging is a non-invasive technique that detects hemodynamic changes during brain activity. This technique relies on the fact that there is an increase of blood oxygenation and blood flow in regions where the brain is active (Huetel et al., 2009). Over the last decade, fMRI has been very attractive for imaging normal brain function, mainly because it is not invasive and does not require patients

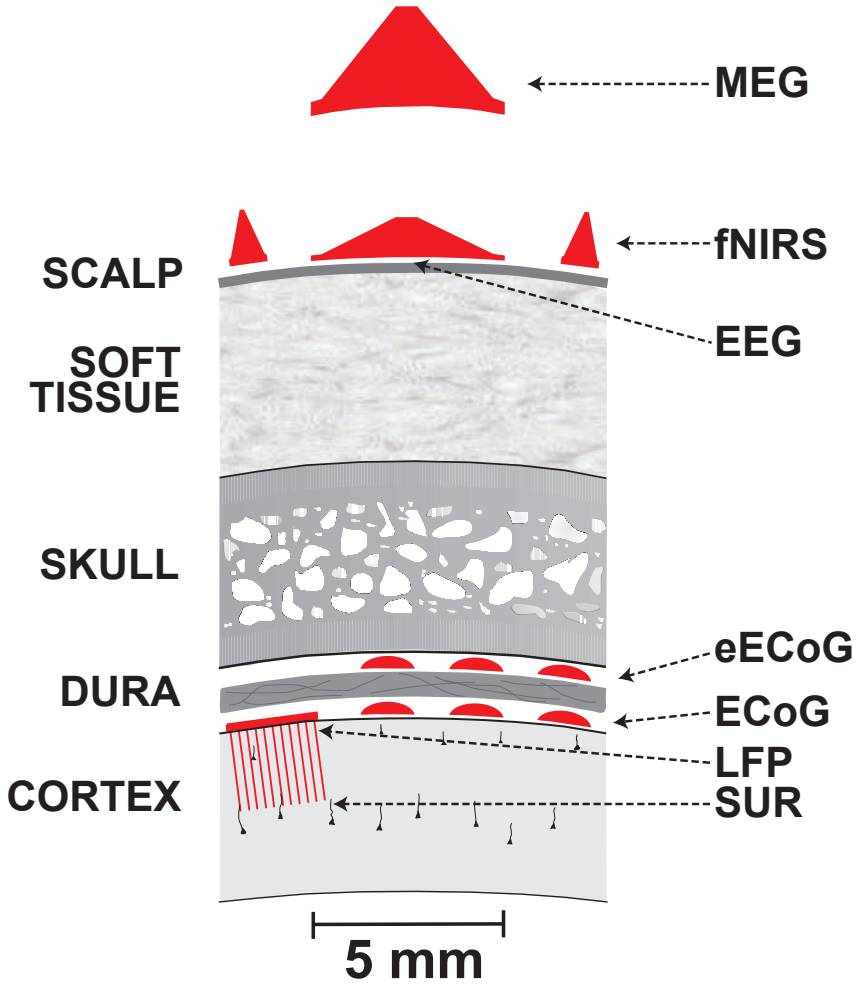

Figure 2.2: Size and location of sensors that acquire brain signals. This figure shows the size and the location of sensors that acquire brain signals. Non-invasive sensors are located on the scalp (for EEG and fNRI) or above the scalp (for MEG) and are typically 10 mm or larger in diameter. Invasive sensors are located on the dura (e.g., epidural ECoG (eECoG)), under the dura (e.g., ECoG) or within the cortex (LFP, SUA) and are typically 2 mm or smaller in diameter. From (Brunner, 2013).

to undergo surgery or be exposed to radiation. Additionally, fMRI provides excellent spatial resolution and full coverage (Kimberley and Lewis, 2007). Its spatial resolution is indeed better than EEG and MEG, but not as good as that of SUR. Standard fMRI scanners can localize brain activity in a spatial range from millimeters to centimeters.

To map brain function, fMRI looks at hemodynamic changes during two conditions (e.g.,visual contrast between red squares and green squares, as shown in Fig.2.3.) This

comparison allows the clinician to detect the brain areas that respond to a particular function. However, these changes are usually observed four to six seconds after the onset of the stimulus, since this is the time it usually takes the vascular system to respond to increased demand for oxygen and glucose. The intrinsic delay between neuronal activity and the blood flow response, in addition to the speed of the scanner and the high brain volume measured, limit the temporal resolution of fMRI to a few seconds. This poor time resolution makes the technique unable to track the high dynamics of neural events and to detect distinct underlying brain physiological processes, such as local cortical processing vs. large-scale oscillatory activity (Aine, 1995; Logothetis, 2008; Logothetis et al., 2001). These limitations, in addition to the high cost for the scanner (e.g., up to multiple million dollars) and need for a shielded room, restrict the utility of fMRI mainly to diagnostic and research applications.

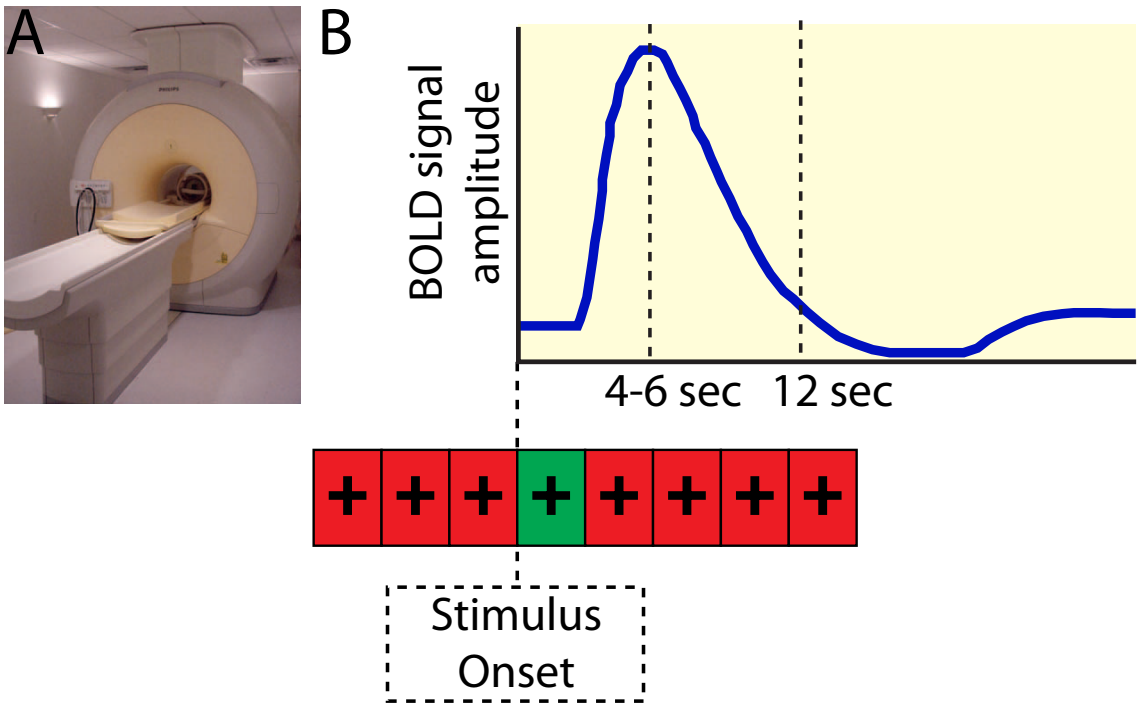

Figure 2.3: **fMRI scanner and BOLD response.** A) fMRI scanner, B) Schematic of blood-oxygen-level dependent (BOLD) response. It peaks at 4-6 sec after stimulus onset.

Positron Emission Tomography (PET)

PET is an imaging technique that measures blood flow or metabolic rate of glucose consumption in the brain using radioactively labelled molecules (i.e., radiotracers). These radiotracers are usually injected into the body to eventually reach the brain through blood circulation. A radiotracer is usually composed of a radioisotope attached to a glucose or oxygen molecule. The radioactive isotope emits a positron (i.e., subatomic particle with the same mass as an electron, and a numerically equal, but positive charge) in the process of its radioactive decay. When this positron collides with an electron, the two particles annihilate each other, and produce two photons traveling in opposite directions. This physical process induces an electromagnetic radiation detected by sensor arrays in the PET scanner. Areas of the brain with high concentration of glucose or oxygen due to high neural activity would produce more radiation detected by the PET scanner. The more neural activity, the more blood, oxygen, and glucose metabolism in the brain tissue, and the more radiation emitted.

PET scans offer better time resolution compared to other metabolic imaging techniques; however, it is limited to monitoring short tasks due to the short-half-life effect of the radioactive tracer. PET is very expensive and exposes subjects to ionizing radiation. For this reason, PET is used less often for research today.

Functional Near-Infrared Spectroscopy (fNIRS)

Like fMRI and PET, this technique also uses hemodynamic changes as an indicator of neural activity. The technique uses a sensor placed on the subject's forehead to detect changes in the amount of hemoglobin oxygen content using near infrared light (Yu-Luen et al., 1999). fNRIS has been used for non-invasive assessment of brain function. However the reliability of this method has not been widely accepted in the clinical and research community, mainly because of the inability to quantify concentration changes in hemoglobin using continuous wave-type instruments and the lack of knowledge of

which regions of the brain are, in fact, sampled during these measurements Sitaram et al. (2007).

2.4 Comparison of the Recording Techniques

The ideal functional neuroimaging technique should be a direct measure of neural activity and should have the following characteristics: high temporal and spatial resolution, high spatial coverage, no invasiveness, no radiation, low implementation cost, low risk of infection, and ease of use. However, up to now, it is not possible to have all these characteristics in a single recording device. In this section, some of these recording technique properties are described, and current functional neuroimaging techniques which exhibit these properties are discussed.

2.4.1 Temporal Resolution

Temporal resolution refers to how closely the measured activity corresponds to the timing of the actual neuronal activity (Kimberley and Lewis, 2007), considering that an action potential takes approximately 0.5-130 milliseconds to propagate across a single neuron (Anderson, 2004). High temporal resolution is a desirable characteristic when it comes to distinguishing the neural activation patterns associated with different stages of stimulus processing. For instance, Potes et al. 2012 and Kubánek et al. 2009 use ECoG signals to track the temporal dynamics of the brain response (every 100 ms) to the sound intensity of the music and the individual traces of finger flexion, respectively.

As discussed above, the temporal resolution of recording techniques based on hemodynamic responses (i.e., fMRI, PET, fNIRS) is limited to a few seconds due to the relatively slow response of the vascular system to any demand of oxygen or glucose and the speed of the device to scan the whole brain. In contrast, recording techniques based on electrical activity responses (i.e., SUR, LFP, EEG, ECoG, and MEG) offer higher temporal

resolution (on the order milliseconds) but at the expense of decreasing spatial resolution.

2.4.2 Spatial Resolution and Coverage

Spatial resolution refers to how well a recording technique can discriminate neuronal activity between two adjacent brain areas. Spatial coverage, on the other hand, refers to how well a recording technique can measure neural activity covering all areas of the brain. High spatial resolution and high spatial coverage are usually desired when researchers and clinicians want to precisely detect and discriminate the brain areas that respond to a particular function.

Among all the recording techniques, fMRI and PET are the only ones to provide both high spatial resolution (ranging from millimeters to centimeters) and high spatial coverage (covering large brain areas, such as Brodmann areas and very small and deep brain structures, such as the hippocampus and amygdala) (Kimberley and Lewis, 2007).

SUR and LFP provide the best spatial resolution since they measure brain activity from single cells or neuronal populations. Nevertheless, they provide the poorest spatial coverage since they cover only a tiny space in the brain. ECoG, EEG, and MEG provide reasonable good spatial coverage, but only ECoG provides better spatial resolution.

2.4.3 Invasiveness Degree and Risk Level

In the context of this discussion, invasiveness refers to the entry of any element or substance into the body with the purpose of recording neural activity of the brain. SUR, LFP, and ECoG require implantation of electrodes within or over the brain. Among them, SUR and LFP are the most invasive since they require insertion of a microelectrode into the brain, thus possibly leading to a high risk of brain infection. ECoG is less invasive and less risky, as long as the electrodes are placed epidurally (right above the dura mater). PET and fMRI are non-invasive in that subjects do not undergo brain

surgery for electrode implantation, but they are exposed to ionizing radiation or strong magnetic fields (Brix et al., 2009). Although no formal studies have investigated in detail the exposure levels used during PET and fMRI, the consensus to the present is that the amount of radiation and magnetic field exposure is too low to affect the normal processes of the body. EEG, MEG, and fNIRS are completely non-invasive and essentially risk-free. They do not involve electrode implantation or exposure to radioactivity or magnetic fields. In general, minimally- or non-invasive techniques tend to provide comprehensive coverage at low risk, but suffer from high cost and/or low spatial resolution and low signal-to-noise ratio.

2.4.4 Implementation Cost

The necessary equipment to record brain signals using fNIR, SUR, LFP, EEG, and ECoG can be very low ($\sim$ 10K USD) compared to the cost of the other technologies (i.e., fMRI, PET, and MEG). The major cost of an fMRI, MEG, or PET experiment is the scanner. The cost of an fMRI scanner is less ($\sim$ 2.5M USD) than for PET, but more expensive than for MEG (Hämäläinen et al., 1993; Hennig et al., 2003; Ioannides, 2006)

2.5 Conclusion

Currently, functional neuroimaging techniques can either instantaneously track the time-course of neural events or reliably locate the occurrence of neural events in the brain, but not both. Often there is a tradeoff between temporal resolution of a measurement and its spatial resolution; it is not possible to have both at the same time using the same recording technique. Techniques with very high temporal resolution such as SUR, LFP, EEG, and MEG can reliably detect the high temporal dynamics of neural activity, but they cannot reliably identify the exact location where that activity is occurring in the brain. On the other hand, techniques with high spatial resolution and coverage such as

fMRI and PET can provide the exact location of neural events in the brain but cannot reliably track the time-course of those events.

Despite its high degree of invasiveness, ECoG represents a good compromise between time and spatial resolution and coverage. ECoG promises to be a powerful and practical technique overcoming most of the technical limitations of the other techniques, as shown in Table 2.1. ECoG has also recently emerged as a promising technique for use in brain research and clinical diagnosis.

Table 2.1: **Comparison of functional neuroimaging techniques.** This table compares the characteristics of the different recording methods.

	SUR	LFP	epidural ECoG	subdural ECoG	EEG	MEG	fMRI	PET	fNIR
temporal resolution	μs	ms	ms	ms	ms	ms	sec	sec	sec
spatial resolution	μm	mm	mm	mm	cm	cm	mm	mm	cm
spatial coverage	very limited	limited	limited	limited	limited	limited	full	full	limited
signal to noise ratio	very high	high	medium	high	low	low	low	low	low
expensive equipment	low	low	low	low	low	high	very high	very high	low
susceptible to artifacts	no	no	no	no	yes	yes	yes	yes	yes
degree of invasiveness	very high	very high	high	high	none	none	very low	very low	none
infection risk	high	high	low	low	none	none	none	none	none

3

Electrocorticography (ECoG)

3.1 Introduction

Wilder Penfield and Herbert Jasper were two groundbreaking researchers who invented the Montreal procedure, a new surgical protocol for patients with epilepsy, to identify and remove the regions of the brain from which seizures originate (i.e., epileptogenic zones). Penfield and Herbert used ECoG recordings in concert with cortical electrical stimulation to identify critical cortical structures responsible for mental functions (i.e., "eloquent cortex") (Penfield and Boldrey, 1937; Penfield et al., 1942; Penfield and Rasmussen, 1950). In this procedure, identification of the epileptogenic zones and eloquent cortex are crucial factors to reduce or eliminate seizures as well as to prevent postoperative neurological deficits. To date, the main clinical purpose of ECoG is to help in the diagnosis and treatment of epilepsy in patients who are resistant to medication. However, for the last decade, it has become clear that ECoG has great potential as a research tool as well.

ECoG measures direct neural activity using a grid of electrodes implanted over the surface of the brain. To place the electrode grid and record ECoG signals, a neurosurgeon must first perform a craniotomy (i.e., a surgical incision into the skull) and place the electrode grid either outside the dura mater (epidural) or under the dura (subdural). The

electrode cables exit the scalp through the incision in the dura and skull, and are then connected to the research and clinical systems for further recordings or stimulation, as shown in Fig.3.1. ECoG offers high temporal and spatial resolution (i.e., in the range of milliseconds and millimeters, respectively), limited spatial coverage, broad bandwidth, high signal-to-noise ratio, and relatively low implementation cost. Although ECoG requires an invasive procedure, it does not require penetration of the cortex. Thereby, it may offer long-term stability and low risk of infection (Margalit et al., 2003; Pilcher and Rusyniak, 1993).

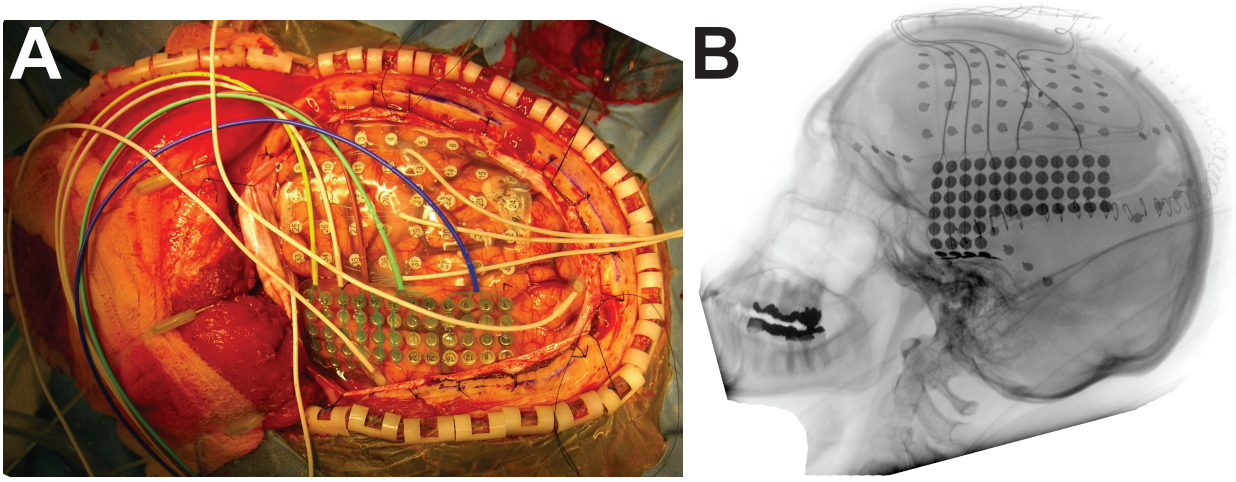

Figure 3.1: **Implantation of ECoG grid.** This figure shows two electrode grids implanted on the surface of the brain of a patient with epilepsy. (A) The cortex is exposed through a craniotomy and an incision of the dura. (B) A lateral X-ray of the skull showing the exact location of the electrode grids.

Current techniques to map brain function have associated advantages and disadvantages which limit, to some extent, their usage in the clinical and research fields. Among these techniques, ECoG promises to be a powerful and practical technique overcoming most of the limitations of the other techniques, and offering potentially new clinical applications as well as more insight in understanding how the human brain works.

This chapter is structured as follows. Section 3.2 provides the reader with current understanding of the electrophysiological processes detected with ECoG. Section 3.3 describes the methods for recording ECoG signals. Section 3.4 demonstrates how to

use these signals for addressing specific neuroscientific questions. Finally, Section 3.5 describes current applications of ECoG in the clinical field.

3.2 Electrophysiological Processes Detected with ECoG

Unlike other neuroimaging techniques, the ability of ECoG to measure electrical brain activity with high signal-to-noise ratio over a wide frequency range (i.e., 0-300 Hz) (Gaona et al., 2011; Staba et al., 2002) has allowed researchers to link current and newly described neurophysiological processes to different electrical rhythms of the brain.

The alpha and mu rhythms are oscillations in the low (8-12 Hz) frequency band. Although the underlying neurophysiological mechanism that creates this low frequency oscillation remains unknown, recent research indicates that this rhythm may play an inhibitory role in the cortex (e.g., visual, auditory, and motor areas) to facilitate transfer of information or to modulate neural activity within the cortex. This neurophysiological process may be realized by neural interactions between the thalamus and cortex (Niedermeyer and Lopes da Silva, 2005; Pfurtscheller and Aranibar, 1977; Pfurtscheller and Lopes da Silva, 1999; Pfurtscheller and Lopes Da Silva, 1999). The alpha rhythm is associated with brain activity in the sensory cortex, whereas the mu rhythm is associated with brain activity in the motor cortex. In general, the amplitude of the alpha rhythm is suppressed over the occipital and temporal lobes with visual and auditory stimuli, respectively; and the amplitude of the mu rhythm is suppressed during actual or imagined movements, particularly on the brain hemisphere contralateral to the movement (Crone et al., 1998a,b; Pfurtscheller and Aranibar, 1977). These amplitude changes in the alpha/mu rhythm are usually narrow in the spectrum (i.e., 8-12 Hz) but very broad in space.

The other major brain rhythm that can be detected with ECoG is gamma. The gamma rhythm is an oscillation in the high (30-300 Hz) frequency band. Recent research has

linked this rhythm to the mean firing rate of neuronal populations in the cortex (Miller et al., 2007). Unlike the mu/alpha rhythms, gamma is very focused in space and has a broad spectral distribution resembling a noise-like phenomenon, i.e., amplitude decreases as frequency increases (Miller et al., 2007) (see Fig. 3.2). The amplitude of gamma rhythm increases during sensory or motor functions, and, more importantly, correlates closely with specific details of these functions (e.g., individual flexion of the fingers (Kubánek et al., 2009) or the sound intensity of music (Potes et al., 2012).) Gamma amplitude has also been tightly correlated to the blood oxygen level dependent (BOLD) signals measured with fMRI (Lachaux et al., 2007a; Niessing et al., 2005), suggesting that increases in local cortical activity might lead to increases in gamma activity as well as to increases in the hemodynamic response.

Alpha/Mu and gamma rhythms are not two independent entities working separately. Coupling between alpha/mu and gamma rhythms have recently been proposed as a mechanism to transfer information from large-scale brain networks to local cortical processing areas. This cross-frequency coupling might be the brain mechanism for coordinating fast processes with slower perceptual or cognitive processes (Canolty et al., 2006; Canolty and Knight, 2010; He et al., 2010).

In summary, the broadband spectrum, the high signal-to-noise ratio, and the high amplitude and fidelity of the brain signals measured with ECoG offer a unique opportunity to explore and identify newly neurophysiological processes, in particular those occurring at very high frequency bands, that could not be identified with any other neuroimaging technique

3.2.1 Thalamocortical Activity

The thalamocortical circuit refers to the continuously ongoing neural activity between the thalamus and cortex. Thalamocortical neurons (TC), reticulothalamic (RT) neurons, and corticothalamic (CT) neurons are the the main elements of this circuit, as illustrated

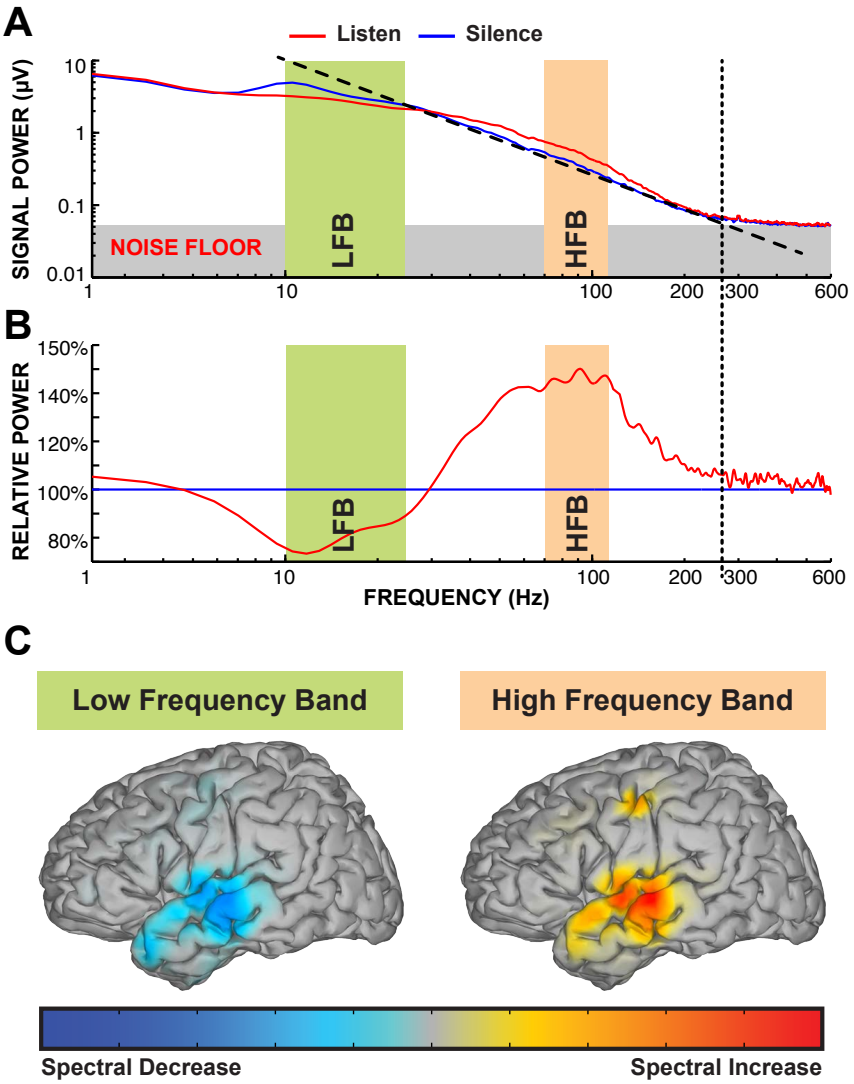

Figure 3.2: **Power spectrum profile during listening and silence tasks.** (A) Power spectrum analysis of ECoG signals recorded during listening (red line) and silence (blue line) tasks reveal a power-law shape. This spectrum shape illustrates how the power signal gets closer to the noise floor in frequencies around 300 Hz (dotted line). (B) Within this frequency range (i.e.,0-300 Hz) the listening task induces a power decrease in the low frequency band (LFB) and a power increase in the high frequency band (HFB). (C) A topographic representation of these power augmentations reveals the involvement of the superior temporal gyrus in the listening task. The color bar indicates the scale used for the topography map: blue reflects spectral decrease, and red–yellow reflects spectral increase. Gray indicates no change. From (Brunner, 2013).

in Fig. 3.3. Intracellular recordings from these neurons in guinea pigs and cats have revealed that they are endowed with very specialized electrophysiological properties (Steriade and Llinás, 1988).

Thalamocortical neurons project their axons to the cerebral cortex and synapse with CT and RT neurons. The intrinsic properties of TC neurons allow them to generate oscillations at 6 and 10 Hz (Steriade and Llinás, 1988), which can be changed in response to external input from the body or by internal feedback from the cortex (Llinás and Ribary, 1998; Llinás et al., 1999). These two intrinsic rhythms allow TC neurons to either oscillate or resonate in reciprocal thalamocortical loops at these two main frequencies. In addition to the oscillatory properties, TC neurons also serve as a relay mechanism that receives either external input from the body to send it to cortical neurons or that receives feedback from cortical neurons to send it back to the body. Corticothalamic neurons are glutaminergic excitatory cells (i.e., they release the neurotransmitter glutamine) mostly found in layer VI of the cortex. These neurons specifically respond to thalamic input at a specific frequency, and exert excitatory and inhibitory influence on thalamic neurons. Both TC and CT neurons make excitatory synaptic contacts (i.e., releasing the neurotransmitter glutamine) to reticular neurons. Reticular neurons, in turn, provide inhibitory synapses (i.e., releasing the neurotransmitter gamma-Aminobutyric acid (GABA)) to TC neurons.

A thalamocortical circuit comprises the specific/sensory loop and the non-specific intralaminar loop (Llinás, 2003; Llinás and Ribary, 1998). The specific/sensory loop starts with external input from the body (i.e., specific/sensory input) entering the ventrobasal thalamus at the "specific" thalamic nuclei (e.g., lateral geniculate nucleus or medial geniculate nucleus). Thalamocortical neurons from these nuclei send this information to the cortex by synapsing with cortical cells in layer IV of the cortex. In a similar way, the nonspecific intralaminar loop starts with internal input from the brain entering the ventrolateral thalamus at the intralaminar "non-specific" nuclei. Thalamocortical neurons from these nuclei send this information to the cortex by synapsing with cortical cells in layers I and VI of the cortex. In this way, cortical cells may integrate sensory perception and information about the internal state of the brain into the thalamocortical circuit (Llinás, 2003; Llinás and Ribary, 1998) (see Fig. 3.4).

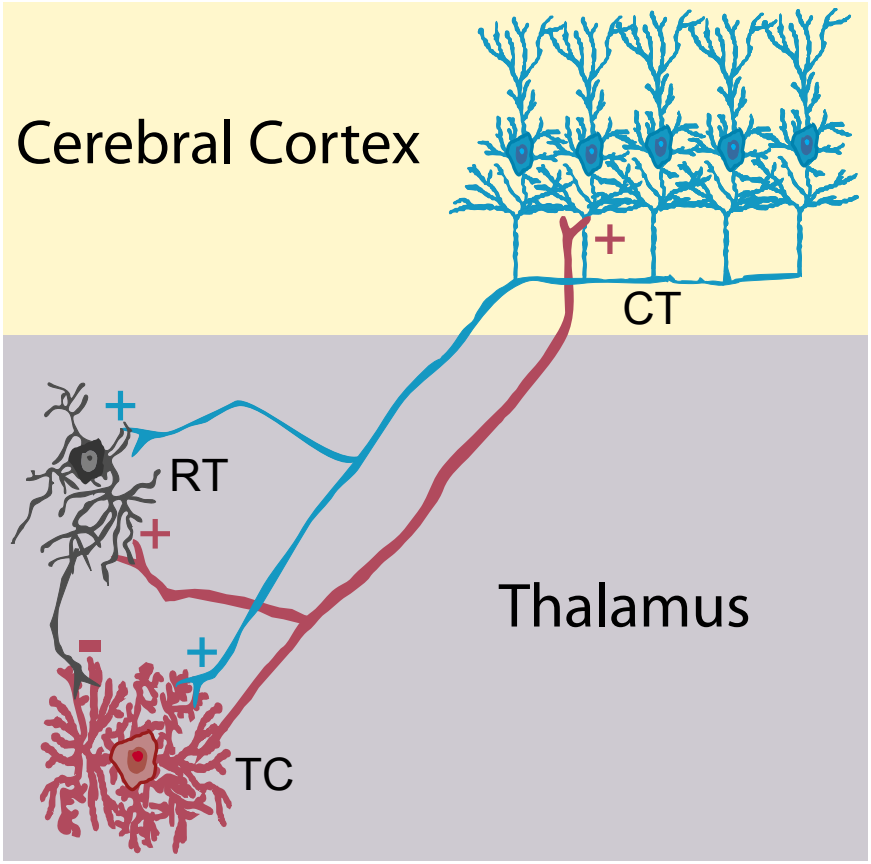

Figure 3.3: **Thalamic and cortical neurons involved in the thalamocortical circuit.** This figure shows the neurons involved in the thalamocortical circuit: corticothalamic (CT), reticulothalamic (RT), and thalamocortical (TC) neurons. The plus symbol corresponds to excitatory synapses (i.e., releasing the neurotransmitter glutamine) and the minus symbol corresponds to inhibitory synapses (i.e., releasing the neurotransmitter GABA).

Established models of the generation of alpha/mu rhythm are derived from animal studies, mainly in dogs and monkeys. Previous studies have linked the origin of this rhythm to neural interactions between the thalamus and cortex (da Silva et al., 1973; Saalmann et al., 2012; Steriade et al., 1990) or to neural interactions within the cortex (Lopes Da Silva and Storm Van Leeuwen, 1977). da Silva et al. 1973 found significant coherence between alpha/mu rhythm that were simultaneously recorded in the cortex and the lateral geniculate and pulvinar nuclei of the thalamus. Saalmann et al. 2012 reported similar results in a visuospatial attention task in monkeys. They found that attention significantly increases the coherence between visual cortex and pulvinar ar-

eas in the alpha/mu and gamma bands (particularly 30-60 Hz). This cross-frequency coupling between thalamocortical areas may be the mechanism by which the brain selectively facilitates the transfer of information across cortical areas (Canolty et al., 2006; Canolty and Knight, 2010; He et al., 2010; Jensen and Mazaheri, 2010). Lopes Da Silva and Storm Van Leeuwen 1977 also linked the origin of alpha/mu rhythm to neural interactions within the cortex. In their study, they found significant coherence between alpha rhythms in relatively close cortical areas (interelectrode distance of 2 mm), and they reported higher intracortical coherence compared to any thalamocortical coherence measured in the same animal.

Despite this body of work in identifying the thalamocortical circuitry, the physiological properties of this network, and the neurophysiological origin of alpha/mu rhythm, more research is needed to better understand the modulation and functional integration between the thalamus and cortex, and the precise neuronal mechanisms that produce the alpha/mu rhythm.

3.2.2 Local Cortical Activity

Unlike other recording techniques, ECoG can measure brain electrical activity over a wide frequency range (0-300 Hz). Changes in the amplitude of the signal over this broadband frequency range have a power-law shape spectrum, are very focused in space, and correlate with functionally specific cortical activity (Miller et al., 2007, 2009).

In the ECoG literature, the term "gamma band" most often refers to the amplitude of the ECoG signal over a specific frequency band (30-170 Hz) (Sinai et al., 2005), a subset of the broad-band ECoG spectrum. The amplitude of the signal in the gamma band increases with respect to baseline during motor execution and planning, auditory processing and visual-spatial attention tasks (Crone et al., 1998a; Gunduz et al., 2011; Kubánek et al., 2009; Miller et al., 2007; Pei et al., 2011, 2010). For instance, Kubánek et al. 2009 and Schalk et al. 2007 reported amplitude increases in the high gamma frequency

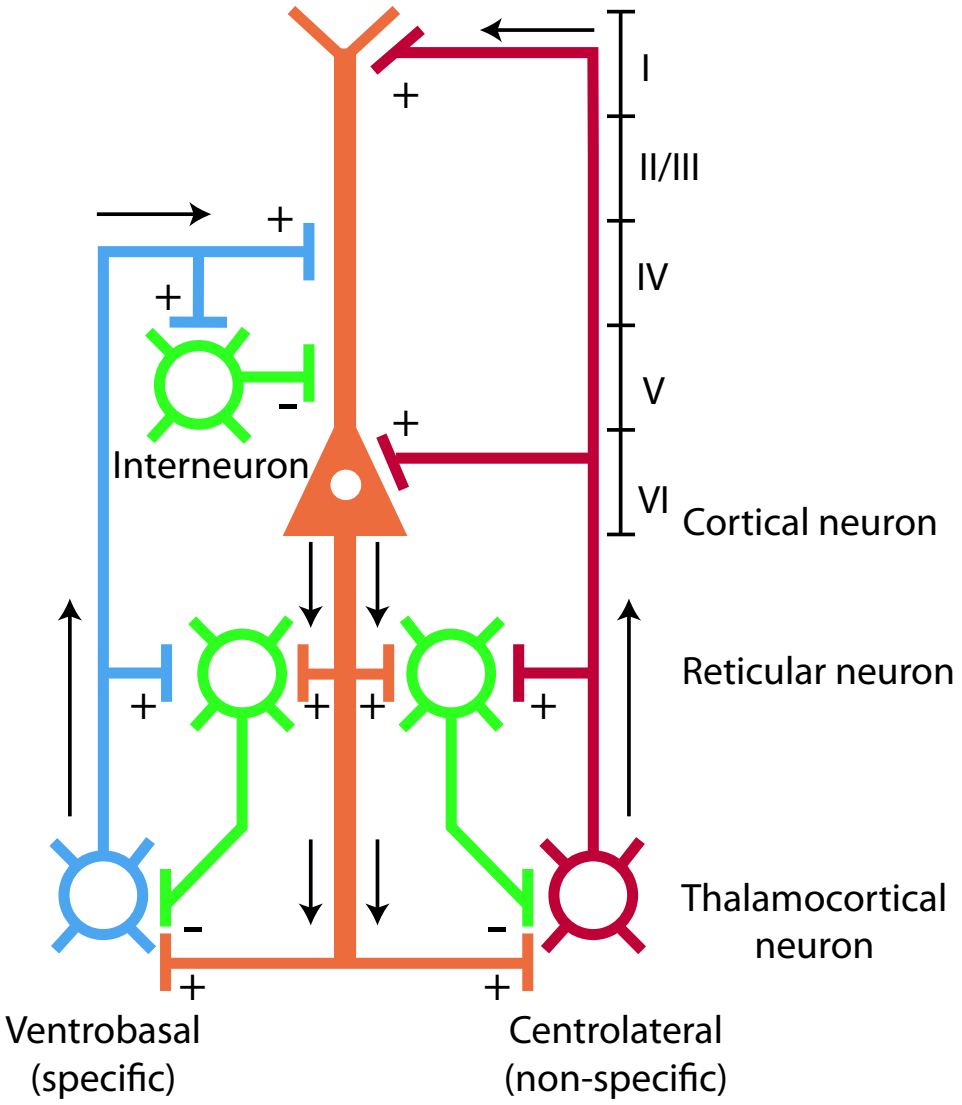

Figure 3.4: **Thalamocortical circuit.** This figure shows the thalamocortical circuit, which is comprised of the specific/sensory loop (in blue) and the non-specific intralaminar loop (in red). The specific/sensory loop starts with external input from the body entering the ventrobasal thalamus at the specific thalamic nuclei. Thalamocortical neurons from these nuclei send information to the cortex by synapsing with cortical cells in layer IV of the cortex. In a similar way, the nonspecific intralaminar loop starts with internal input from the brain entering the ventrolateral thalamus at the intralaminar non-specific nuclei. Thalamocortical neurons from these nuclei send the information to the cortex by synapsing with cortical cells in layers I and VI of the cortex. In this way, cortical cells integrate sensory perception and information about the internal state of the brain into the thalamocortical circuit. Modified figure from (Llinás, 2003).

band ($\sim$ 70-170 Hz) during flexion of individual fingers and hand movements. More importantly, the time course of high gamma in relevant cortical areas was used to decode

the time course of the finger flexion and the kinematic parameters of hand movements. Thus, gamma activity has been proposed as a robust and general indicator of local cortical function.

Although numerous studies report changes in the broadband spectrum of the ECoG signal during execution and planning of specific tasks, the underlying neurophysiological mechanism that produces this broadband phenomenon remains unclear. One possible explanation of this phenomenon comes from SUR and LFP studies in monkeys and humans (Fries et al., 2001; Manning et al., 2009; Pesaran et al., 2002). These studies report that increases in the broadband power spectrum of the local field potentials are related to increases in the firing rate of single-neuron action potentials. This finding provides empirical evidence that broadband spectral changes of the ECoG signals might be related to the mean firing rate of the neuronal population beneath each electrode.

Figure 3.5 from (Miller, 2010) describes a simple neurophysiological model to relate increases in the broadband spectrum of ECoG signals to increases in the firing rate of presynaptic action potentials. (A) Poisson-distributed presynaptic action potentials arrive at a neighboring neuron. The power spectral density (PSD) of these action potentials events over time has a flat, frequency-independent form (i.e., a "white noise" shape, with spikes coming with equal probability at every frequency; blue trace in (G). (B) At the synapse between the two neurons, each arriving action potential triggers release of a neurotransmitter and postsynaptic current influx. As shown in the central schematic neuron, this results in a gradient of charge density within the dendritic arbor. (C) The temporal shape of the postsynaptic current smears out the PSD, giving it a $\frac{1}{f^2}$ form, with a "kink" at a particular frequency determined by the decay time, τ, of the postsynaptic current (here $\sim$ 70 Hz), shown with a gray arrow in (G). (D) In this model, the inputs from 6000 such synaptic currents are integrated over time and space, simulating the time-dependent change in transmembrane charge concentration. The associated transmembrane potential produces a time-dependent current across the dendritic membrane.

(E) The combined effect of synaptic and transdendritic current influx/efflux induces a gradient of current-source density in the surrounding medium. The time dependence of transmembrane potentials are mimicked by the local field potential (LFP), and likely by the macroscale (ECoG) potential as well. (F) The PSD shifts associated with changes in mean firing rate from presynaptic inputs are broadband in nature (spread across all frequencies), with a characteristic $P \sim \frac{1}{f^{\chi}}$ form (i.e., the power in the PSD falls off with increasing frequency according to the exponent, χ). (G) The $P \sim \frac{1}{f^{\chi}}$ PSD structure might emerge from the combinations of three simple processes: Poisson-distributed input spikes (reflected in the rate measured by (Manning et al., 2009)); a characteristic postsynaptic current with exponential decay, which produces a $\frac{1}{f^2}$ form following a kink (gray arrow) at a frequency determined by the decay time at the synapse; and the integration of inward currents over time in the dendrite (as in D and E) to shape the PSD. Thus, Miller 2010 asserts that an increase in the firing rate of action potentials will likely result in an increase in the broadband spectrum of the electrical activity measured at larger spatial scales.

Up to the present, the consensus from established ECoG research is that broad-band spectral changes reflect local cortical processes, closely related to the mean firing rate of neuronal ensembles, and that these cortical processes can be synchronized or modulated by neuronal signals from other brain structures such as the thalamus (Canolty and Knight, 2010; Saalmann et al., 2012).

3.3 Methods for Collecting and Recording ECoG Signals

In this section, the methods implemented at the Wadsworth Center lab for collecting and recording ECoG signals are described. The goal of this section is to provide the reader with a sequence of steps necessary for collecting and displaying data for research or clinical purposes.

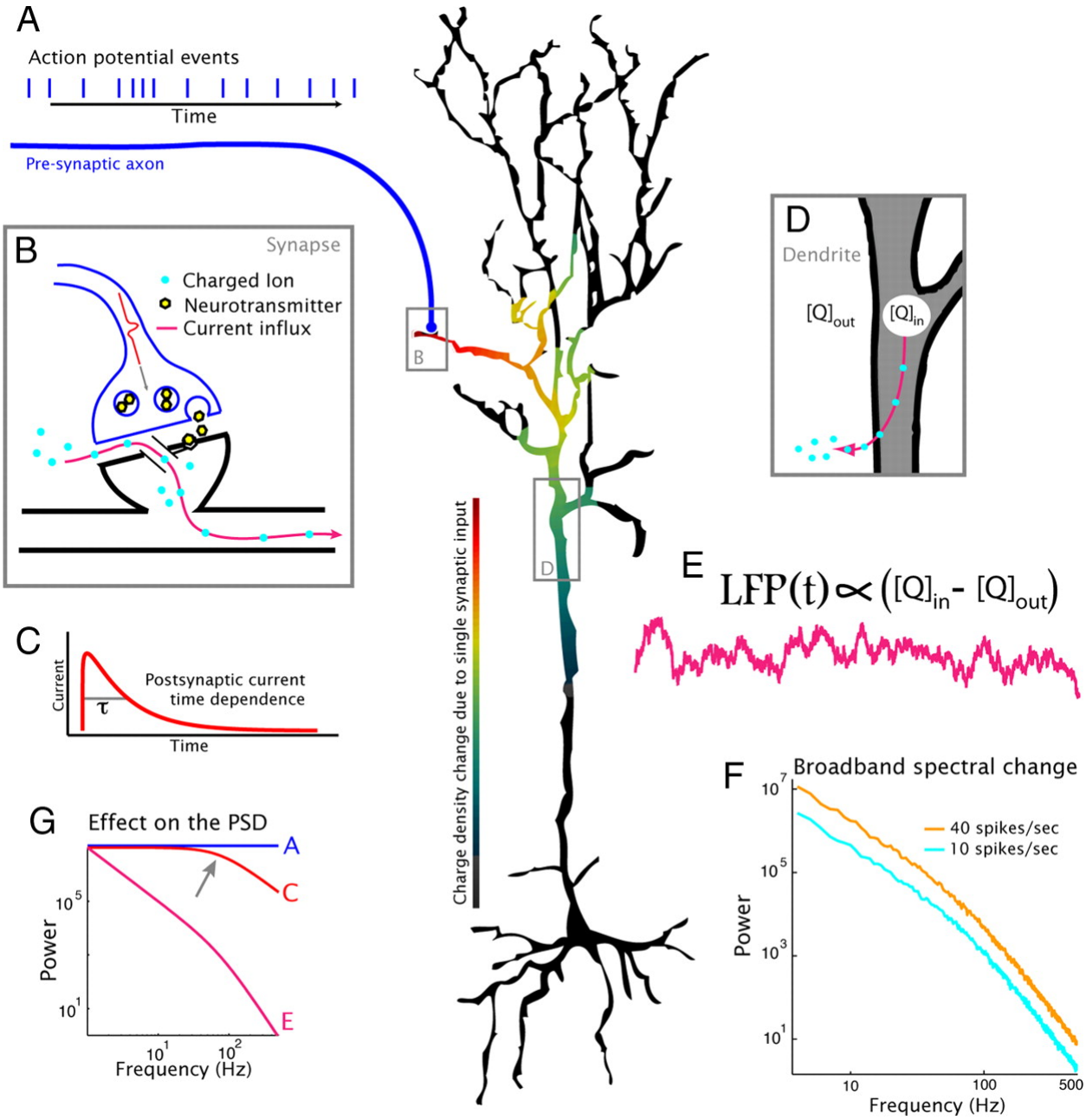

Figure 3.5: **A heuristic model for how broadband spectral increases might emerge from increases in presynaptic action potentials (APs) firing rate.** See text for a full description of the figure. Figure adopted from (Miller, 2010)

.

3.3.1 General Overview

According to the Centers for Disease Control and Prevention (CDC), epilepsy is a serious chronic neurological disorder affecting the life of 2.3 million adults and 467,711

children under 17 years of age in the United States [1]. Although medications and other treatments have been effective in some people with epilepsy, many of them still suffer from seizures that limit their daily activities. Epilepsy surgery is an alternative procedure to treat drug-resistant epileptic patients (i.e., refractory epilepsy). This procedure aims to remove the epileptogenic area with the hope of minimizing or removing epileptic seizures. When epileptic seizures are associated with brain lesion areas previously identified by brain imaging, resection of these areas can lead to seizure control in 60-80% of patients (Spencer and Huh, 2008).

Prior to brain resection, patients typically undergo temporary implantation of subdural electrode arrays for the purpose of localization of the epileptogenic focus and the eloquent cortex. During this procedure, a neurosurgeon first performs a craniotomy to open the patient's skull and then implants the electrode grids and/or electrode strips over the cortex, typically beneath the dura layer. An electrode grid (Ad-Tech Medical Corp., Racine, WI) usually consists of 8 $\times$ 8 platinum- iridium electrodes of 4 mm in diameter (2.3 mm exposed) embedded in silicon, and spaced with an inter-electrode distance of 1 cm. An electrode strip typically consists of 4 to 6 electrodes in a single line. (See Fig. 3.7.)

After electrode implantation, the patient is continuously monitored and his or her brain electrical activity is continuously recorded over a period of 5-12 days to localize the epileptogenic focus. Electrical stimulation is delivered through the electrode array to map eloquent cortex, so that long-term neurological deficits after brain resection can be minimized. At the end of the monitoring and electrical stimulation periods, electrode explantation and brain resection are performed in a single procedure, as shown in Fig. 3.6.

Although the primary purpose of this procedure is clinical, it also provides a new opportunity to acquire human ECoG data for neuroscientific research. All patients who

[1] Morbidity and Mortality Weekly Report (http://www.cdc.gov)

willingly decide to participate in the research protocol, previously approved by the hospital's institutional review board, sign an informed consent. The research protocol for each patient is partly determined by the brain coverage (electrode locations) and the results of the screening procedure (Brunner et al., 2009).

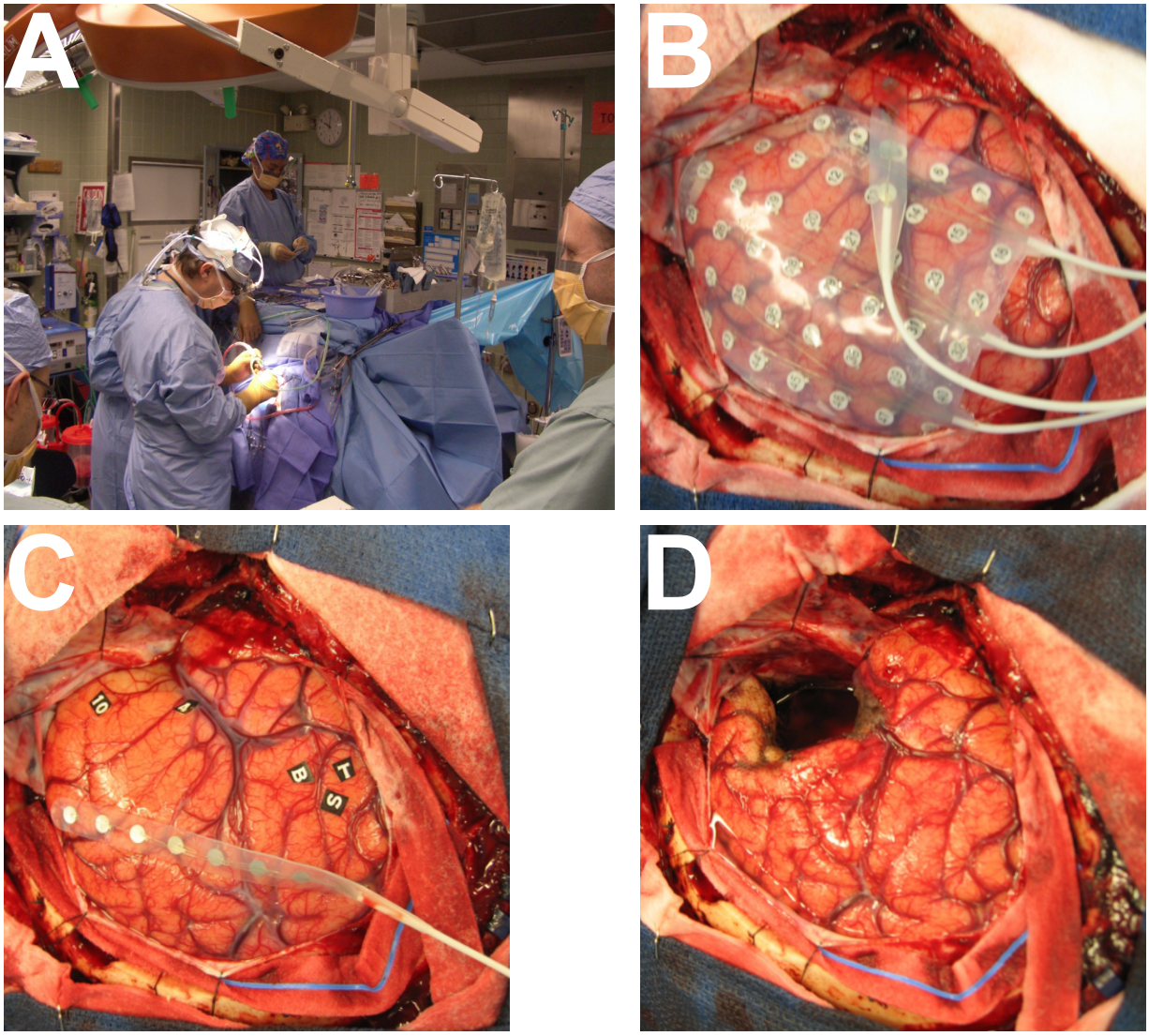

Figure 3.6: **ECoG procedure.** This figure outlines the surgical procedure. (A, B) First, patients undergo temporary implantation of subdural electrode arrays. (C) Second, delineation and label of eloquent cortex using electrical cortical stimulation. (D) Finally, electrode explantation and brain resection of the epileptogenic zone.

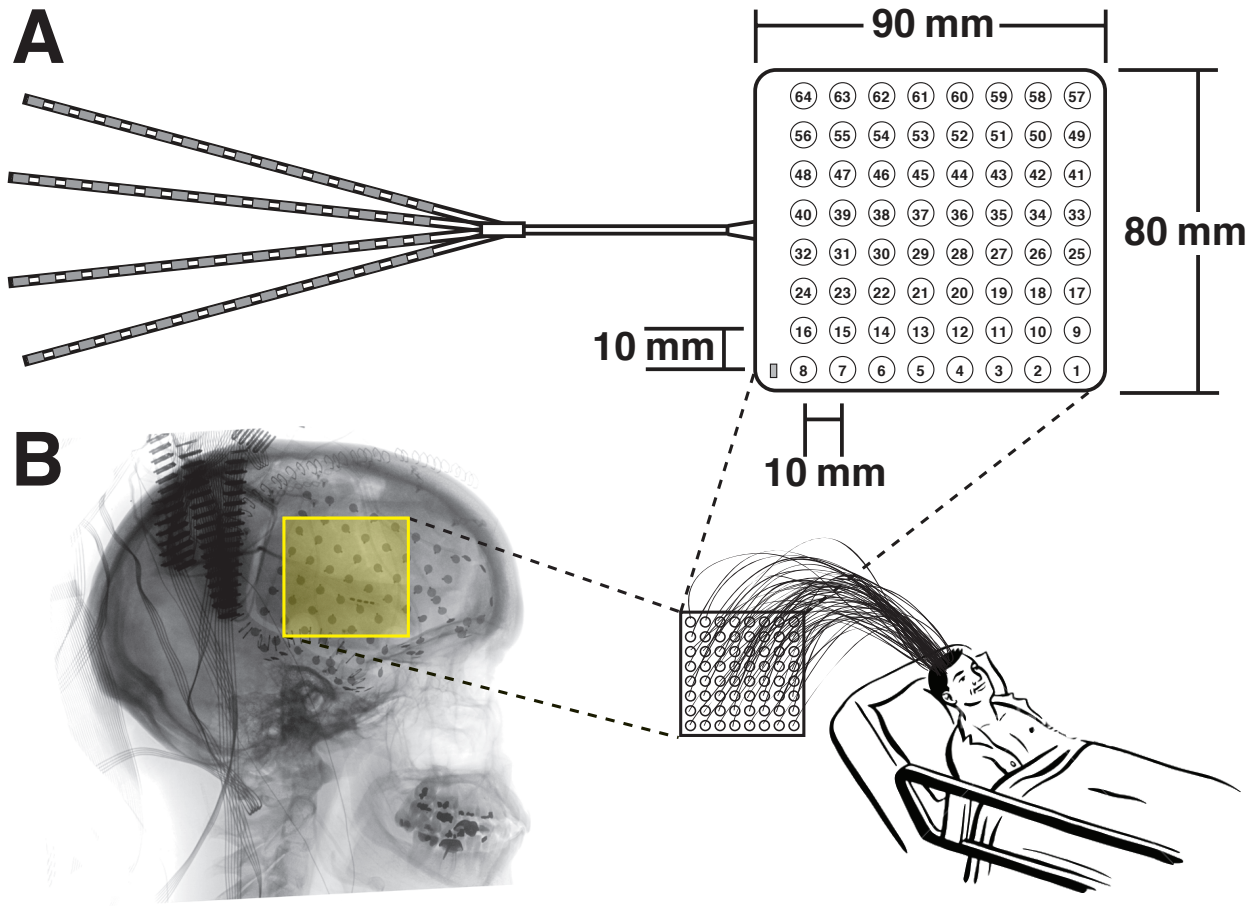

Figure 3.7: **Details of ECoG implant.** This figure shows an electrode grid implanted on the surface of the brain. (A) An 8×8 electrode grid. (B) The electrode grid is sealed under the dura, skull, and scalp, with the cables tunneled through the incision in the dura to exit the scalp.

3.3.2 Brain Model Generation and Electrode Localization

A three-dimensional (3D) subject-specific brain model and an accurate localization of the implanted electrodes are necessary to identify and visualize the functional areas of the brain. To create this brain model and reliably localize each electrode on the subject-specific brain's surface, pre-operative T1-weighted structural magnetic resonance imaging (MRI) (1.5 Tesla (T) or 3T) of the patient's head is collected with the following specifications: 256×256 pixels per slice, full field of view, no interpolation, 1 mm slice width, and preferably sagittal cross-sections. Digital photographs of the electrodes in situ, the neurosurgeon's notes of the location of the electrodes and strips, post-operative skull

X-ray images, and high resolution brain computerized tomography (CT) scans (1 mm slice width, skin to skin, no angle) are also collected. At this point, Curry software (Neuroscan Inc., El Paso, TX) is then used to create a 3D cortical model of the patient's brain as well as to localize the implanted electrodes. These results are then co-registered with the post-operative CT images, skull X-ray images, and digital photographs, as shown in Fig. 3.8.

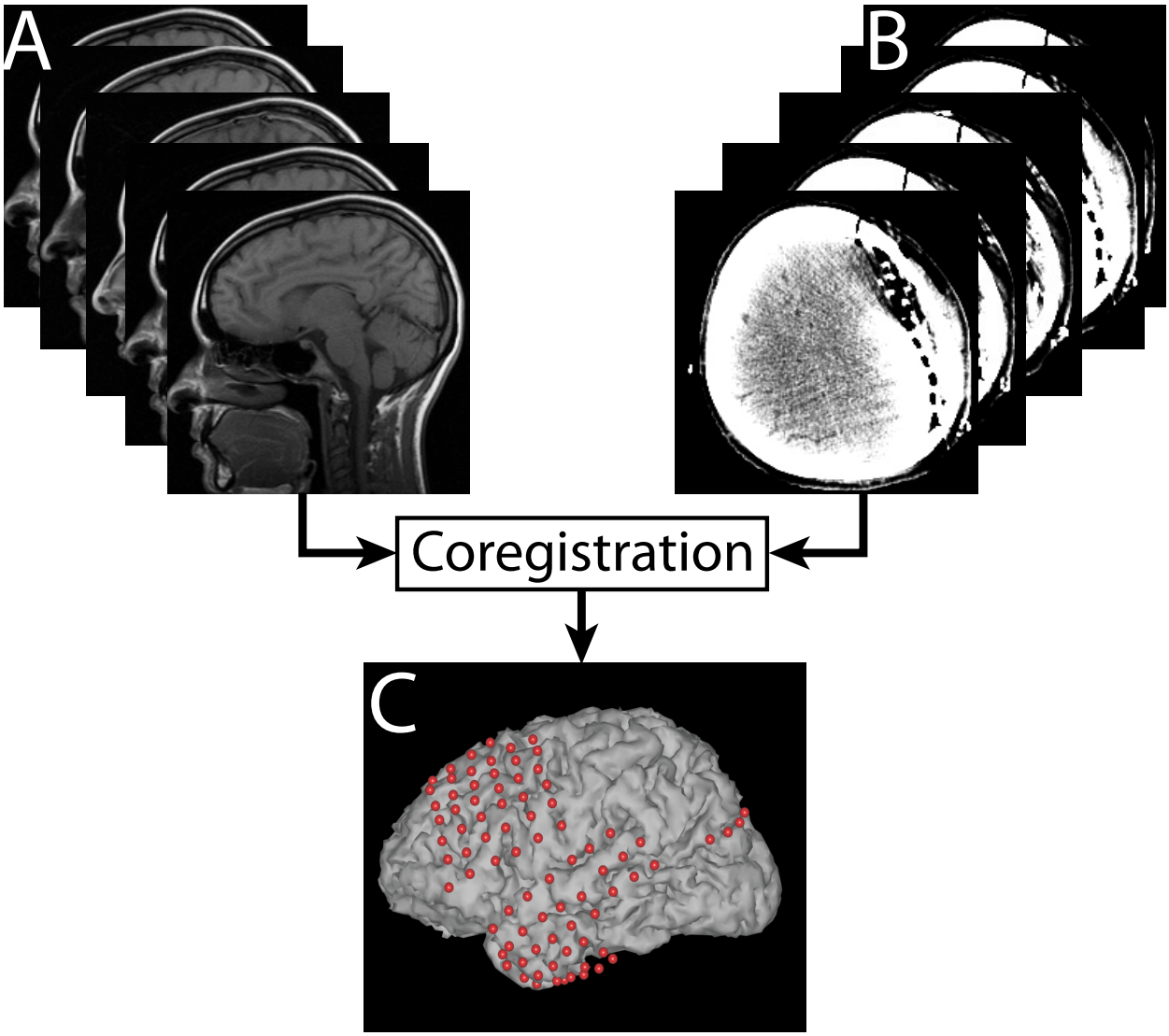

Figure 3.8: **Subject-specific brain model and electrode localization.** This figure illustrates the procedure to generate a subject-specific brain model and to localize the implanted electrodes. (A) Set of magnetic resonance images (MRI). (B) Set of computerized tomography (CT) scans. (C) Brain model generation, coregistration, and electrode localization using Curry software.

3.3.3 Hardware and Software

To record ECoG signals for research purposes without interfering with the clinical recordings, the brain electrical activity measured at the ECoG electrodes is split, in order to feed into the clinical and research systems simultaneously, using splitter connectors depicted in Fig. 3.9a. The clinical system at the Epilepsy Monitoring Unit at the Albany Medical Center in Albany, New York, is a 192-channel Nihon-Kohden Neurofax monitoring system, and the research system consists of eight synchronized 16-channel g.USBamp amplifier/digitizer units (g.tec, Graz, Austria). The research system is FDA-approved for invasive recordings and has a very low noise-floor in the high frequency range. ECoG signals in the research system are typically referenced to an electrocorticographically silent electrode (i.e., a location that was not identified as eloquent cortex), recorded at 1200 Hz, synchronized with stimulus presentation, and stored using BCI2000 software (Schalk et al., 2004; Schalk and Mellinger, 2010). BCI2000 is a general-purpose software system for data acquisition, stimulus presentation, and brain monitoring applications. Since time with the patients to record ECoG data is limited, BCI2000 is an ideal software platform that ensures flexibility, robustness, and the ability to launch an experiment at the touch of a button. BCI2000 is comprised of four modules: an Operator module that provides a graphical interface to the investigator; a Source module that handles the acquisition of the signals; a Signal Processing module that extracts brain features and translates them into output signals; and an Application module that delivers stimuli and provides feedback to the subjects. All these modules communicate with each other via a network-capable protocol, as shown in Fig. 3.9b.

3.3.4 Experimental Session

Before proceeding with any experimental session, it is verified that the signals measured from the implanted electrode array provide useful information about the subject's brain

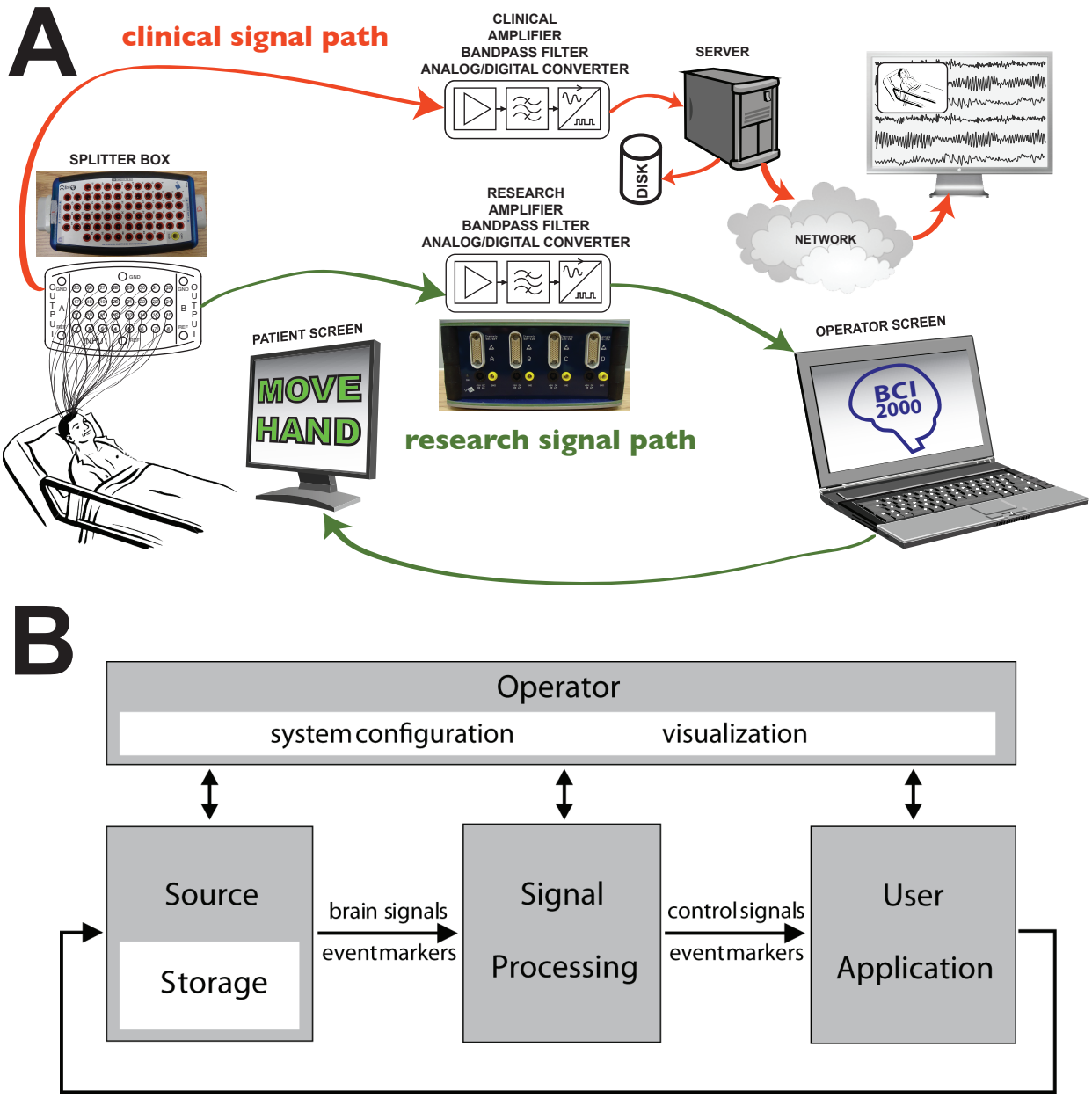

Figure 3.9: **Bedside monitoring systems.** This figure shows the clinical and research monitoring systems used at the Epilepsy Monitoring Unit at the Albany Medical Center. (A) Left, ECoG signals are split, routing signals to the clinical and research amplifiers through a splitter box; Middle, clinical and research biosignal amplifiers; Right, interface to the investigator. BCI2000 software is present only in the research monitoring system. (B) BCI2000 modules.

activity. Verification protocol includes running a real-time screening session consisting of four predetermined tasks (each task lasting for 15 seconds) interleaved with resting periods of the same duration. The subjects are visually cued by the words “hand",

“tongue", “kiss", “listen", or “rest", which are presented on a computer screen. The cue for “hand" prompts the subject to open and close the hand contralateral to the side of the grid placement. The cue for “tongue" prompts the subject to protrude and retract the tongue. The cue for “kiss" prompts the subject to continuously performed lip gestures mimicking. The cue for “listen" prompts the subject to carefully listen to a story. And the cue for “rest" prompts the subject to relax and avoid any movement. One run consists of one repetition of this sequence (hand-rest, tongue-rest, kiss-rest, and listen-rest). It is typical to record one initial run in order to familiarize the subject with the tasks, and five more runs for the screening session (total time of 12 minutes). By the end of the screening session, mapping results of hand/oral motor functions and sensory function are obtained, as shown in Fig. 3.10. These results are the basis for planning the subsequent experiments.

A number of different experiments may be conducted with any given patient. However, they depend on electrode coverage of the patient’s brain, the results of the screening session, the patient’s endurance and willingness to participate, and the patient’s clinical state (e.g., post-operative facial swelling, pain, or discomfort). Patients are notified and instructed about the tasks they would be requested to perform before each experimental session starts. Throughout the session, the patient’s behavior and ECoG signals are continuously monitored for suspected seizures. ECoG data and event markers are recorded and saved using BCI2000.

3.4 Techniques to Analyze ECoG Signals

Electrical signals recorded from the surface of the brain by ECoG are useful for communication, clinical diagnosis, and neuroscience research. However, before these signals can be used, they must first be preprocessed to unmask the underlying neural patterns of interest. After preprocessing, the ECoG signals are then transformed, mainly in the

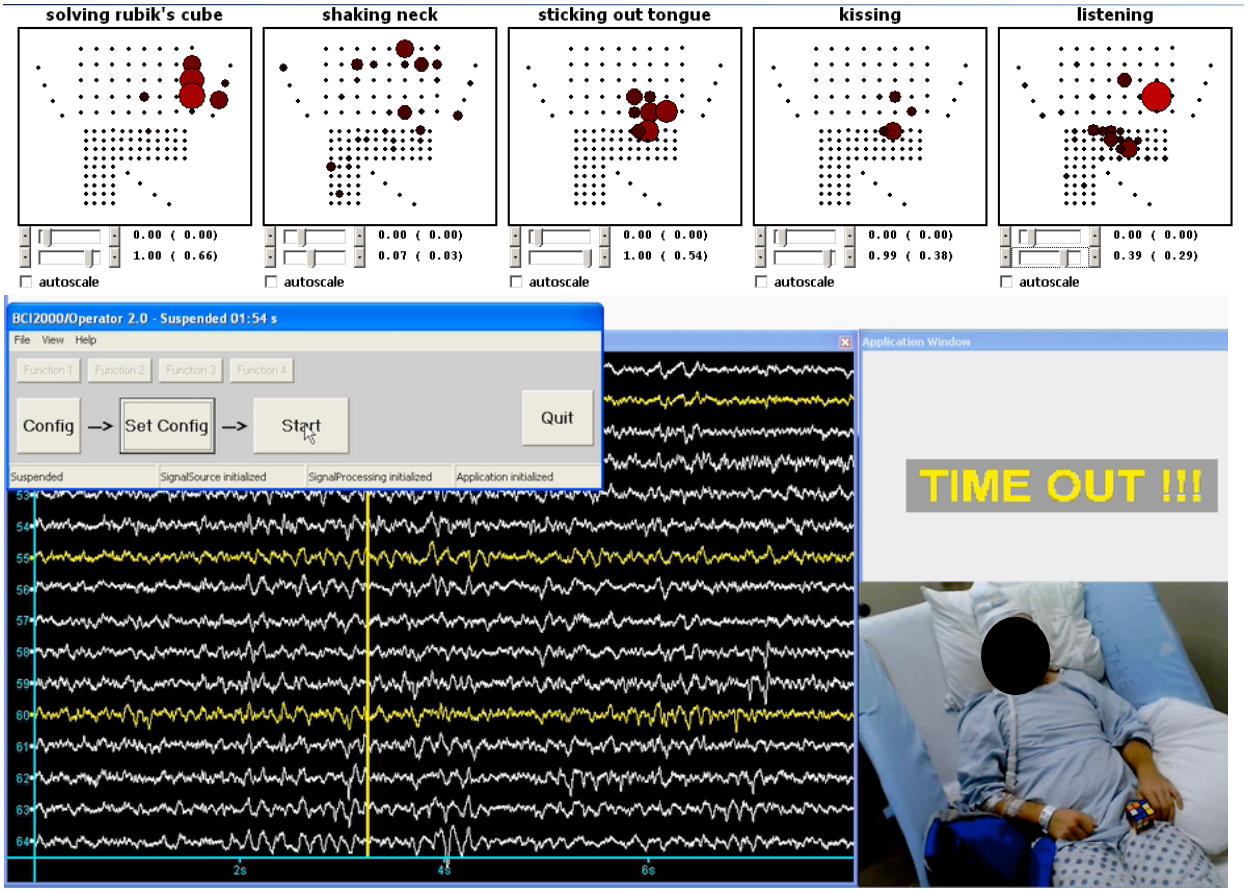

Figure 3.10: **Real-time screening session.** This figure shows the real-time screening session using BCI2000 and SIGFRIED (Signal modeling For Real-Time Identification and Event Detection) (Brunner et al., 2009).

frequency domain, so that task-related features such as the power in the gamma band can then be used for subsequent classification or regression. Further validation of the classification or regression results must be accomplished using statistical analyses.

In this section, the techniques developed to analyze ECoG signals during each of these three stages (i.e., preprocessing, feature extraction, and statistics) are discussed.

3.4.1 Preprocessing

The goal of preprocessing is to increase the signal-to-noise ratio and isolate the signals of interest. ECoG signals are less sensitive to noise and artifacts than are EEG signals. However, ECoG signals can be easily contaminated with power-line noise (e.g., 50-60

Hz) or artifacts (e.g., patient movement or epileptic spikes) that may obscure, distort, or completely misrepresent true underlying brain signals.

The first step in preprocessing is to remove the drift and direct current offset of the ECoG signals. To do this, a zero-phase infinite impulse response (IIR) high-pass filter at 0.1 Hz is applied, using the *filtfilt* Matlab command. The next step, a very commonly used but very subjective approach, is to visually inspect the ECoG recordings. In this step, signals with high spike activity or noise due to a false or broken contact are manually identified and excluded from further analysis.

Next, a common average reference (CAR) spatial filter is applied to enhance local ECoG activity over a single electrode while reducing noise common to all ECoG electrodes. The CAR filter functions as a high-pass spatial filter because it accentuates components with highly focal distributions (Nunez et al., 1994). Line noise or motion artifacts common to all electrodes should be reduced or removed after applying a CAR filter. Nevertheless, in practice, not all ECoG electrodes are contaminated with line noise or motion artifacts. Therefore, a CAR filter must be carefully applied to the data since it could otherwise worsen the quality of the signals (Desmedt et al., 1990; Ludwig et al., 2009).

Let $x_{i,t}$ denote the ECoG signal from electrode i at time t. The output of the CAR filter is then represented as

$$\hat{x}_{i,t} = x_{i,t} - \frac{1}{N}\sum_{i=1}^{N} x_{i,t} \tag{3.1}$$

After applying a CAR filter to the ECoG signals, the power spectral density (PSD) of the signal at each electrode is estimated, using the Welch's overlapped segment averaging estimator (Welch, 1967). Based on each estimated PSD frequency series, electrodes whose signals are still contaminated with line noise are identified and visually inspected for the potential application of a second-order IIR notch filter at 60 Hz and its harmonics.

3.4.2 Feature Extraction

The goal of feature extraction is to transform the recorded and preprocessed ECoG signals into task-related features, as illustrated in Fig. 3.11. The most commonly used features for ECoG are the power of the signal in the mu (8-12 Hz) and gamma (30-170 Hz) frequency bands because these two particular features have been shown to be amplitude modulated during motor, sensory, or cognitive tasks (Crone et al., 2001, 1998a,b).

It is highly desirable to compute these ECoG features in short time windows (e.g., 50-100 ms) to capture and track the high temporal dynamics of neural activity. However, the choice of the length of the window entails a trade-off between temporal resolution and frequency resolution. A short time window provides high temporal resolution at the expense of low frequency resolution. This time-frequency trade-off is the main drawback of power spectrum estimators based on the Fourier transform.

Changes in the power spectrum of the ECoG signal can be estimated using different methods such as digital filters, Welch's periodogram, wavelets, or autoregressive (AR) models. In this dissertation, only digital filters are used to estimate the power of the signal in the two frequency bands of interest. Many other EEG/ECoG studies have used it in similar contexts, with results similar to those obtained with the other estimators (i.e., wavelets, AR).

Digital Filter The simplest and most straightforward approach to estimate the power spectrum of the ECoG signal in a specific frequency band is to use a bank of finite impulse response (FIR) or IIR filters. Since most of the ECoG signal analyses are accomplished off-line, causal filters are not required, and therefore they can be designed to have zero phase response. Zero-phase filters are useful when the ECoG features must be synchronized with the time course of the task (e.g., moving a joystick or listening to music). After filtering the ECoG signals from each electrode with this bank of filters, the envelope in each frequency band is extracted by computing the magnitude of the

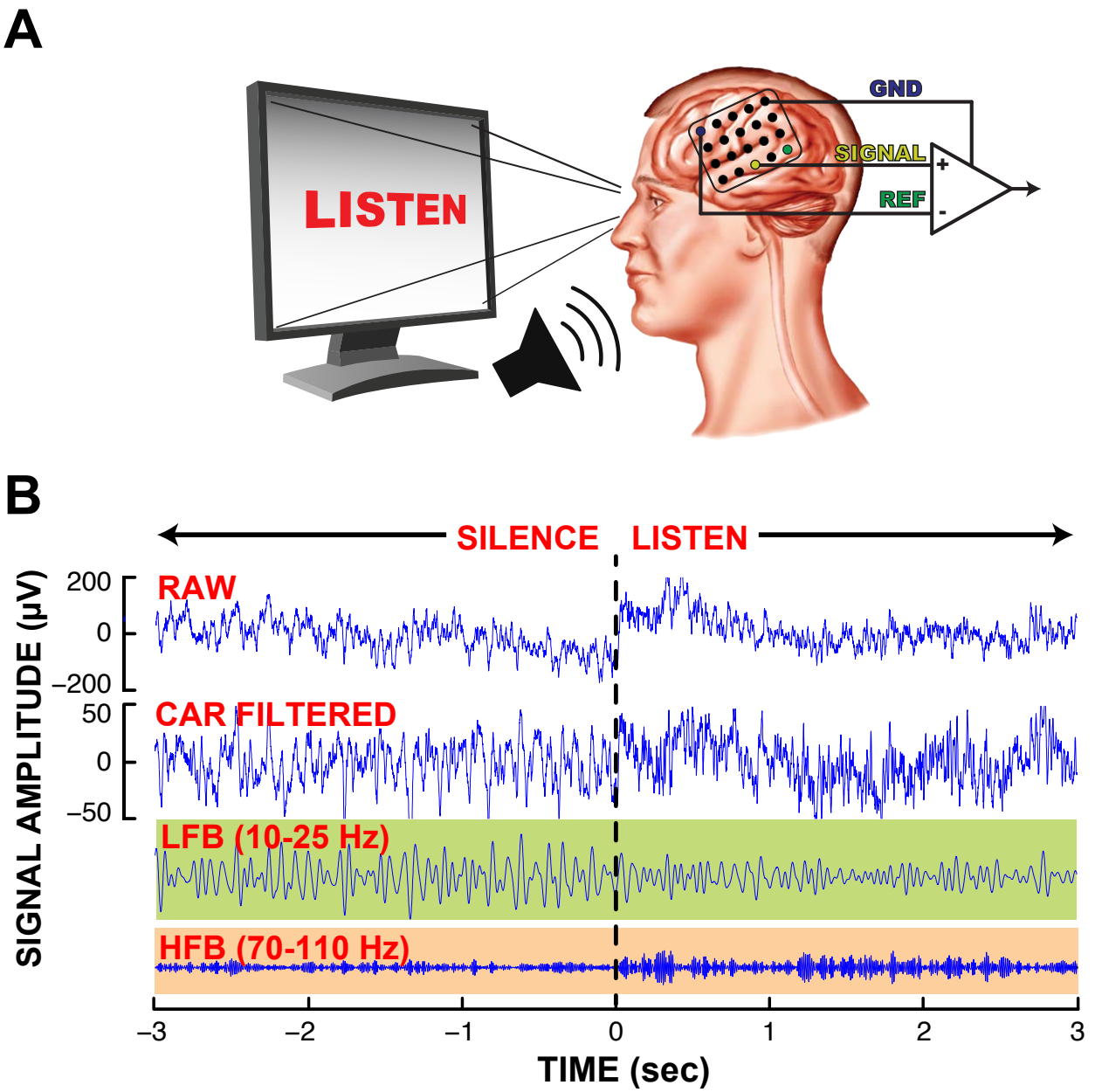

Figure 3.11: **Preprocessing of the ECoG signal.** This figure shows the preprocessing steps necessary to enhance the ECoG features related to the task. (A) After a period of silence, the subject is presented with listening task, while ECoG signals are recorded from the superior temporal gyrus. (B) The task-related modulation of the raw ECoG signals cannot be revealed by visual inspection. However, after CAR filtering and band-pass filtering, the resulting signals reveal the task-related modulation in the low and high frequency bands. From (Brunner, 2013).

analytic signal. The power of the envelope is computed and the result is resampled to 10 Hz. Thereby, an estimate of the power of the signal at each frequency band is obtained

every 100 ms.

Welch's Method Welch's method is used to estimate the power of a signal at different frequencies. Compared to the standard periodogram, Welch's method reduces noise in the estimated power spectra at the expense of reducing frequency resolution. In this method, the signal is split into L segments, using a Hamming window, overlapped by 50%. After this, the squared magnitude of the discrete Fourier transform of each segment is computed and averaged across all L segments to reduce the variance of the individual power measurements. This results in an array of power measurements vs. frequency bins that can be averaged over a frequency band to estimate the power in the bands of interest.

Wavelet Transform Wavelet transform is suitable for analysis of the time-frequency characteristics of nonstationary signals. Compared to power spectrum estimators based on Fourier transforms, wavelets can provide high temporal and frequency resolution simultaneously. This is achieved by using a wavelet function that is shifted along the signal at various scales. The wavelet transform in the continuous case can be seen as a convolution between the signal $x(t)$ with the wavelet function $\psi_{s,\tau}(t)$

$$w(s,\tau) = \int_{-\infty}^{\infty} x(t)\psi^*_{s,\tau}(t)\,dt \tag{3.2}$$

where $\psi_{s,\tau}(t)$ is the wavelet coefficient that corresponds to the frequency associated with the scale s and the time τ of the wavelet function $\psi_{s,\tau}(t)$; where the symbol * indicates the complex conjugate; and where the wavelet function $\psi_{s,\tau}(t)$ is a scaled and shifted version of the mother wavelet $\psi(t)$

$$\psi_{s,\tau}(t) = \frac{1}{\sqrt{s}}\psi\left(\frac{t-\tau}{s}\right) \tag{3.3}$$

Adaptive AR Models An AR model is a linear representation of a random process. The AR model specifies the output as a variable that linearly depends on its previous p values. Mathematically, the AR model of order p of the signal $x(t)$ can be described as

$$x(t) = \sum_{i=1}^{p} a_i x(t-i) + \epsilon(t) \tag{3.4}$$

where a_i is the i-th filter coefficient, and $\epsilon(t)$ is white noise with mean of zero and variance σ^2.

The coefficients of the AR model are usually estimated using the Yule-Walker, Burg, or forward-backward algorithms. The resulting coefficients can then be used to estimate the power spectrum of the ECoG signal $x(\omega)$ as

$$x(\omega) = \frac{1}{\left|1 - \sum_{i=1}^{p} a_i e^{-ji\omega}\right|} \tag{3.5}$$

Selection of the model order p of a given signal is a key factor in reliably estimating the spectrum of the signal. If the model order is too low, the resulting spectrum would be too smooth. In contrast, if the model order is too high, the spectrum would result in spurious peaks. To select the right order of an AR model, the variance σ^2 must be estimated and an order selection criterion (Bayesian information criterion (SBC) or Akaike Information criterion (AIC)) must be evaluated for AR(p) models of successive orders $p_{min} \leq p \leq p_{max}$.

AR spectral estimation provides better frequency resolution for shorter time segments than those based on Fourier Transform (Krusienski et al., 2006). Nevertheless, AR spectral estimation performs poorly when the signal is not stationary (Florian and Pfurtscheller, 1995).

3.4.3 Statistical Analysis

Identifying task-related neural signals is typically accomplished by investigating the statistical relationship between brain activity and a particular aspect of the task (e.g., time course of sound intensity as in (Potes et al., 2012)) or between brain activity across subjects (Potes et al., 2013). The most familiar measure of dependence between two random variables is the Pearson correlation coefficient, which is sensitive only to linear relationships. Other measures of dependence, more sensitive to nonlinear relationships, are Spearman's and Kendall's rank correlation coefficient and mutual information. Unlike the Pearson correlation, these tests are non-parametric, as they do not rely on any assumptions on the distributions of the random variables. In this dissertation, Spearman's correlation and mutual information is used to identify task-related brain activity.

Statistical dependence between two variables does not imply a causal relationship (Aldrich, 1995). Measures of causality such as Granger causality are, therefore, mainly used to estimate causal interactions between brain regions, because they provide a more stringent criterion for information flow rather than just simple correlation with some lag-lead relationship. Section 3.4.3.2 will outline a method to infer causal relationships between neural activity.

3.4.3.1 Measures of Dependence

Pearson Correlation is a measure of the linear correlation between two random variables. Pearson correlation between two variables is defined as the covariance of the two variables divided by the product of their standard deviations. The Pearson correlation coefficient takes on values from -1 to $+1$, indicating perfectly increasing and decreasing linear fits, respectively. The mathematical representation of the Pearson correlation for a sample population of the random variables X and Y is defined as

$$r = \frac{\sum_{i=1}^{n} (X_i - \bar{X})(Y_i - \bar{Y})}{\sqrt{\sum_{i=1}^{n} (X_i - \bar{X})^2}\sqrt{\sum_{i=1}^{n} (Y_i - \bar{Y})^2}} \tag{3.6}$$

where $\bar{X} = \frac{1}{n}\sum_{i=1}^{n} X_i$ and $\bar{Y} = \frac{1}{n}\sum_{i=1}^{n} Y_i$ are the sample means of X and Y, respectively, and n is the total number of samples. In the context of ECoG analysis, X could be gamma features and Y the time course of the task (e.g., finger flexion), or X and Y could be gamma features from two different subjects. The disadvantage of Pearson correlation is that it captures only linear relationships and is very susceptible to outliers. Thus, if any of the random variables X or Y is particularly noisy, the Pearson correlation coefficient could result in a high correlation value, even if the variables are not linearly correlated. Therefore, a measure of dependence less susceptible to outliers and more sensitive to nonlinear relationships is desired in ECoG signal analysis.

Spearman's Correlation measures the relationship between two random variables using a monotonic function. Unlike Pearson correlation, Spearman correlation is less susceptible to outliers since its computation relies on the distribution of the rank of the random variables instead of the raw numbers. Spearman correlation is mathematically defined as the Pearson correlation of the ranked variables (Myers and Well, 2003), and also takes on values from -1 to $+1$.

Kendall's Correlation measures the similarity of the orderings of the data when ranked by each of the quantities. Similar to Spearman's correlation, Kendall's correlation is less susceptible to outliers, does not require the data to be normally distributed, and captures not only linear but also monotonic relationships. Kendall's correlation looks at the difference between the probability that any two points will agree on the relative ranks of the variables compared to the probability that they will disagree. The Kendall's correlation coefficient can be defined as

$$\tau = \frac{\text{Number of concordant pairs} - \text{Number of discordant pairs}}{\frac{1}{2}n(n-1)} \tag{3.7}$$

where the number of concordant pairs is defined as the condition where both $x_i > x_j$ and $y_i > y_j$ or both $x_i < x_j$ and $y_i < y_j$. The number of discordant pairs is defined as the condition where $x_i > x_j$ and $y_i < y_j$, or $x_i < x_j$ and $y_i > y_j$. If $x_i = x_j$ or $y_i = y_j$, the pairs are neither concordant nor discordant. The pairs $(x_1, y_1), (x_2, y_2), \ldots, (x_n, y_n)$ are the observations of the joint random variables X and Y, respectively. Similar to Pearson and Spearman's correlation, Kendall's correlation coefficient takes on values from -1 to $+1$.

Mutual Information measures the mutual dependence between two random variables. It indicates how much information in one random variable X is uncertain knowing the other random variable Y. In other words, the more mutual information between X and Y, the less uncertainty there is in X knowing Y or Y knowing X. Mutual information is most commonly measured in logarithms of base 2 (bits). The mathematical representation of the mutual information between the random variables X and Y is defined as

$$I(X;Y) = \sum_{x \in X} \sum_{y \in Y} p(x,y) log \left(\frac{p(x,y)}{p(x)p(y)} \right) \tag{3.8}$$

where $p(x,y)$ is the joint probability distribution function (pdf) of X and Y, $p(x)$ is the marginal pdf of X, and $p(y)$ is the marginal pdf of Y. Thus, if X and Y are independent random variables, then $p(x,y) = p(x)p(y)$, and I(X,Y) = 0.

3.4.3.2 Measures of Causality

Measures of causality can be used in neuroscience research to identify and quantify causal interactions between brain regions. Current measures of causality based on AR models include bivariate Granger causality, partial directed coherence, and directed

transfer functions. Other measures of causality that are not based on AR models but based instead on information theory are entropy, transfer entropy, and mutual information. The reader is referred to (Greenblatt et al., 2012) for a review of the different methods to measure connectivity in human brain electrophysiological data. The goal of this section is to not compare the myriad of metrics to measure functional connectivity. Rather, focus is placed only on providing the theoretical framework behind Granger causality, which is the metric used to estimate causal interactions between different recordings across subjects, as detailed in Chapter 6.

Granger causality is a statistical test to determine whether one time series is useful in forecasting another (Granger, 1969). Granger causality makes two important assumptions about the data: (1) that it is covariance stationary; and (2) that it can be adequately described by a linear model. If these two assumptions are not met, Granger causality results must be carefully interpreted. Granger causality from Y to X (i.e., $Y \rightarrow X$) exists if adding past values of X and Y (i.e., full model) provide more information about future values of X than when only past values of X (i.e., restricted model) are considered. In the context of ECoG signals, X or Y are time series representing alpha or gamma activity in a particular electrode location and subject. Consider the full model as

$$x(t) = \sum_{i=1}^{p} a_i x(t-i) + \sum_{j=1}^{p} b_j y(t-j) + \epsilon(t) \tag{3.9}$$

and the restricted model as

$$x(t) = \sum_{i=1}^{p} a_i x(t-i) + \eta(t) \tag{3.10}$$

where: $x(t)$ and $y(t)$ are two time series; $\epsilon(t)$ and $\eta(t)$ are white noise with means zeros and variances σ_1^2 and σ_2^2 respectively; p is the maximum number of lagged observations included in the model; and a_i, b_j are the coefficients of the AR models. The value of

σ_1 measures the accuracy of the autoregressive prediction of $x(t)$ based on its previous values and previous values of $y(t)$. In contrast, the value of σ_2 measures the accuracy of the autoregressive prediction of $x(t)$ when only its past values are considered. According to Granger 1969, if σ_1 is less than σ_2, then y(t) is said to have a causal influence on x(t). This causal influence can be quantified as

$$F_{y\to x} = \ln\frac{\sigma_2}{\sigma_1} \tag{3.11}$$

$F_{y\to x} = 0$ when there is no causal influence from $y(t)$ to $x(t)$, and $F_{y\to x} > 0$ when there is.

3.5 Clinical Applications

3.5.1 Real-Time Functional Mapping

Mapping by electrical cortical stimulation (ECS) is the gold standard to identify the eloquent cortex. However, this process is time consuming and can even induce seizures due to the after-discharges produced after stimulation. Thus, a passive functional mapping such as that provided by SIGFRIED (Signal modeling For Real-Time Identification and Event Detection) (Brunner et al., 2009) may be valuable in providing an initial estimate of the eloquent cortex. The SIGFRIED results may be confined or refined with ECS if necessary. SIGFRIED interprets changes in the brain's electrical activity, which is passively recorded from electrode grids that are already implanted in the surface of the patient's brain for clinical purposes. Within minutes, SIGFRIED can identify, on a 2D or 3D topographical display that is updated in real time as the patient performs different tasks, the brain locations in which brain activity changes in response to the task. SIGFRIED and ECS mapping results have exhibited substantial concurrence.

3.5.2 Electrical Cortical Stimulation (ECS)

Electrical cortical stimulation is usually performed in concert with ECoG recording for functional mapping of the cortex and identification of the eloquent cortex. Electrical stimulation is typically delivered between pairs of adjacent electrodes at different frequency and currents, at 2-4 mA for somatosensory stimulation, and near 15 mA for cognitive stimulation. During ECS mapping, the patient must be alert and interactive since the patient must describe sensations, name pictures, read aloud, repeat sentences, and comprehend oral sentences. Identification of the eloquent cortex using this procedure is critical to minimize possible post-operative neurological deficits due to surgical damage to these areas.

3.5.3 Brain Computer Interfaces (BCI)

A brain-computer interface (BCI) uses brain signals to restore some lost function. ECoG is a promising technique for real-world BCI applications for people with motor disabilities. This is mainly due to its higher spatial resolution, better signal-to-noise ratio, wider frequency range, very high communication rates, and less training requirements when compared to scalp-recorded EEG. Recent studies have shown that ECoG allows for accurate single-trial detection of evoked responses, and it thereby supports very high communication rates. The communication rate of ECoG-based P300 BCIs have been shown to be 3-4 times faster than what had previously been reported in EEG-based P300 BCI studies (i.e., 1.4 to 4.5 characters per minute) (Brunner et al., 2011).

3.6 Conclusion

This chapter presented the theoretical background of ECoG. Compared to the characteristics offered by other neuroimaging techniques, ECoG is an excellent compromise between time and spatial resolution and spatial coverage. Because of this, ECoG has

allowed researchers to explore the brain in ways never before possible. Nonetheless, collecting ECoG data for research purposes is not an easy task. It primarily depends on the patient's endurance and collaboration. Time with the patient is a limited resource. Therefore, ECoG experiments must be optimally planned to be executed effectively. Gathering ECoG data also requires a highly multidisciplinary and cooperative team to solve problems in engineering, neuroscience, computer science, neurosurery, neurology, and statistics. Together with regulatory, organizational, and technical difficulties, this situation impedes systematic and controlled studies using large numbers of subjects. Despite these difficulties, ECoG is an emerging technology that has positive impact not only on research but also on pre-surgical epileptic evaluation.

4

Auditory Processing

4.1 Introduction

Human's ears are continuously exposed to different types of sounds. As time passes, certain sounds are associated with certain people or experiences that are faced in daily life. This ability, that is often taken for granted, is accomplished due to complex processes taking place in the auditory system and in the brain. Acoustic signals striking the eardrum are transformed into neural signals that then travel through different structures of the brain to ultimately reach the thalamus and the cortex. It is in the cortex where these signals are then further processed and transformed to allow the perception of sound.

The aim of this chapter is to outline a theoretical framework in auditory processing, so that the reader can grasp the main points discussed in the next two chapters. This chapter is organized as follows: Section 4.2 describes the difference between sound stimulus and perception. Sections 4.3 and 4.4 describe the anatomical structures, functions, and pathways that comprised the auditory and central nervous systems. Section 4.5 describes the areas of the cortex engaged in the perception of sound, mainly loudness and pitch. Finally, Sections 4.6 and 4.7 describe the existing pathways from the thalamus to the cortex as well as from distinct areas of the cortex.

4.2 Sound Stimulus and Perception

Sound is a mechanical wave that causes pressure changes in some medium such as air or water. Sounds in the environment such as those produced by people speaking, machines, and in nature have different amplitudes and frequencies. The amplitude of a sound measures the difference in pressure between the minimum and maximum peaks of the sound wave. The amplitude of a sound is typically measured in decibels (dB) relative to a reference value, which is usually the sound pressure threshold of human hearing at 1KHz (20 μPa). A sound with relative amplitude of 0 dB is barely audible by humans, whereas a sound with relative amplitude of 140 dB, equivalent to the sound generated by a jet engine at takeoff, is extremely loud. Thus, the sound pressure level is closely associated with the perception of loudness. The frequency of a sound refers to how often the particles of the medium vibrate when a wave passes through a medium. The frequency is measured in number of cycles per second (Hz). Humans can perceive frequencies in the range of 20 Hz to 20,000 Hz. The frequency of a sound is closely related to the pitch of a sound. That is, a sound with low frequency is perceived as a sound with low pitch (e.g., the sound of a tuba), whereas a sound with high frequency is perceived as a sound with high pitch (e.g., the sound of a piccolo).

4.3 Peripheral Auditory System

The peripheral auditory system comprises the outer, middle, and inner ear. The main function of this system is to amplify and transduce sound waves into electrical signals. In addition to protecting the inner structures of the ear, the outer brain amplifies the sound waves and then directs them through the external auditory canal. Once the amplified sound waves reach the end of the external auditory canal and make the tympanic membrane vibrate, three small bones in the middle ear (i.e., the ossicles) transduce the air waves coming from the outer ear into fluid waves that propagate inside the liquid

of the cochlea. The cochlea, a main structure of the inner ear, contains specialized cells (inner hair cells) that bend back and forth in response to sound stimulus, thus causing alternating bursts of electrical signals flowing from the cochlear nerve to auditory areas of the cerebral cortex, as demonstrated in Fig. 4.1.

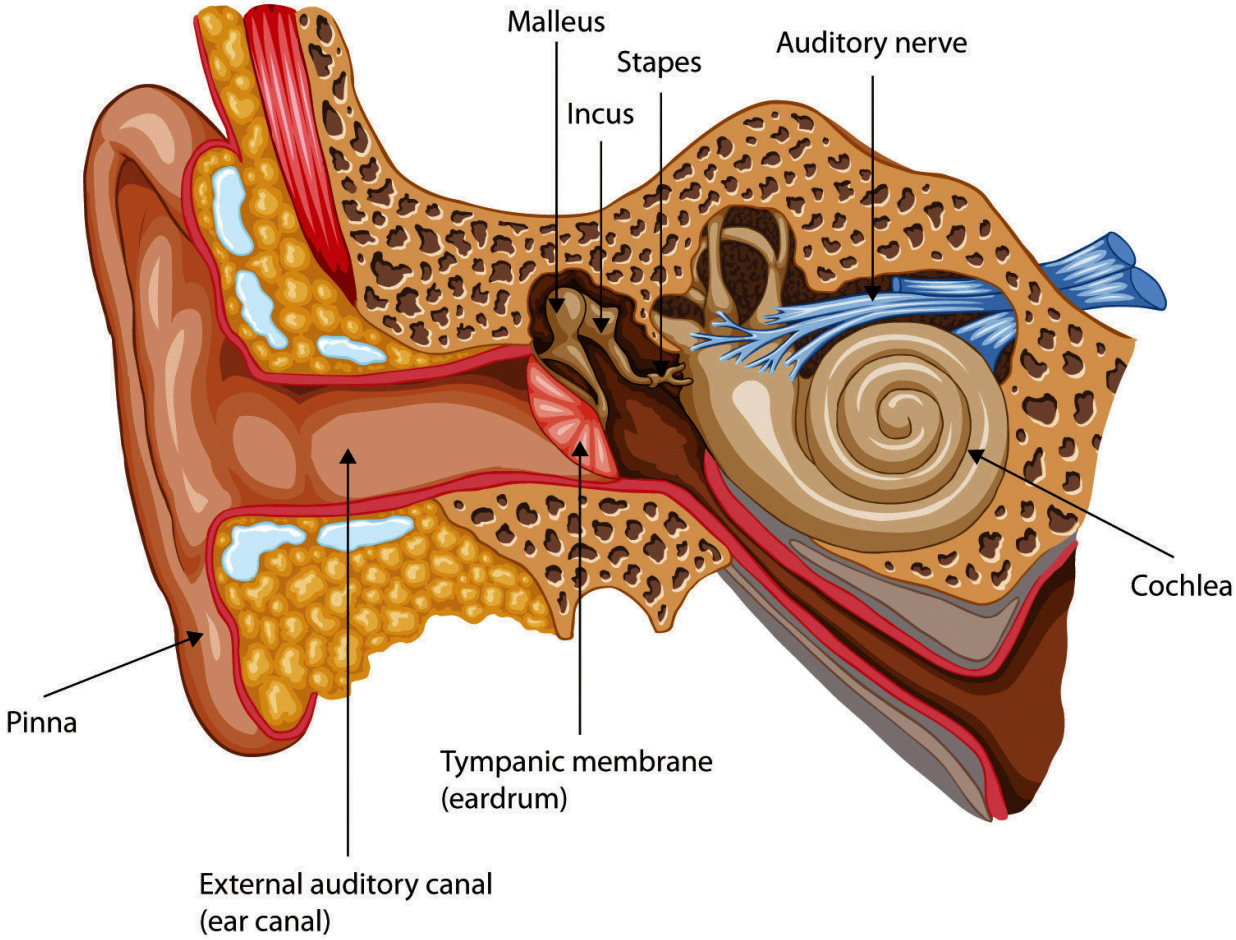

Figure 4.1: **Peripheral auditory system.** This figure shows the parts of the human ear: the outer, middle, and inner ear. The sound waves first reach the outer ear to then be amplified and transmitted to the eardrum through the auditory canal. The ossicles (i.e., malleus, incus, and stapes) transduce the sound vibrations into fluid waves that propagate inside the liquid of the cochlea. The hair cells respond to these vibrations by transmitting electrical signals through the cochlear nerve. Figure reproduced from (Stangor, 2010).

4.4 Central Auditory System

The central auditory system comprises the cochlea and subcortical and cortical structures of the brain. The main function of the central auditory system is to transmit electrical signals that contain information about the sound stimulus from the cochlea to auditory receiving areas in the cortex. The electrical signals generated by the hair cells leave the inner ear through the cochlear nerve to sequentially synapse with different subcortical structures of the brain (see Fig. 4.2). The first subcortical structures to synapse with are the cochlear and superior olivary nuclei. The axons of the cochlear nerve bilaterally project to the cochlear nucleus and then continue to the superior olivary nucleus. Both nuclei are tonotopically organized (i.e., organized according to the frequency information of the sound stimulus). From the superior olivary nucleus, auditory signals continue traveling to the inferior colliculus and the medial geniculate nucleus of the thalamus. This thalamic nucleus is also tonotopically arranged and plays a key role in relaying auditory information to auditory cortical areas.

4.5 Cortical Areas Related to Auditory Perception

Auditory objects might be seen as acoustic features produced by different sound sources (e.g., voice or musical instruments) that can be perceptually correlated to human brain responses (e.g., loudness and timbre). Auditory perception of these acoustic features has been extensively studied using several neuroimaging techniques (Bendor and Wang, 2005, 2006; Bilecen et al., 2002; Jäncke et al., 1998; Johnsrude et al., 2000; Langers et al., 2007; Penagos et al., 2004; Potes et al., 2012; Zatorre, 1988).

Loudness perception has been closely associated with the temporal features of the sound stimulus (e.g., sound intensity) (Jäncke et al., 1998; Langers et al., 2007; Potes et al., 2012). Langers et al. 2007 and Jäncke et al. 1998 used fMRI in humans to study brain cortical responses during sound stimulus at different intensities. Both studies

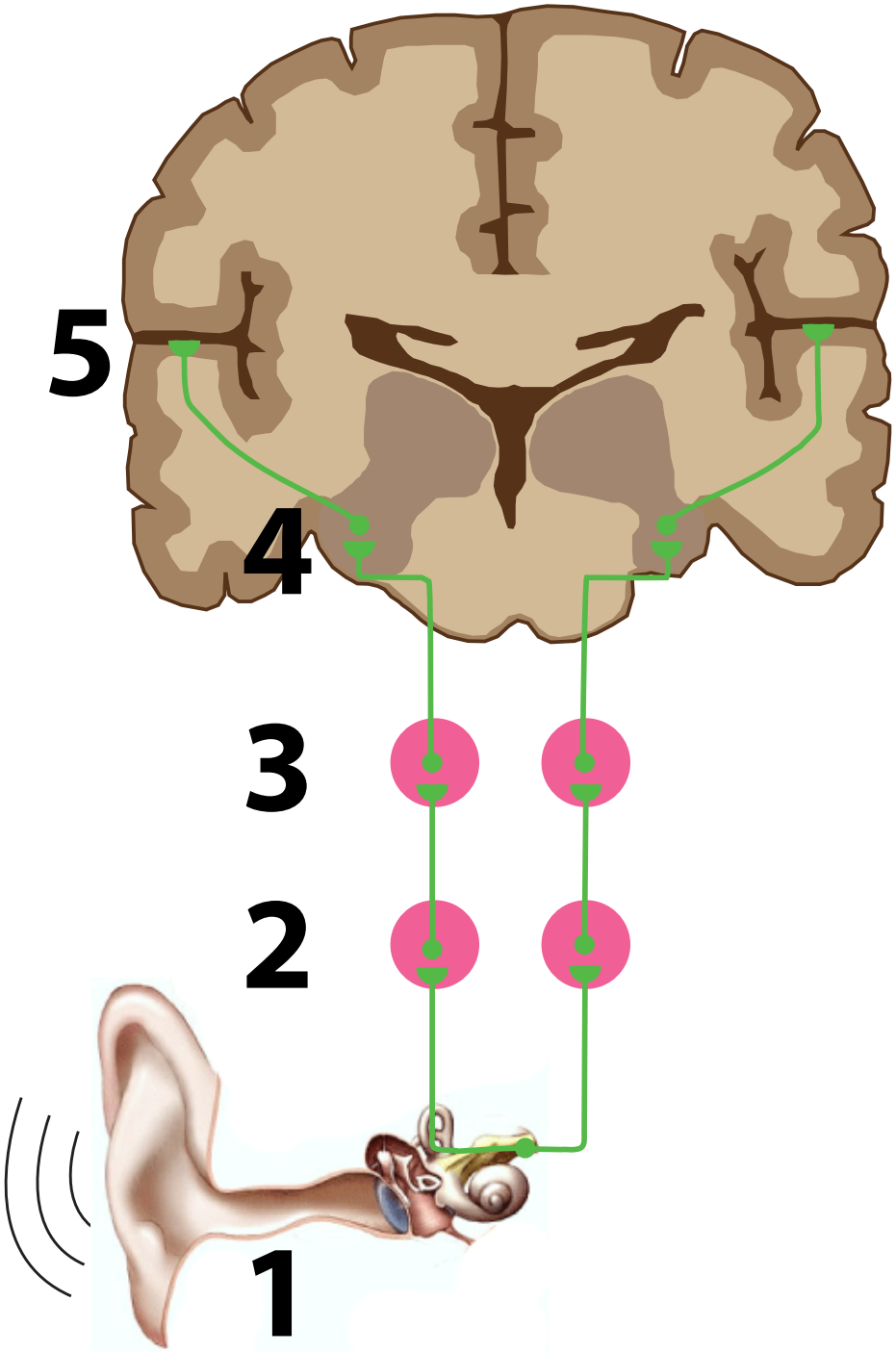

Figure 4.2: **Central auditory system.** This figure shows the subcortical and cortical structures involved in auditory processing (Zatorre et al., 2002). (1) cochlear nerve, (2) superior olivary nuclei, (3) inferior colliculus, (4) medial geniculate nuclei, (5) primary auditory cortex.

showed linear increments in blood flow as sound intensity level linearly increases. Increments in blood flow were mainly located in the Heschl's gyrus and in the primary and secondary auditory cortices (Brodmann area (BA) 41, 42). In a similar study, Bilecen et al. 2002 reported drift activations from ventral to dorsal and from lateral to medial in the transverse temporal gyrus as sound intensity increases. Recently, Potes et al. 2012 reported that ECoG activity recorded from the posterior part of the superior temporal gyrus as well as from an isolated area in the precentral gyrus was highly correlated with the sound intensity of the music.

Pitch perception, on the other hand, has been closely associated with the frequency features of the sound stimulus (Bendor and Wang, 2005, 2006; Johnsrude et al., 2000; Penagos et al., 2004; Zatorre, 1988). Auditory studies in animals have shown that neurons lateral to the primary auditory cortex are sensitive to changes in pitch (Bendor and Wang, 2005, 2006). This view has been also supported by human lesion and fMRI studies (Johnsrude et al., 2000; Penagos et al., 2004; Zatorre, 1988), suggesting that Heschl's gyri and surrounding cortex in the right cerebral hemisphere are important in extracting the pitch from a complex auditory stimulus.

4.6 Corticocortical Pathways

From an anatomical perspective, the auditory cortex can be defined as those areas of the cortex that receive significant input from the medial geniculate nucleus of the thalamus (Hackett, 2011). Although in humans it remains unclear which areas of the cortex receive direct input from this thalamic nucleus, recent neuroimaging and electrophysiological studies generally agree that human auditory cortex mostly comprises the superior temporal cortex (including Heschl's gyrus), the planum temporale, and the posterior superior temporal gyrus. (See Fig. 4.3.)

For decades, most auditory research focused on studying the primary auditory cor-

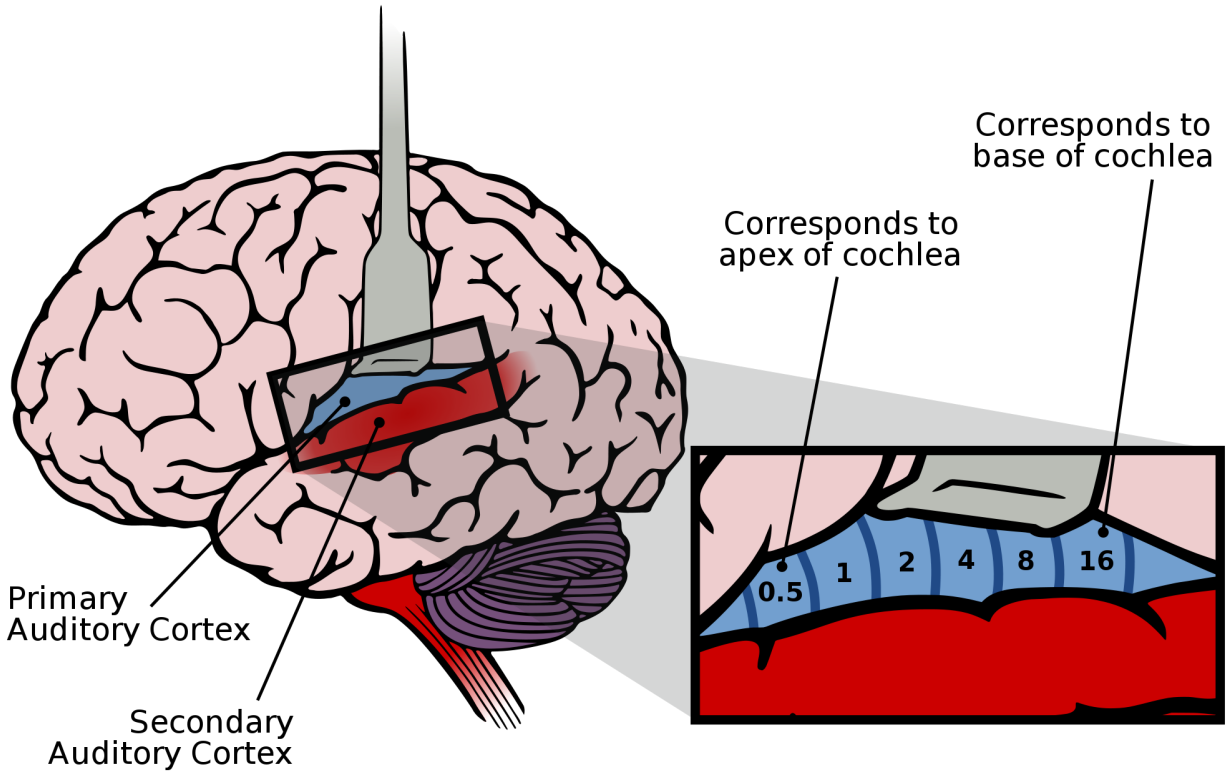

Figure 4.3: **Primary and secondary auditory cortex.** This figure shows the primary and secondary auditory cortex. The primary auditory cortex is organized tonotopically (i.e., sounds are organized according to the frequency). Figure reproduced from (Chittka and Brockmann, 2005).

tex. Now, however, with the advance of new neuroimaging techniques, more recent studies have discovered additional auditory-related areas, extending beyond the auditory cortex, that play a key role in complex auditory processing. For instance, cortical areas such as the auditory association area (Brodmann area 42), posterior and inferior parts of the superior temporal gyrus, and premotor area have been found to be activated during the processing of complex auditory stimulus such as music or speech (Potes et al., 2012).

This important neuroscientific advance has allowed researchers to devise novel models of cortical auditory processing. These models propose that auditory information is processed by an interconnected network in which auditory areas are organized in a multilevel hierarchy. Similar to the visual dual-pathway model, the auditory dual-pathway

model proposes two largely segregated processing streams useful for identification of objects and localization of sounds in space (Rauschecker, 1998; Rauschecker and Scott, 2009; Rauschecker and Tian, 2000; Zatorre et al., 2007). This model suggests that after auditory information reaches the primary auditory cortex, it then travels along the superior temporal gyrus to follow two main streams: ventral and dorsal. The ventral stream, also known as the *"what"* stream, starts in the anterior part of the temporal cortex and then extends to prefrontal areas. This stream is thought to be specialized for processing auditory objects that are invariant in time (Warren et al., 2005; Zatorre et al., 2004). In contrast, the dorsal stream, also known as the *"where"* stream, starts in the posterior part of the temporal cortex and extends to the parietal and prefrontal cortices. The dorsal stream has been shown to be relevant for sound localization and for tracking time-varying auditory objects (Griffiths and Warren, 2002; Zatorre et al., 2007). Recent research has postulated this stream as a mechanism to decompose and process auditory-motor information (Zatorre et al., 2007). In this view, it is thought that the posterior superior temporal gyrus (STG) plays an important role in decomposing the various types of sound and integrating those of motor relevance with the prefrontal, premotor, and motor regions through the dorsal stream (Griffiths and Warren, 2002).

4.7 Thalamocortical and Corticothalamic Pathways

Reciprocal neural interactions between thalamus and cortex provide a gain control mechanism in the transmission and modulation of information from the periphery to the cortex (Lee, 2012; Lee and Sherman, 2008, 2009; Ryugo and Weinberger, 1976; Sherman and Guillery, 2002). It was thought that the role of the thalamus was just to convey information from the periphery to primary cortical areas. This simplistic view of the thalamus has now evolved into a more multifaceted view, including roles in modulating intracortical activity and in synchronizing widespread cortical activity (Lee and Sherman, 2008,

2009).

Auditory information is conveyed from the cochlear nerve to the thalamus and then to the primary auditory cortex. From there, the conventional view is that information is processed along a hierarchical series of corticocortical projections. Complementary to this view, Lee 2012; Lee and Sherman 2008, 2009 suggest that higher-order thalamic nuclei (i.e., the dorsal division of the medial geniculate nucleus (MGN)) mediates transfer of information from one cortical area to the next via a corticothalamocortical pathway.

Evidence from animal studies suggests that the MGN is subdivided into the ventral, dorsal, and medial divisions (Calford and Aitkin, 1983; Lee and Sherman, 2008; Winer, 1984). The ventral division receives tonotopic inputs from the central nucleus of the inferior colliculus and projects to primary auditory cortical areas. The dorsal division receives non-tonotopically inputs from the dorsal cortex of the inferior colliculus and projects primarily to secondary non-tonotopic auditory areas. Finally, the medial division receives non-tonotopic and polymodal inputs from the lateral cortex of the inferior colliculus and projects to all areas of auditory cortex.

The ventral and dorsal divisions of the MGN are anatomically and physiologically similar. Both divisions project to cortical layers 4 and 6 of the primary and secondary auditory cortices, respectively, as shown in Fig. 4.4. These anatomical and physiological findings suggest that the non-tonotopic thalamocortical connections coupled with the descending feedforward connections from layer 5 of the primary auditory cortex to the dorsal division of the MGN establish a potential alternate route for information flow between cortical areas (Lee, 2012).

Therefore, processing of low- and high-level aspects of the auditory stimulus is not only carried out by corticocortical interactions but also by reciprocal communication between the thalamus and cortex.

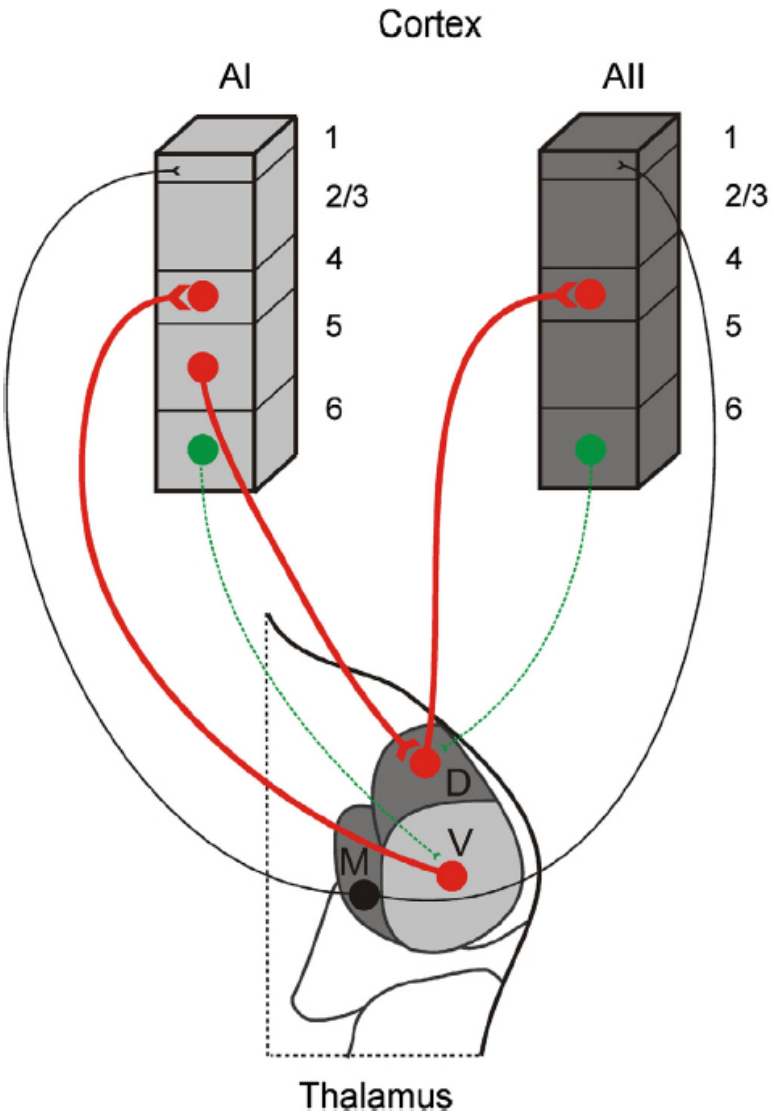

Figure 4.4: **Thalamocortical connections mediating higher order auditory processing**. Primary auditory cortex (AI) receives ascending information from the ventral division of the MGN ending in layer 4, while the secondary auditory cortex (AII) receives information from the dorsal division of the MGN (red thick lines). Feedforward corticothalamic projections from layer 5 (red lines) of AI establish a corticothalamocortical route for information transfer between AI and AII. In contrast, feedback corticothalamic projections from layer 6 of AI and AII are not primary conduits of information flow, but rather modulate thalamic activity in the ventral and dorsal divisions of the MGN, respectively (green dashed lines). Calbindin-expressing neurons in the medial division of the MGN project widely to multiple cortical areas (black thin lines), targeting apical dendrites in layer 1 primarily. These projections have the potential to synchronize activity across broad cortical territories. Light gray shading (tonotopic nuclei and areas), dark gray shading (non-tonotopic nuclei and areas). Figure reproduced from (Lee, 2012)

.

4.8 Conclusion

This chapter provides the reader with the theoretical basis of auditory processing. The different structures of the ear and brain make humans capable of perceiving the distinct physical characteristics of sound and, more importantly, understanding the meaning of spoken words. By the physical characteristics of a song, humans can perceive its loudness, pitch, timbre, or rhythm and decide whether it is pleasant or not. Moreover, certain songs are remembered and linked to specific life experiences. If the song has lyrics, the spoken words can be interpreted and their meaning understood. Despite the great advances in auditory processing, how the brain is capable of executing all these amazing functions is still unknown. The aim of the next two chapters is to shed light on this matter, particularly in understanding the neurophysiological processes during music processing.

5

ECoG Activity during Listening to Music

5.1 Introduction

The neural substrates underlying the processing of complex sounds, such as voice or music, have not yet been fully elucidated (Griffiths and Warren, 2004; Kumar et al., 2007; Leaver and Rauschecker, 2010; Zatorre et al., 2004). Many studies on music perception and auditory processing have focused on the low-level acoustic features that compose complex sounds. For instance, loudness perception was found to be correlated to temporal acoustic features (e.g., sound intensity) within an auditory stream (Platel et al., 1997; Reiterer et al., 2008; Zatorre and Belin, 2001). Auditory processing of these acoustic features (i.e., sound intensity) has been extensively studied using functional magnetic resonance imaging (fMRI), positron emission tomography (PET), and scalp-recorded electroencephalography (EEG). These studies have identified cortical representations of sound intensity processing mainly in the primary and secondary auditory cortices (Jäncke et al., 1998; Langers et al., 2007; Mulert et al., 2005). fMRI (Jäncke et al., 1998; Langers et al., 2007) or combined fMRI/EEG studies (Mulert et al., 2005; Thaerig et al., 2008) found a linear relationship between blood flow or electrical activity in the primary auditory cortex and sound intensity level. Other studies (Brechmann et al., 2002;

Hart et al., 2003; Tanji et al., 2010; Yetkin et al., 2004) showed a relationship between sound intensity and the spatial extent of BOLD activations in the auditory cortex.

All these studies cited in the previous paragraph investigated brain responses to specific static features of simple auditory stimuli. Despite this body of work, it is unclear to what extent brain signals encode dynamic acoustic features (such as the time course of sound intensity) in a continuous stream of music. Functional neuroimaging techniques (e.g., fMRI or PET) depend on metabolic processes (such as the hemodynamic response) and therefore measure signals that are produced by neuronal mass activity (Logothetis, 2008). These techniques cannot readily differentiate between different underlying physiological processes (such as local cortical processing vs. large-scale oscillatory activity) and have low temporal resolution (Aine, 1995; Shibasaki, 2008). On the other hand, EEG recordings provide electrophysiological measurements with high temporal resolution, but cannot capture local cortical processing that is reflected in high frequency field potentials, and also suffer from low spatial resolution (Nunez and Srinivasan, 2005). For instance, a recent EEG study by (in Schaefer et al., 2010) was able to differentiate seven different musical fragments based on single-trial event-related potentials. However, they could not accurately localize functionally significant areas due to the low spatial specificity of scalp recordings.

Electrocorticographic (ECoG) recordings from the surface of the brain combine high temporal resolution with relatively high spatial resolution. ECoG activity in the high gamma range (i.e., ∼70-170Hz) is generally regarded as an accurate indicator of local cortical processing. For example, ECoG has been found to reflect higher-order auditory processing (Boatman-Reich et al., 2010; Crone et al., 2001; Edwards et al., 2005, 2009; Sinai et al., 2009) and aspects of speech or auditory perception (Crone et al., 2001; Edwards et al., 2009; Lachaux et al., 2007a; Pasley et al., 2012; Ray et al., 2003; Sinai et al., 2009). Nevertheless, which ECoG features and locations encode dynamic aspects of acoustical features in continuous music has remained unknown.

The goal of this study was to determine the ECoG features and the cortical regions that are related to sound intensity of continuous music. Results from eight human subjects demonstrate, for the first time, that ECoG high gamma activity recorded from auditory and premotor and motor cortices accurately reflect the time course of the music's sound intensity.

5.2 Materials and Methods

5.2.1 Subjects and Data Collection

The subjects in this study were eight patients with intractable epilepsy (four women and four men) who underwent temporary implantation of subdural electrode arrays for the purpose of localization of seizure foci prior to surgical resection. Table 6.1 summarizes the subjects' clinical profiles. All of the subjects gave informed consent to participate in the study, which was approved by the Institutional Review Board of Albany Medical College. Preoperative Wada testing (Wada and Rassmussen, 1960) determined language lateralization to the left hemisphere in subjects A, B, C, D, E, and G; and bilateral language dominance in subject F. Language lateralization was not determined for subject H. None of the subjects had a history of hearing impairment. The implanted electrode grids (Ad-Tech Medical Corp., Racine, WI) consisted of platinum-iridium electrodes that were 4 mm in diameter (2.3 mm exposed), embedded in silicon, and were spaced with an inter-electrode distance of 1 cm. (The temporal lobe grid of subject F had electrodes with a 6 mm inter-electrode distance.) The total number of implanted electrodes were 99, 96, 83, 109, 58, 120, 58, and 59 for subjects A to H, respectively. Grid placement and duration of ECoG monitoring were based solely on the requirements of the clinical evaluation without any consideration of this study. Each subject had postoperative anterior-posterior and lateral radiographs, as well as computer tomography (CT) scans to verify grid locations (see Figure 5.1).

Table 5.1: **Clinical profiles of the subjects that participated in the study.** All of the subjects had normal cognitive capacity and were functionally independent. Language lateralization (LL) was based on the Wada test.

Subject	Age	Sex	Handedness	LL	Seizure Focus	Grid Locations	# of Elec.
A	24	M	R	L	Right temporal	Right fronto-parietal	64
						Right temporal	35
B	29	F	R	L	Left temporal	Left fronto-parietal	64
						Left temporal	23
						Left temporal pole	3
						Left occipital	6
C	30	M	R	L	Left temporal	Left frontal	40
						Left temporal	35
						Left temporal pole	4
						Left occipital	4
D	26	F	R	L	Left temporal	Left frontal	64
						Left temporal	35
						Left temporal pole	4
						Left occipital	6
E	45	M	R	L	Left temporal	Left fronto-temporal	54
						Left temporal pole	4
F	29	F	R	Bilateral	Left temporal	Left frontal	40
						Left temporal	68
						Left temporal pole	4
						Left orbital pole	4
						Left occipital	4
G	45	F	L	L	Left temporal	Left frontal	31
						Left temporal	27
H	60	M	R	NA	Left temporal	Left temporal	17
						Left parieto-occipital	42

The subjects were instructed to listen attentively to the song "Another Brick in the Wall - Part 1" (Pink Floyd, Columbia Records, 1979) while ECoG activity was recorded using the general-purpose software BCI2000 (Schalk et al., 2004; Schalk and Mellinger, 2010) that was connected to eight g.USBamp biosignal acquisition devices (g.tec, Graz, Austria). The song was 3:10 minutes long, digitized at 44.1 kHz in waveform audio file format, and binaurally presented to each subject using in-ear monitoring earphones (12 to 23.5 kHz audio bandwidth, 20 dB isolation from environmental noise). The sound volume was adjusted to a comfortable level for each subject.

ECoG signals were referenced to an electrocorticographically silent electrode (i.e., a

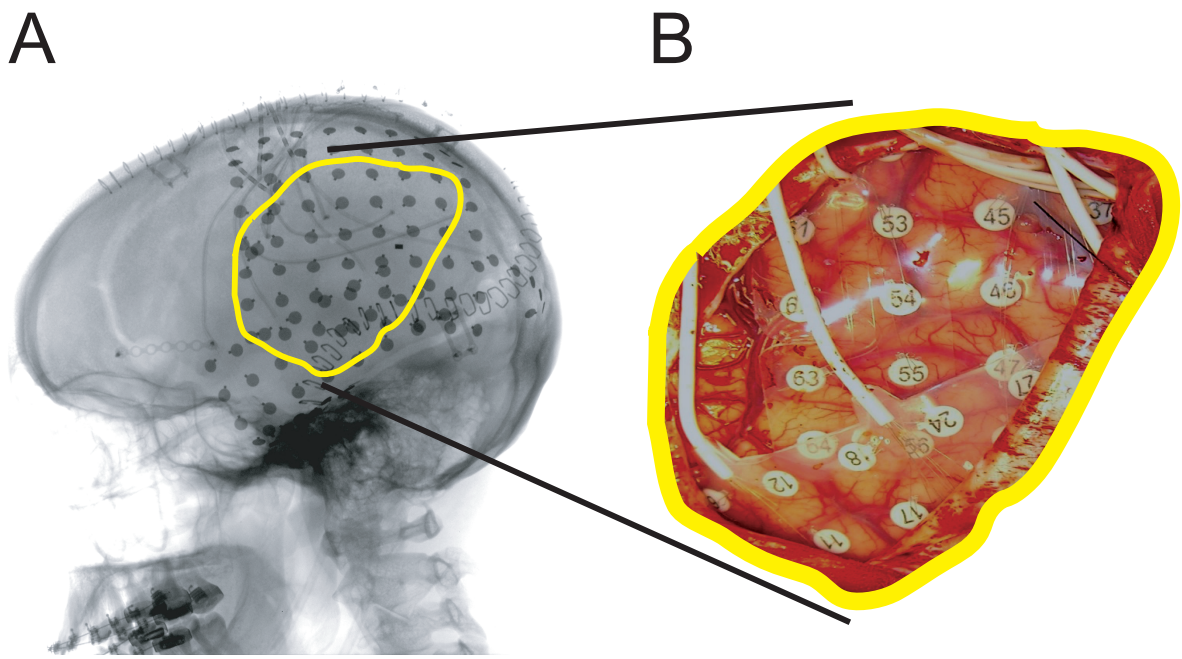

Figure 5.1: **ECoG implant.** Example of an implanted subdural grid in Subject B. (A) Lateral radiograph indicating grid position. (B) Subdural grid placed over left fronto-parietal and temporal lobes.

location that was not identified as eloquent cortex by electrocortical stimulation mapping), digitized at 1200 Hz, synchronized with stimulus presentation, and stored with BCI2000. The recordings were visually inspected offline for environmental artifacts and interictal activity. Channels that did not clearly contain ECoG signals were removed from further analyses, which left 97, 86, 82, 104, 56, 108, 57, and 53 channels for subjects A to H, respectively.

5.2.2 Cortical Mapping

Curry software (Neuroscan Inc., El Paso, TX) was used to create subject-specific 3D cortical brain models from high-resolution pre-operative magnetic resonance imaging (MRI) scans. MRIs with post-operative computer tomography (CT) images were co-registered. For each grid electrode, the stereotactic coordinates and functional area according to the Talairach Atlas (Lancaster et al., 2000) were extracted. 3D cortical template provided

by the Montreal Neurological Institute (MNI) [1] was used for cross-subject analysis and for subject A analysis, whose brain model was not available. Finally, the electrode locations were projected onto the subject-specific brain models shown in Figure 5.2 to render activation maps using custom MATLAB software.

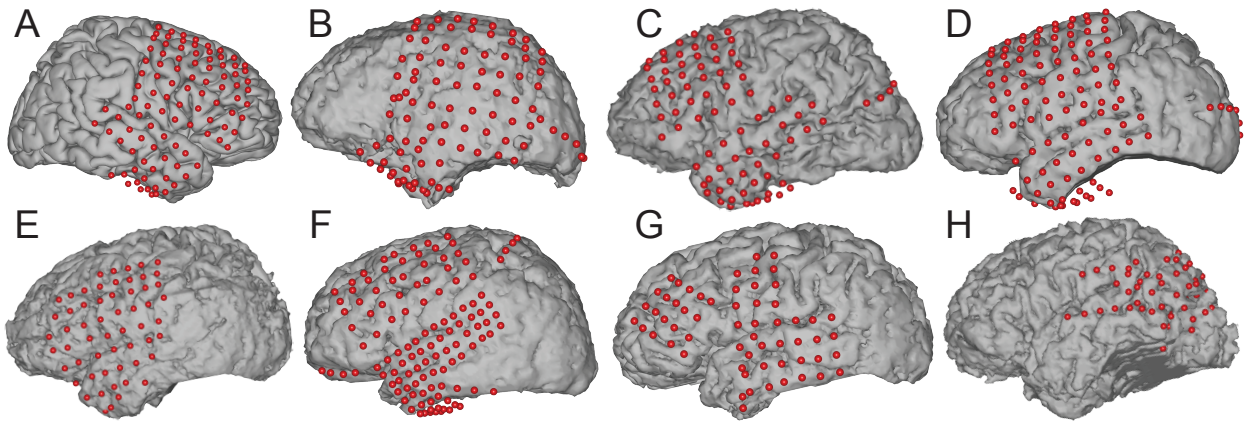

Figure 5.2: **Subject-specific brain models and projected electrode locations for Subjects A to H.** (The MNI brain was used for subject A because his brain model was not available.)

5.2.3 Extraction of ECoG Features

The spectral amplitudes of the ECoG signals in the mu (8-12 Hz), beta (18-24 Hz), low gamma (35-45 Hz) and high gamma (70-170 Hz) bands were of interest because these frequency bands have been shown in previous ECoG studies to be task-related (e.g., motor movement (Miller et al., 2007; Schalk et al., 2007), speech production (Pei et al., 2011), or auditory processing (Pasley et al., 2012; Sinai et al., 2009)). To extract these amplitudes, all frequencies below 0.1 Hz were removed from the ECoG signals using a high-pass filter. A common average reference (CAR) spatial filter then removed spatial noise common to all ECoG channels. ECoG signals from each channel were band pass filtered at mu, beta, low gamma, and high gamma frequency bands (i.e., ECoG features). Next, the magnitude of each of these ECoG features was computed, followed by a low

[1] http://www.bic.mni.mcgill.ca

pass filter at 0.5 Hz. Similar results were obtained when using a low pass filter with different cut-off frequencies (e.g., 1 Hz and 3 Hz). Finally, ECoG signals in each band were downsampled to 10 Hz.

5.2.4 Extraction of Sound Intensity

The analysis of the ECoG correlates of the song was approached by studying its relationship with the song's sound intensity. To do this, the sound intensity was calculated as the average power derived from non-overlapping 10 ms segments of the song. Sound intensity was smoothed by applying a low pass filter at 0.5 Hz and then downsampled to 10 Hz. Figure 5.3 shows an example of the time course of ECoG high gamma activity in temporal cortex derived from Subject B and illustrates its relation to the time course of sound intensity. This figure also illustrates a time-frequency representation of the ECoG signal recorded from the superior temporal gyrus.

5.3 Results

5.3.1 Relevant Cortical Locations

First, the cortical locations and frequency bands (i.e., the ECoG features) that were related to sound intensity were identified. To do this, the pairwise Spearman's correlation [2] coefficient (r) and its significance (i.e., p-value) between sound intensity and each of the different ECoG features at each location were calculated. The resulting correlation coefficient (r) has a t-distribution with df$=$ 1798 degrees of freedom. For those locations with significant correlation coefficients (i.e., $r > 0.3$ and p-value < 0.01 after Bonferroni correction), the negative logarithm of the corresponding p-values (i.e., $-log_{10}(p)$) were

[2] Spearman's (non-parametric) correlation method was used rather than Pearson's (parametric) correlation, because Spearman's correlation is less sensitive to outliers in the data.

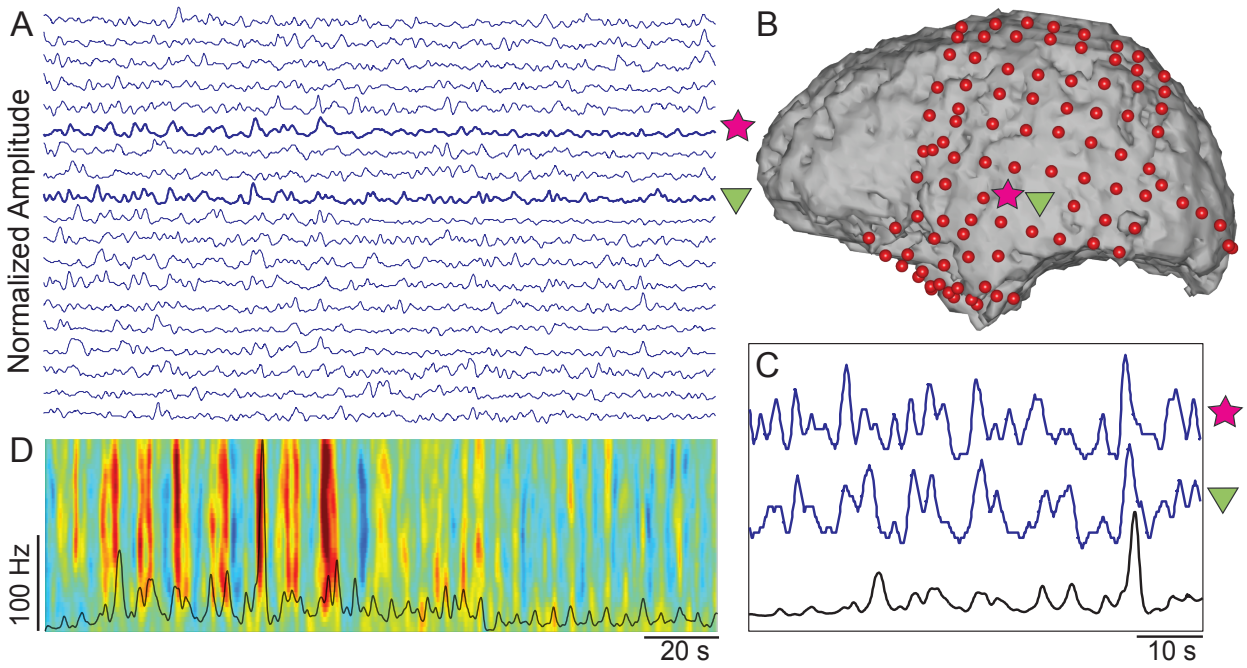

Figure 5.3: **Example of ECoG activity and its relationship with sound intensity in subject B.** A) Time course of normalized high gamma amplitudes (blue traces) extracted from channels located in the left temporal lobe. B) Locations that exhibit a time course that is correlated with sound intensity are indicated with colored symbols and are shown on the subject's brain model. C) Magnification of time course of sound intensity (black trace) and high gamma of the indicated locations (blue traces). D) Time-frequency representation of the ECoG signal recorded from the cortical location indicated by the star symbol in B. The time course of sound intensity is shown in black.

projected onto the corresponding individual brain model [3]. The negative logarithm of the p-value has been used in several previous studies (Gunduz et al., 2011; Kubánek et al., 2009; Schalk et al., 2007) to visualize results from similar correlation analyses. This metric is additive, so it can be used to show average brain activation across multiple subjects. The resulting topographies are shown in Figure 5.4 for each subject and ECoG feature. These topographies show that high gamma band activations in or close to the superior temporal gyrus and precentral gyrus are significantly correlated with sound intensity. Similar topographies were obtained when a low pass filter with different cut-off frequencies (e.g.,1 Hz and 3 Hz) was applied to each ECoG feature and sound intensity

[3]Note that a $-log_{10}(p)$ of 2 and higher is statistically significant at a confidence level of 99% (i.e., $p < 0.01$).

as described in sections 5.2.3 and 5.2.4.

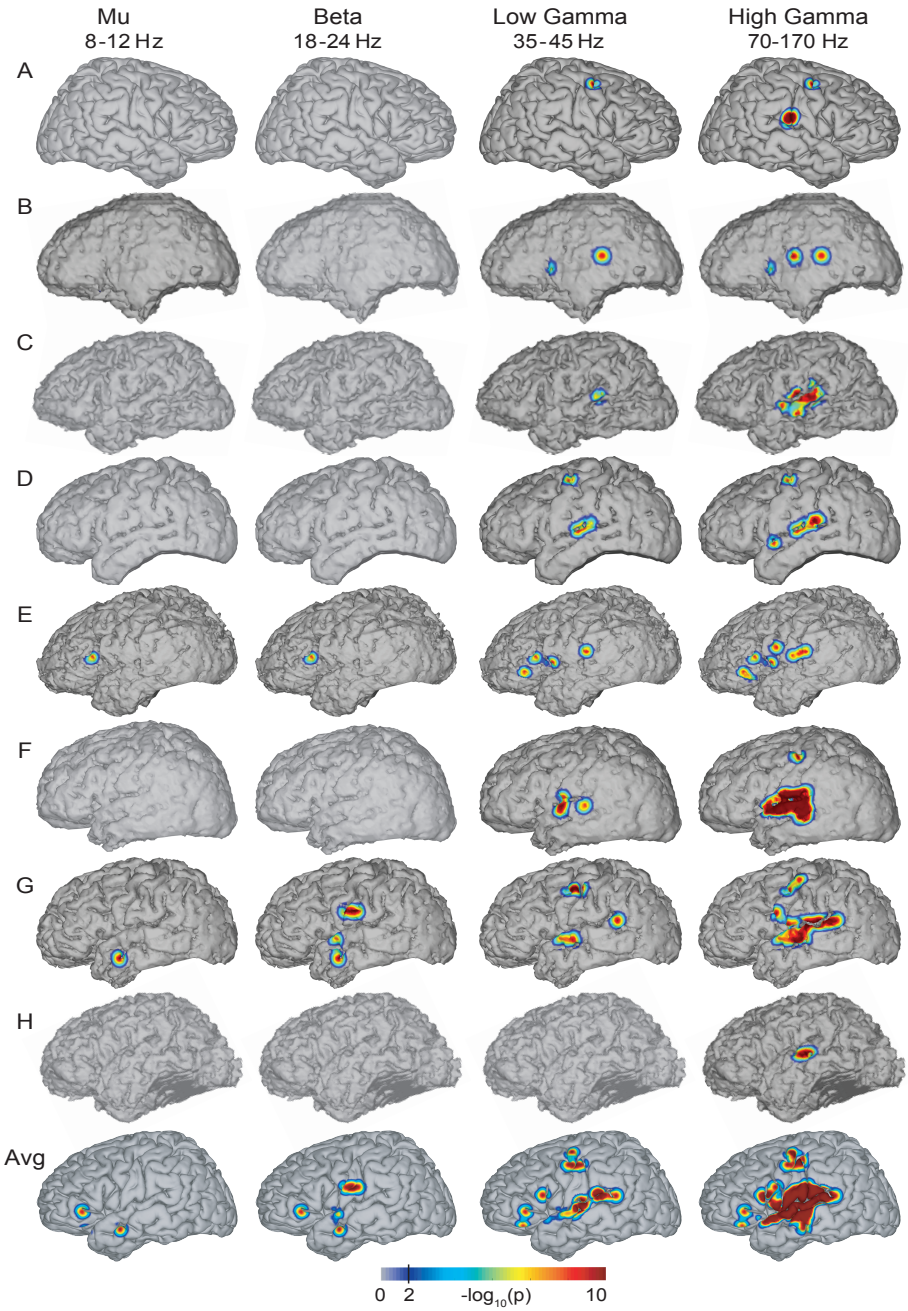

Figure 5.4: **Significance of cortical areas for sound intensity processing.** This figure shows the spatial distribution of $-log_{10}(p)$ values obtained from the (univariate) correlation between sound intensity and each ECoG feature. The last row corresponds to the average spatial distribution of $-log_{10}(p)$ values for subjects with electrode grids implantedonly in the left brain hemisphere (i.e., subjects B to H). Values larger than 2 are statistically significant at a confidence level of 99% (see vertical line in color bar). High gamma activations are focused mainly over the superior temporal gyrus and precentral gyrus.

From all these cortical locations, locations in the superior temporal gyrus and precentral gyrus that had the highest correlation coefficients between ECoG high gamma and sound intensity were determined, resulting in two identified locations for each subject. (Only subjects A, D, F, and G had locations with significant correlation coefficients in precentral gyrus.) Across all subjects, these locations were tightly clustered in the posterior part of the superior temporal gyrus and the dorsal part of precentral gyrus, respectively. Table 5.2 shows the correlation coefficients between each ECoG feature (mu, beta, low gamma, and high gamma) and sound intensity for the superior temporal gyrus locations for all subjects. Figure 5.5 and Figure 5.6 show these cortical locations in superior temporal gyrus and precentral gyrus, respectively, as well as the time course of sound intensity and ECoG high gamma at the respective location. Results confirm the importance of these areas for auditory processing found in previous neuroimaging studies (Brechmann et al., 2002; Chen et al., 2009; Griffiths and Warren, 2002; Hart et al., 2003; Jäncke et al., 1998; Langers et al., 2007; Popescu et al., 2004; Yetkin et al., 2004; Zatorre et al., 2007), an ECoG study (Edwards et al., 2010), and EEG studies (Mulert et al., 2005).

Table 5.2: **Correlation coefficient between ECoG features and SI.** Correlation coefficients computed between sound intensity and different ECoG features: mu (8-12 Hz), beta (18-24 Hz), low gamma (35-45 Hz), and high gamma (70-170 Hz) located over the posterior part of the superior temporal gyrus.These results demonstrate that high gamma activity yields the highest correlation in all subjects.

ECoG Feature / Subject	A	B	C	D	E	F	G	H	Avg
Mu	-0.14	0.1	-0.17	0.02	-0.04	-0.32	-0.4	-0.23	-0.15
Beta	-0.13	0.16	-0.03	0.11	0.11	-0.11	-0.33	-0.1	-0.04
Low gamma	0.16	0.37	0.31	0.22	0.31	0.11	0.30	0.02	0.23
High gamma	0.43	0.53	0.45	0.52	0.50	0.43	0.51	0.58	0.49

ECoG high gamma activity for all these locations and for all subjects with grids implanted in the left hemisphere were averaged, separately for superior temporal gyrus and precentral gyrus, and the two time series at different time lags were correlated. The

maximum correlation coefficient r = 0.70 was obtained at lag τ = 110 ms, which suggests that ECoG high gamma activity in auditory cortex precedes ECoG high gamma activity in premotor/motor cortex by 110 ms (Fig. 5.7). Finally, Figure 5.8 shows the spatial relationship of the location identified in precentral gyrus with locations classified as hand or face motor cortex using electrical stimulation mapping and/or passive functional ECoG mapping (Brunner et al., 2009). The location found to be related to auditory stimulation in this study was different from hand or face motor locations in all subjects.

5.4 Discussion

5.4.1 The Role of ECoG Gamma Activity in Sound Processing

This study shows for the first time that the time course of high gamma ECoG activity is highly correlated to the sound intensity of a continuous stream of music. While neural activity correlated to sound intensity was mostly identified in the superior temporal gyrus, an additional isolated area in the precentral gyrus also showed a relationship with sound intensity in subjects A, D, F, and G. (It is quite possible that the absence of this location in the other subjects can be attributed to the limited spatial resolution of our recordings.) This area was not classified as hand or face motor cortex using electrical stimulation mapping or passive real-time ECoG mapping in any of these four subjects. This suggests that the corresponding location is in fact related to a distinct aspect of auditory processing rather than to somatosensory or motor processing. However, future research is needed to determine the specific functional relevance of activations in the precentral gyrus such as rhythm processing (Zatorre et al., 2007) or speech processing (Edwards et al., 2010).

The average gamma activity in the superior temporal gyrus was highly correlated (r = 0.84) with the average gamma activity from the precentral gyrus, and was leading it by 110 ms. These results might be explained by previous findings in fMRI studies (Chen

et al., 2009; Griffiths and Warren, 2002; Popescu et al., 2004; Zatorre et al., 2007) where it is suggested that the posterior part of the superior temporal gyrus might act as a neural hub decomposing the various types of sound and integrating those of motor relevance with the prefrontal, premotor, and motor regions through a dorsal pathway. Results of this study also support the hypothesis that activity in the high gamma band, in contrast to activity at lower frequencies, co-localize with hemodynamic responses measured with fMRI during sound intensity processing (Hermes et al., 2011; Jäncke et al., 1998; Lachaux et al., 2007a; Langers et al., 2007; Logothetis et al., 2001). Although the neurophysiological origin of high gamma activity in ECoG is still a matter of some debate, recent research supports the hypothesis that it is a reflection of the mean firing rate of the neuronal population directly beneath the electrode contact (Manning et al., 2009; Miller, 2010). The concurrence of these results with fMRI studies in humans and single-unit studies in primates, and ECoG's high temporal and relatively high spatial resolution, strongly encourage further study of high gamma ECoG activity and its relationship to other acoustic features.

5.4.2 Current Experimental Limitations

The present results are encouraging, and could not have readily been derived using other imaging techniques. At the same time, there will ultimately be limits to what can be achieved by using the currently limited subject population used in this study. This study, like practically all human ECoG studies to date, relied on electrode grids implanted for clinical reasons. Thus, grid coverage is incomplete and variable across subjects. Given the limited number of subjects with grids implanted over the right (1 subject) and left (7 subjects) brain hemispheres, further research is needed to determine potential hemispheric differences during music processing. The physical and cognitive condition and level of cooperation of each patient are impaired and/or variable. In addition, auditory stimulation was not highly controlled during the experiment. This relatively

uncontrolled experimental situation is in contrast to typical neuroscientiPc studies, in which experimental conditions are usually highly controlled. Finally, the subjects in the study are epileptic patients, and thus may have some degree of functional reorganization compared to non-epileptic individuals. Variability in the correlation values at the same cortical locations across subjects might be explained by variances introduced by different sources such as grid coverage, physical and cognitive condition, and the subject's specific neuroanatomy. Despite these issues, the results presented in this and other ECoG studies are usually consistent with expectations based on the neuroanatomy or on results from other imaging modalities.

While the subjects had broad spatial coverage, including coverage of the temporal lobe, the analytical detail of the results is limited in spatial resolution by the inter-electrode distance (0.6-1 cm) of the implanted grids. Grid electrodes with smaller contacts and inter-electrode distances have recently been implanted and used to study language processing (Kellis et al., 2009; Wilson et al., 2006). Increased resolution of the ECoG grids will likely improve and further refine our understanding of underlying ECoG physiology.

The placement of the electrode grids in this study was based on the clinical needs of the patients for the localization of epileptic foci, which typically originate from a single hemisphere. Hence, it was not possible to investigate brain lateralization of acoustic processing as suggested in (Belin et al., 1998; Gourévitch et al., 2008; Platel et al., 1997; Zatorre and Belin, 2001). For instance, these studies demonstrated specialization of the right hemisphere for fine spectral changes such as the pitch. Comprehensive access to both hemispheres, which will likely remain impractical, would allow for a more complete analysis of auditory processing.

5.4.3 Future Work

This study demonstrated the relationship of ECoG features with sound intensity in a continuous stream of music. Future work may investigate the relationship between ECoG features and other aspects of sounds or their perception, such as loudness perception. Loudness perception is a subjective measure that cannot be universally measured by a single metric and can be affected by several acoustic parameters such as sound intensity, bandwidth, and duration. Decoding of perceived loudness from brain signals may have important applications for the calibration of stimulation levels of cochlear implants. Currently, these levels are adjusted by an audiologist and have to be frequently reprogrammed due to implant scar formation or habituation.

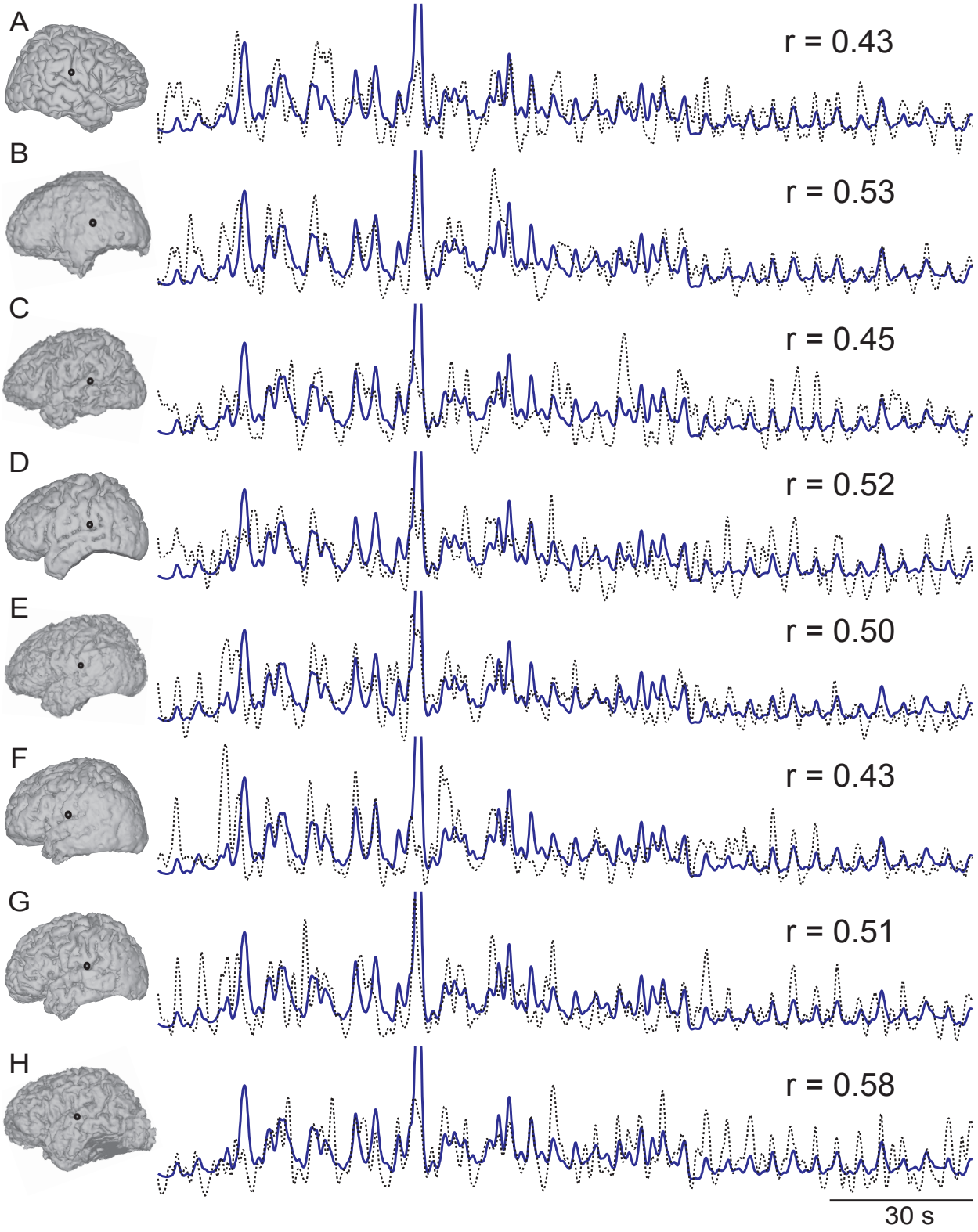

Figure 5.5: Cortical locations (black dots) in the posterior part of the superior temporal gyrus with the highest correlation between ECoG high gamma (dashed black trace) and sound intensity (blue trace). The respective correlation coefficients, *r*, for each subject are also given.

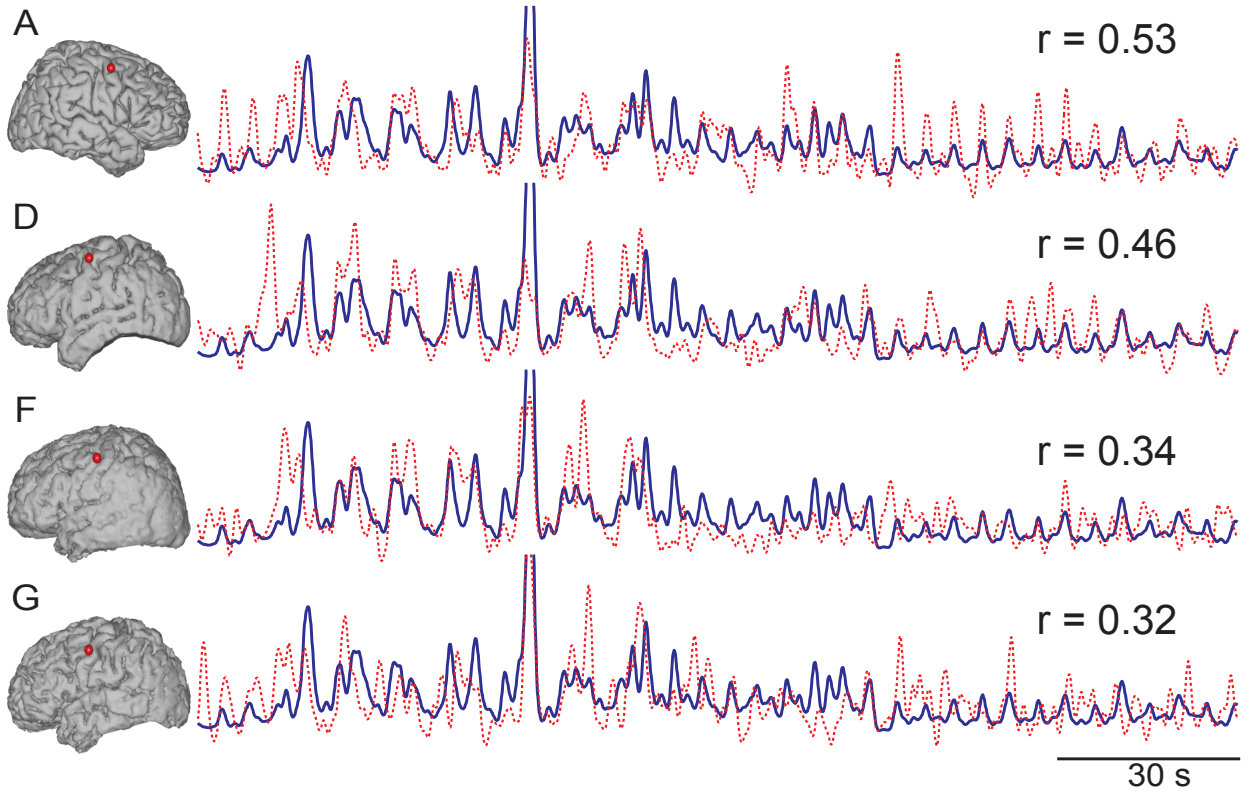

Figure 5.6: Cortical locations (red dots) in the dorsal part of the precentral gyrus with the highest correlation between ECoG high gamma (dashed red trace) and sound intensity (blue trace). (Only subjects A, D, F, and G had locations with significant correlation coefficients.) The respective correlation coefficients, r, for each subject are also given.

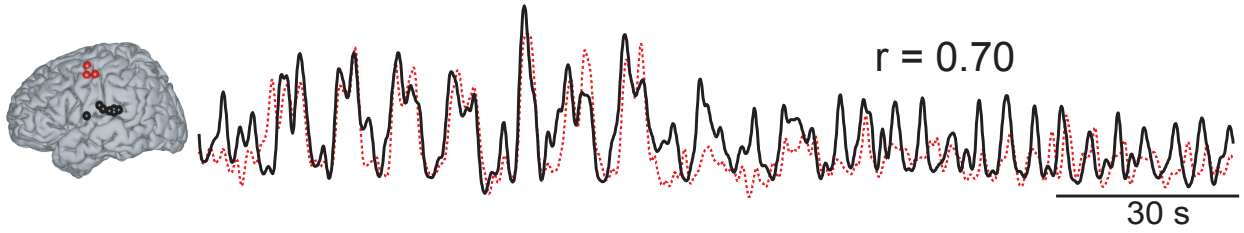

Figure 5.7: Left: Locations in the superior temporal gyrus and precentral gyrus identified in Figures 5.5 and 5.6. Right: Average time course of ECoG high gamma for these locations in the superior temporal gyrus (black trace) and the precentral gyrus (dashed red trace). Subject A who has grid implanted in the right brain hemisphere was not considered to compute the average. The corresponding correlation coefficient, r, is also given.

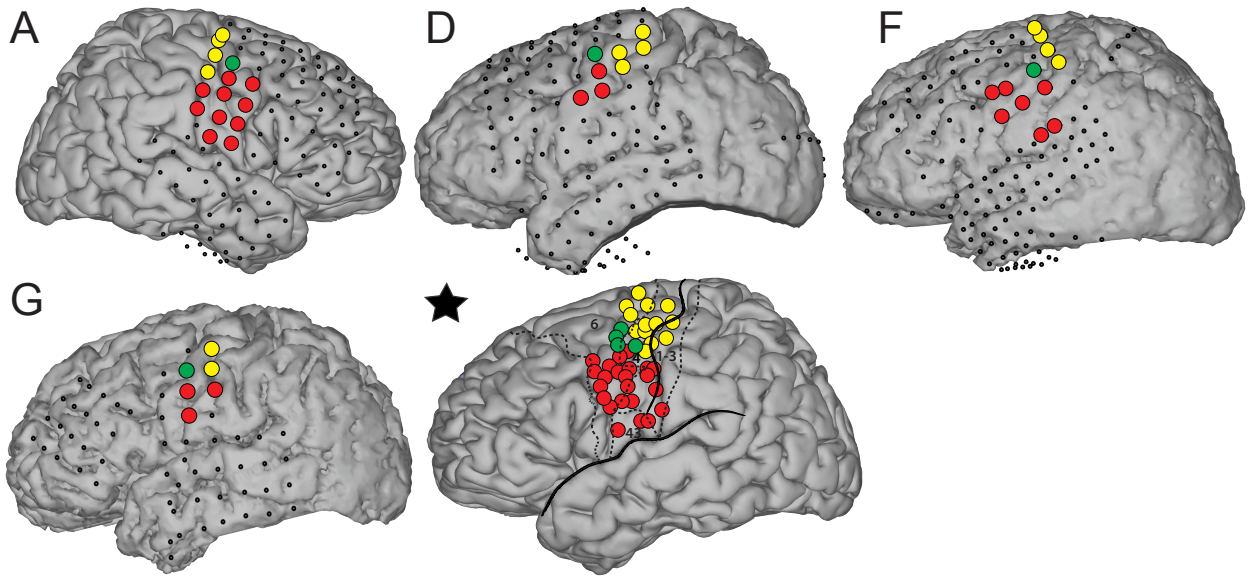

Figure 5.8: **Cortical mapping of face (red circles) and hand (yellow circles) motor areas identified using electrocortical stimulation mapping and/or real-time passive ECoG mapping (Brunner et al., 2009)**. Coverage of all other electrodes is shown using small black dots. Electrodes in green are the same locations from subjects A, D, F, and G shown in Figure 5.6. The brain figure marked with a star shows the MNI brain, the locations of all highlighted electrodes for subjects A, D, F, and G, as well as relevant cortical landmarks.

6

Spatio-Temporal Relationship of ECoG Activity During Music Processing

6.1 Introduction

Music is a perceptual experience that engages many cognitive processes within different regions of the brain (Lauren et al., 2006). Over the past few decades, numerous studies using hemodynamic and electrophysiological imaging techniques (fMRI/PET and EEG/MEG, respectively) have attempted to uncover the neural underpinnings of music processing. For instance, a recent fMRI study by Vinoo et al. in 2012 investigated the BOLD responses related to the processing of timbre, rhythm, and tone while subjects listened to music. Other neuroimaging studies investigated the relationship between sound intensity and brain activity in auditory cortex (Brechmann et al., 2002; Hart et al., 2003; Mulert et al., 2005; Tanji et al., 2010; Thaerig et al., 2008; Yetkin et al., 2004), and EEG studies determined relationships between rhythm and pitch and EEG components during listening and imagination of melodies (Schaefer et al., 2009).

These and other studies have made important progress in identifying those brain regions whose activity changes with the perception of different individual musical features (e.g., sound intensity, rhythm, pitch), but most of them have been constrained to highly

controlled experiments using artificial stimuli (e.g., presenting tones at different intensities or pitches). This is unfortunate, because cortical processing of artificial stimuli may differ in important ways from the processing of complex natural stimuli (such as music), and because evidence suggests that the brain employs general principles that govern the processing of complex natural stimuli (Hasson et al., 2010, 2004). In addition to experimental constraints, methodological limitations have not allowed the simultaneous evaluation of the temporal and spatial dynamics related to music processing. For instance, fMRI and PET measure brain metabolic activity with excellent spatial resolution but reduced temporal resolution (several seconds). Thus, they cannot track the rapid moment-to-moment variations related to processing of continuous music. Conversely, EEG and MEG measure brain electrical activity with excellent temporal resolution but poor spatial resolution (several centimeters) and cannot reliably ascribe activity changes to particular brain areas.

Electrocorticographic (ECoG) recordings from the surface of the brain have recently been used to study the neural dynamics during processing of complex sounds, in particular speech (Edwards et al., 2009; Lachaux et al., 2007b; Pasley et al., 2012; Sinai et al., 2009). This relatively new imaging technique combines high temporal resolution with high spatial resolution and coverage. It can also detect different neurophysiological processes that subserve sensory, motor/language, or cognitive functions (Crone et al., 1998a; Hermes et al., 2011). These processes include ECoG modulations in the alpha (8-12 Hz) and high gamma (70-110 Hz) frequency bands. Activity in the alpha band seems to reflect interactions between the thalamus and the cortex (da Silva, 1991; Steriade et al., 1990; Zhang et al., 2004), and may facilitate information transfer to task-related cortical areas by inhibiting neural activity in task-unrelated areas (Jensen and Mazaheri, 2010). On the other hand, activity in the high gamma band seems to reflect task-related activity of neural populations directly underneath the electrodes (Crone et al., 2001, 1998a; Miller et al., 2007, 2009; Schalk et al., 2007).

Despite this body of work, the most salient spatial and temporal relationships of these neural processes during music processing remain undefined. To address this issue, electrical activity from electrodes implanted on the brain's surface of ten human subjects while they were listening to music were recorded. This data was then used to define the cortical locations that modulate alpha or gamma activity during music processing and to define their temporal and causal relationships. Results implicate perisylvian structures as well as an unexpected and distinct area in superior premotor cortex, and establish the differing spatial and temporal contributions of alpha and gamma activity.

6.2 Materials and Methods

6.2.1 Subjects and Data Collection

Electrical activity from intracranial electrodes of ten epileptic subjects (four men, six women) who were listening to a complex natural auditory stimulus (the song "Another Brick in the Wall - Part 1" (Pink Floyd, Columbia Records, 1979)) was recorded. These subjects underwent temporary implantation of subdural electrode arrays to localize the epileptogenic focus and to delineate it from eloquent (i.e., functional) cortical areas prior to brain resection. Table 6.1 summarizes the subjects' clinical profiles. All of the subjects gave informed consent to participate in the study, which was approved by the Institutional Review Board of Albany Medical College. None of the subjects had a history of hearing impairment. The implanted electrode grids consisted of platinum-iridium electrodes that were 4 mm in diameter (2.3-3 mm exposed) and spaced with an inter-electrode distance of 0.6 or 1 cm. The total numbers of implanted electrodes were 96, 83, 109, 58, 120, 58, 59, 98, 134, and 98 for the different subjects, respectively. Electrodes were implanted on the left hemisphere for all subjects, as shown in Fig. 6.1. ECoG signals were digitized at 1200 Hz, synchronized with stimulus presentation, and stored using the BCI2000 software platform (Schalk et al., 2004; Schalk and Mellinger, 2010). ECoG

signals were recorded while the subjects were listening to the song, which was 3:00 min long, digitized at 44.1 kHz in waveform audio file format, and binaurally presented to each subject using in-ear monitoring earphones. In addition, the same amount of ECoG signals were recorded while subjects were at rest with eyes open. The individual ECoG recordings were visually inspected and those electrodes that did not contain clean ECoG signals or had interictal activity were removed. This procedure left 86, 82, 103, 56, 108, 57, 53, 93, 110, and 92 electrodes for the different subjects for further analysis.

Table 6.1: **Clinical profiles of the subjects that participated in the study.** All of the subjects had normal cognitive capacity and were functionally independent.

Subject	Age	Sex	Handedness	Seizure Focus	# of Elec.
A	29	F	R	Left temporal	86
B	30	M	R	Left temporal	82
C	26	F	R	Left temporal	103
D	45	M	R	Left temporal	56
E	29	F	R	Left temporal	108
F	45	F	L	Left temporal	57
G	60	M	R	Left temporal	53
H	17	F	L	Left temporal	93
I	28	M	R	Left temporal	110
J	25	F	R	Left temporal	92

6.2.2 Cortical Mapping

The brain anatomy of each subject was defined using pre-operative magnetic resonance imaging (MRI) scans, and the location of the electrodes using post-operative computer tomography (CT) imaging. A 3D surface model of each subject's cortex was created from the MRI images, and co-registered it with the location of the electrodes given by the CT images using Curry Software (Compumedics NeuroScan), and transformed the 3D model and electrode locations into Talairach space (see Fig. 6.1).

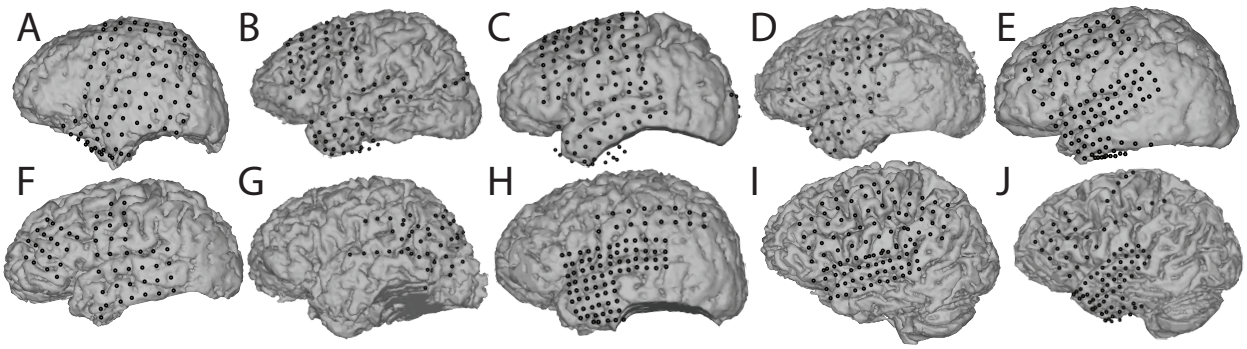

Figure 6.1: **Subject-specific brain models and locations of implanted and analyzed electrodes.** The brain model template marked with a star shows the approximate location of implanted electrodes from all subjects.

6.2.3 Extraction of ECoG and Sound Features

To extract the time course of alpha and high gamma activity, the ECoG signals from each electrode at each specific frequency band (i.e., 8-12 Hz and 70-110 Hz) were filtered using an IIR band-pass filter, and spatially distributed noise common to all ECoG electrodes was removed using a common average reference (CAR) spatial filter. The envelope of the ECoG signal (i.e., the magnitude of the analytic signal) in each frequency band was computed. Finally, the natural logarithm of the envelope power (i.e., squaring each element of the envelope and then computing the natural logarithm) was computed and the result resampled to 10 Hz. To extract the song's sound intensity, the average power derived from non-overlapping 10 ms segments of the song was computed. The sound intensity was then smoothed by applying a low pass IIR filter at 5 Hz and resampled the result to 10 Hz. The total length of the alpha, high gamma, and sound intensity time courses are 1800 samples each. All filtering operations were performed forwards and then backwards (using Matlab's `filtfilt` command) to avoid an introduction of a group delay. The following analyses then determined those locations or interactions across locations that contained alpha or gamma activity that was related to music processing.

6.2.4 Intersubject Correlation (ISC) Analysis

Identifying task-related neural signals is typically accomplished by comparing brain activity during two conditions (e.g., task vs. baseline) or by correlating brain activity to a particular aspect of the task (e.g., time course of sound intensity as in (Potes et al., 2012)). However, these approaches either require many repetitions of task and rest periods (to minimize the effect of spontaneous brain activity changes that are not related to the task) or a very specific hypothesis about what aspect of the task may be reflected in brain signals. Thus, these approaches are not amenable to identifying the most relevant neural processes related to processing of a continuous piece of music. However, recent research (Hasson et al., 2010, 2004) has established that it is possible to identify such processes by studying brain signals exclusively across (rather than within) subjects.

Based on this idea, task-related neural signals were identified as those correlated across subjects. This approach ensured that all neural signals identified with this procedure are related to the processing of music since ECoG modulations resulting from the presentation of music were the only aspect that linked neural signals from one subject to neural signals from another subject. It also ensured that the results represented only task-related neural signals that were common across subjects. Because the location of the electrodes varied across subjects, it was not possible to compare activity changes at the identical location across subjects. Instead, for each electrode location in each subject, all electrodes from all other subjects that were in close proximity ($<$1 cm) to that electrode were identified. This permitted comparison of brain activity from one individual to brain activity from other subjects. For each such pair of electrodes, the average Talairach coordinate was computed, which resulted in a total of 15107 locations (336$\pm$210 per subject combination) that formed the basis for the study's analyses. For each of these locations/electrode pairs, and separately for ECoG activity in the alpha and high gamma bands, the pairwise Spearman correlation coefficient (intersubject correlation (ISC) r) and its significance (i.e., p-value) was computed. The statistical significance of

the resulting correlation coefficients was computed using a bootstrapping randomization test in which the envelope samples for each frequency band and for each channel were randomly scrambled (i.e., 1000 times) across time. The same procedure was repeated for all locations and all combinations of subjects (i.e., $\binom{10}{2} = 45$ combinations). Next, all locations whose p-values were significantly different than chance after Bonferroni correction for 15107 locations (i.e., $p < \frac{0.01}{15107} = 6.6e^{-7}$) were determined. The negative logarithm of the corrected p-values ($-log_{10}(p)$) for each electrode was then projected on to the 3D brain cortical template provided by the Montreal Neurological Institute (MNI).

To determine causal relationships between the time course of average alpha activity (calculated across all locations) and the time course of average gamma activity, Granger causality (Granger, 1969) was calculated using a model order of 10, suggested by the Bayesian information criterion (BIC) (Schwarz, 1978). Finally, the lag between activity in these two time courses was determined by identifying the time of the peak of the cross-correlation function.

6.2.5 Intersubject Granger Causality (ISG) Analysis

Pairs of locations whose activity time course were related to each other causally and were also related to music processing were established. To do this, causal interactions between different recording sites across subjects at alpha and high gamma frequencies were estimated using bivariate Granger causality. There is Granger causality from $\boldsymbol{X}$ to $\boldsymbol{Y}$ (i.e., $\boldsymbol{X} \rightarrow \boldsymbol{Y}$) if adding past values of $\boldsymbol{X}$ and $\boldsymbol{Y}$ (i.e., full model) provide more information about future values of $\boldsymbol{Y}$ compared to when only past values of $\boldsymbol{Y}$ (i.e., restricted model) are considered. In this analysis, $\boldsymbol{X}$ or $\boldsymbol{Y}$ are time series representing alpha or high gamma activity in a particular electrode location and subject. For the visualization of causal interactions identified with the Granger causality analyses, directed arrows that connected two specific locations on an MNI brain were used. In the analyses, all possible (630800) pairs of electrode locations across subjects were considered.

To select the best model order for Granger causality, the Bayesian information criterion (BIC) (Schwarz, 1978) was computed across all pairs of electrodes, which resulted in a model order of 10. To validate the goodness-of-fit of each autoregressive (AR) model, the residuals (i.e., the errors) were checked to see if they were serially uncorrelated using the Durbin-Watson test (Durbin and Watson, 1950); the consistency of the model was examined using the procedure described in (Mingzhou et al., 2000); and the adjusted coefficient of determination (R^2) was evaluated using the procedure described in (Colin and Frank, 1997). All significant Granger causality connections had consistency and R^2 values greater than 80%, and all the residuals passed the Durbin-Watson test.

To assess the statistical significance (i.e., p-value) of the Granger causality between two locations $\boldsymbol{X} \rightarrow \boldsymbol{Y}$, the null hypothesis (i.e., the full model does not fit the data better than the restricted model) was tested using the F-statistic $\mathbf{F} = \frac{(\mathbf{RSS_F} - \mathbf{RSS_R})(\mathbf{n}-\mathbf{3k})}{\mathbf{RSS_R}(\mathbf{k})}$, where RSS_F and RSS_R were the residual sum of squares of the full and restricted model, respectively, k was the model order (i.e., k=10), and n was the number of observations (i.e.,1800). To determine statistical significance (i.e., a p-value), the F-statistic was compared to an F-distribution with $(k, n-3k)$ degrees of freedom. The null hypothesis was rejected if the p-value was less than $1.58e^{-8}$ after Bonferroni correction for all possible connections (i.e., p-value $< \frac{0.01}{630800} = 1.58e^{-8}$). The critical value of the F-distribution with $(10, 1770)$ degrees of freedom was 0.0145.

Application of bivariate Granger causality is known to be susceptible to spurious connections (i.e., connections that are either mediated or confounded by another time series, e.g., alpha or high gamma activity in a particular channel and subject). To account for this known potential confound, all spurious connections were removed from the resulting set of statistically significant causal interactions using the approach described in (Haley et al., 2010). To display only large cortical networks, short connections (i.e., those with a distance less than 1 cm) were removed. From the resulting connections, the connections that were in close proximity (i.e., connections whose start or end points

were in a distance less than 1 cm) were then selected.

6.3 Results

6.3.1 Spatial Relationship

The spatial relationship of locations whose alpha or high gamma activity was related to music processing were investigated first. Specifically, the results shown in Fig. 6.2a highlight those locations whose alpha (upper panel) or gamma (lower panel) activity was significantly modulated by music processing (left panels) as opposed to the rest condition (i.e., relaxing on a bed with eyes open, right panels). The black dots and colored areas in the brain figures identify these locations and their corresponding accumulated $-log_{10}(p)$ values. A total of 500 significant locations were found across all subjects, the two frequency bands, and the task and rest conditions. Specifically, for the ECoG recordings during the task condition, 80 locations had significant alpha-ISC values (mean correlation $\pm$ standard deviation across the 80 locations: r = 0.13 $\pm$ 0.02, max r = 0.19) and were primarily located in areas close to primary auditory cortex (Fig. 6.2a, top-left). Moreover, 412 locations had significant gamma-ISC values (r = 0.15 $\pm$ 0.03, max r = 0.27) and were not only located in areas close to primary auditory cortex but also over auditory association areas as well as in a distinct but previously largely unrecognized area in premotor cortex (Fig. 6.2a, bottom-left). In contrast, for the ECoG recordings during rest, only 8 (Fig. 6.2a, top-right) (mean correlation $\pm$ standard deviation across the eight locations: r = 0.001 $\pm$ 0.13, max r = 0.14) and 0 (Fig. 6.2a, bottom-right) locations had significant alpha-ISC and gamma-ISC values, respectively. The number of locations with significant alpha- and gamma-ISC values during the task was larger than those during rest (Fisher's exact probability test, two-tail, p=4.51e-7 for alpha, p=1.88e-75 for gamma). These results are summarized in Fig. 6.2b. While ECoG activity during the task was correlated across subjects in the alpha and high gamma bands, this was not the

case for the beta (12-30 Hz, 1 location) and low gamma (35-50 Hz, 17) frequency bands (see Fig. 6.3.) It is important to note that the results only minimally depend on the specific metric (i.e., correlation) used here as very similar results were obtained when the mutual information metric was used instead of the correlation metric.

Figure 6.2: **Intersubject correlation analysis.** (A) Topographical distribution of accumulated negative log of the significance of the ISC values during the task (left panels) and rest (right panels) conditions for ECoG activity in the alpha (top row) and high gamma (bottom row) bands. Values larger than 2 are statistically significant at a confidence level of 99% (see vertical line in color bars). (B) Number of locations with significant ISC values at each frequency band and for task (left) and rest (right) and the total number of significant locations (277). The dashed lines on the brain topographies outline the spatial coverage of the intersubject analyses.

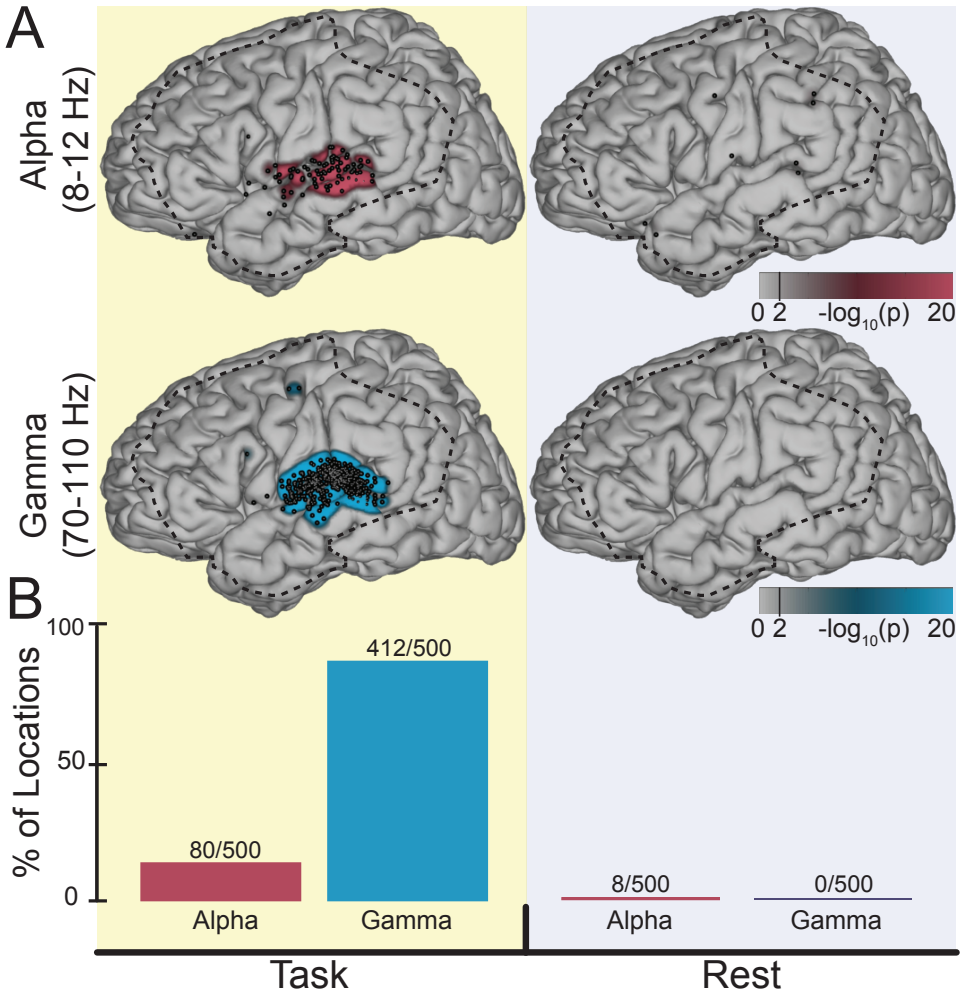

6.3.2 Temporal Relationship

The temporal relationship across alpha activity, high gamma activity, and the song's sound intensity was also investigated. For this, the time courses of alpha and high gamma activity across all locations where activity was significantly correlated across individuals were first investigated. Then, the three averaged time courses of alpha activity, high gamma activity, and the song's sound intensity were correlated with each other. The results are shown in Fig. 6.4 and reveal a significant negative correlation between alpha and high gamma activity (r = -0.52), indicating that high gamma activity augmentation in auditory cortical areas during auditory processing is accompanied by alpha activity suppression (see also (Crone et al., 2001)). Significant positive correlation between high gamma activity and sound intensity (r= 0.37) and significant negative correlation between alpha activity and sound intensity (r = -0.3) were found. ($p<0.0001$, Spearman's correlation, n=1800.) These results are in line with previous studies (Potes et al., 2012). The scatter plots shown in Fig. 6.4b further illustrate these relationships. Importantly, Granger causality analyses revealed that high gamma activity predicted alpha activity ($p << 1e^{-8}$), but not vice versa, and cross-correlation analysis indicated that the onset of high gamma activity preceded alpha activity by 280 ms.

6.3.3 Relationships with Anatomical and Neurophysiological Models

Results were then set in relation to established anatomical models of auditory function and to current theories of the generating origin of alpha and high-gamma activity. Specifically, previous studies have shown that neurons in the medial geniculate nucleus of the thalamus send auditory information to the cortex through projections that terminate in primary auditory cortex (Steriade et al., 1990). In addition, neurons in auditory cortex have projections back to the thalamus. Theoretical considerations suggest that thalamo-cortical projections (Fig. 6.5a) contribute to oscillations at low frequencies (6-12

Hz) (Llinás et al., 1999), and recent experimental evidence in animals is beginning to confirm the important role of thalamic modulation of cortical activity (Saalmann et al., 2012). In contrast, the predominant theory of the physiological origin of the activity in the high gamma band suggests that it reflects the average firing rate of cortical neurons directly underneath the electrodes (Miller, 2010; Miller et al., 2009).

The results identified significant alpha-ISC values only in locations close to primary auditory cortex, and thereby link anatomical structures with thalamocortical connections to oscillatory electrophysiological activity and its hypothesized originating mechanism (Fig. 6.5b, c). In addition, the results identified significant gamma-ISC values in larger perisylvian areas that have previously been implicated in auditory processing (Griffiths and Warren, 2002; Hackett, 2008; Vinoo et al., 2012; Zatorre and Belin, 2001; Zatorre et al., 2002, 2004, 2007). Together with the findings that high gamma and alpha activity are negatively correlated, and that high gamma activity predicts alpha activity, the results presented here support the hypothesis that activity in the alpha band reflects interactions between the thalamus and the cortex (Hackett, 2008; Saalmann et al., 2012; Zatorre et al., 2007), and that these interactions are driven by local neuronal activity in early auditory cortex.

6.3.4 Causal Relationships

Finally, all possible combinations of locations across subjects (i.e., 630800) were tested for causal relationship in the alpha and high gamma frequency bands. This analysis did not identify any significant connection for either the task or the rest conditions in the alpha frequency band, nor for the rest condition in the high gamma frequency band. Yet, it identified 68 significant connections for the task condition in the high gamma frequency band (Fig. 6.6a). After removing spurious connections and identifying the most salient connections, these results were reduced to 10 connections (Fig. 6.6b). No significant connection for the task or rest conditions was identified in any of the other frequency

bands (i.e., beta and low gamma), as shown in Fig. 6.7. It is remarkable that out of 630800 possible connections, the 10 statistically significant connections are all in line with current understanding of cortical auditory processing. Furthermore, the negative results in the rest conditions suggest that the results reflect a highly robust account of the most salient causal relationships between different brain regions involved in music processing. Final results suggested a causal relationships of high gamma activity between distinct locations in early auditory pathways within superior temporal gyrus (STG) and posterior STG, between posterior STG and inferior frontal cortex, and between STG and the newly identified location in premotor cortex (Fig. 6.6b). Thus, the results provide the first direct electrophysiological verification of long-standing hypotheses about the key functional connections related to auditory processing. At the same time, they also highlight a new and unexpected functional connection directly from areas close to early auditory cortex to a distinct location in superior parts of premotor cortex. Because the results did not reveal music-related alpha activity in the same location, they suggest that that functional connection may be realized by cortico-cortical projections rather than common driving input from subcortical structures such as the thalamus.

6.4 Discussion

6.4.1 The Role of Alpha and High Gamma Activity in Music Processing

In the present study, the ECoG activity in the alpha and high gamma bands were related to music processing. Spatial, temporal, and causal relationships of ECoG activity were characterized, and the results were related to the established understanding of the physiological origin of alpha and gamma activity, and current understanding of central auditory processing. From an anatomical perspective, recent animal and human research

suggests that signals related to auditory input are relayed from the medial geniculate nucleus of the thalamus to auditory core areas that include primary auditory cortex and adjacent areas where they are processed to extract low-level aspects of auditory stimuli (e.g., sound intensity). Auditory signals then travel from core areas to higher-order areas (e.g., anterior and posterior parts of the STG) to process more complex aspects of auditory stimuli (e.g., timbre, pitch, or melody).

From a functional perspective, there is substantial evidence that brain oscillations in the alpha band might reflect neural interactions between the thalamus and the cortex (da Silva et al., 1973; da Silva, 1991; Hughes and Crunelli, 2005) and might modulate the firing rate of local cortical activity (Haegens et al., 2011; Saalmann et al., 2012). Other studies have suggested that brain activity in the high gamma band reflects the firing rate of the cortical neuronal population beneath each electrode (Cardin et al., 2009; Miller, 2010; Miller et al., 2009; Ray and Maunsell, 2011). This view is supported by many studies that have defined strong temporal or spatial relationships of gamma activity recorded at specific locations with specific aspects of motor, perceptual, or cognitive function (Crone et al., 2001, 1998a; Kubánek et al., 2009; Potes et al., 2012; Schalk et al., 2007).

Integrating this anatomical and functional evidence, one may expect to find task-related activity in the alpha band only close to core areas (i.e., areas that have thalamocortical connections), and task-related activity in the high gamma band not only in core areas but also in higher-order areas (because all those cortical areas are presumed to be involved in auditory processing). Similarly, causal interactions between different cortical sites should be identified primarily between the gamma band and not other frequency bands. Results from this study provide the first direct electrophysiological confirmation of these expectations.

First, the locations of significant alpha-ISC values highlighted core areas Fig. 6.3c, whereas the locations of significant gamma-ISC values highlighted not only core areas

but also other cortical areas that have been proposed to be activated in established cortical auditory models (Griffiths and Warren, 2002; Hackett, 2008; Kaas and Hackett, 1999; Zatorre and Belin, 2001; Zatorre et al., 2002, 2007). Second, functional connectivity analyses identified significant causal interactions exclusively at high gamma but not at other frequencies. Third, cortical interactions at high gamma (see Fig. 6.6) were generally consistent with current understanding of cortical auditory processing. Fourth, the results are consistent with the hypothesis that thalamo-cortical projections transmit auditory information from the thalamus to early auditory cortex, from where cortico-cortical projections relay the results to other perisylvian areas to extract complex auditory features (Kumar et al., 2007; Zatorre et al., 2007; Zhang et al., 2004).

6.4.2 Implications

The present results advocate the use of ECoG and more natural paradigms to obtain a comprehensive picture of music processing. First, the approach described in this study provides a novel, robust, and very specific method to identify the most common aspects of task-related brain activity, which is currently typically evaluated within subjects by either comparing brain activity during a task to brain activity during rest, or by relating brain activity to a specific aspect of the task (e.g., sound intensity, kinematic parameter). Second, the approach implemented here provides the basis for functional rather than anatomical co-registration of brains of different individuals of the same or even different species (Mantini et al., 2012). Third, results suggest that high gamma activity and alpha activity are negatively correlated, and that high gamma activity predicted alpha activity and preceded it by 280 ms. Hence, higher gamma amplitudes, which have been shown to be related to higher stimulus intensity (Potes et al., 2012), lead to decrease in alpha amplitudes presumably related to an increase in cortical excitability. This evidence provides a link between higher stimulus intensity and a resulting higher cortical excitability. Thus, it may suggest a general mechanism for prioritizing different competing sensory

streams, and could also be useful in explaining different types of stimulus-driven or internally-generated (covert or overt) forms of attention. In other words, results suggest that it is possible that the interactions between stimulus intensity, gamma activity, and alpha activity may point to a principal mechanism of auditory or even other functions. Fourth, established functional models of auditory processing have emerged from meta-analyses of several functional neuroimaging studies under highly controlled experiments. This relatively indirect approach has left room for subjective interpretation and controversial hypotheses. With further validation, the method described here may allow for a more direct verification and extension of these functional models.

6.4.3 Future Research Questions

The present study provides new information about the neural mechanisms engaged in music processing, but also raises a number of important questions. First, the results presented here suggest an important interplay between cortical and thalamic activity. Investigation of this interplay would necessitate simultaneous recordings from the thalamus and from different areas of the cortex, and experimental manipulations that modify external or internal parameters (e.g., stimulus intensity, stimulus modality, or attention). Second, the data-driven results determined the cortical locations involved in auditory processing. However, their functional relevance, in particular regarding the location in superior premotor cortex, is currently unclear. Third, the functional relevance of the causal relationships between different brain areas is currently largely undefined. For example, could the functional connection between posterior STG and inferior frontal cortex identified by the analyses (Fig. 6.6b) be related to the processing of lyrics in the music? Finally, the methods presented here transform multi-subject data into common and readily interpretable representations using a rigorous processing and statistical framework. Thus, this approach could form the basis for studies addressing questions that could not be answered with previous subject-specific analytic methods.

Figure 6.3: Topographical distribution of accumulated negative log of the significance of the ISC values during the task (left panels) and rest (right panels) conditions for ECoG activity in the alpha (8-12 Hz), beta (12-30 Hz), low gamma (35-50 Hz), and high gamma (70-110 Hz) bands. Values larger than 2 are statistically significant at a confidence level of 99% (see vertical line in color bar).

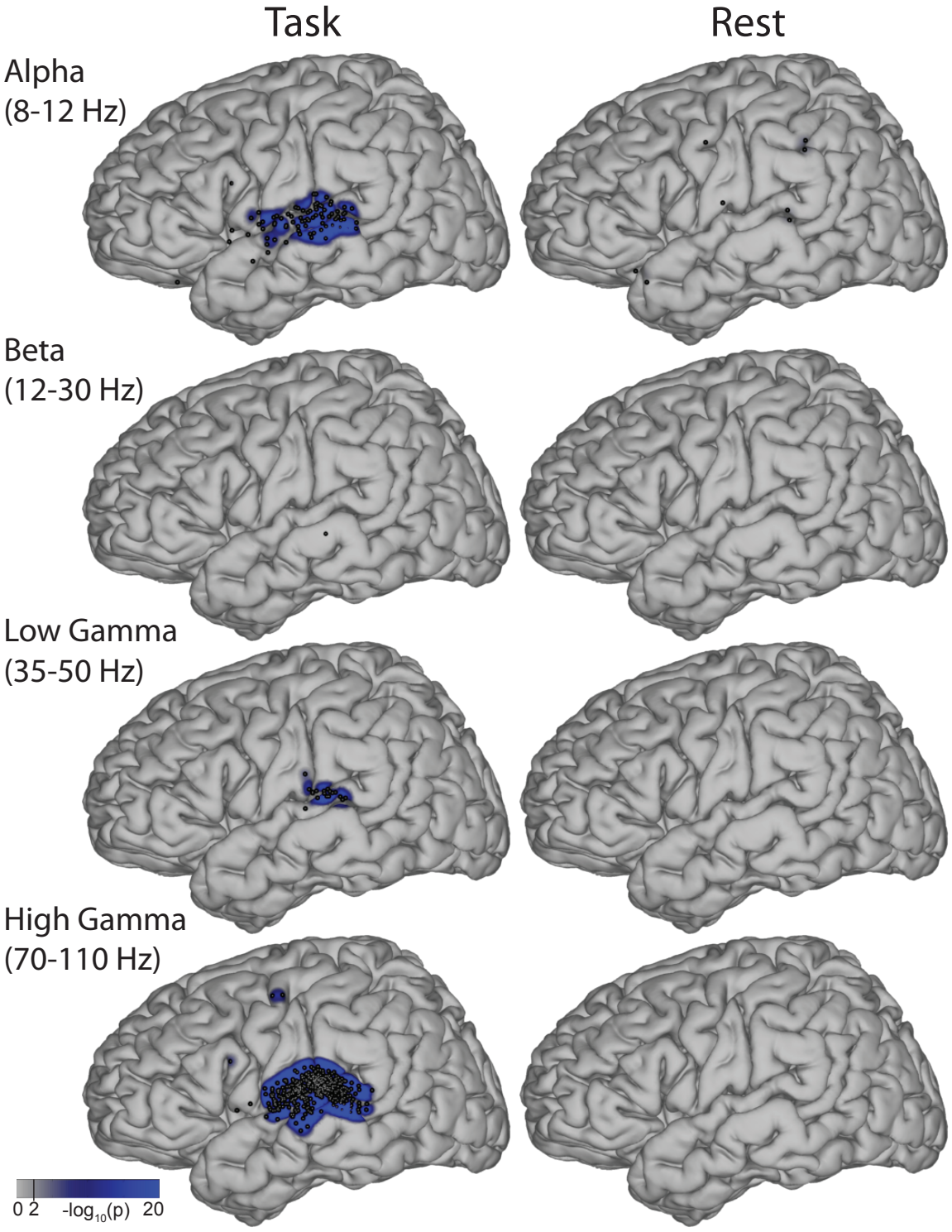

Figure 6.4: **Temporal relationship between alpha, high gamma, and sound intensity.** (A) Representative part of the time course of the sound intensity (black trace) and the average time course of ECoG gamma (blue trace) and alpha (red trace) activity. (B) Scatter plots illustrate the relationship between these three variables for all data points, as well as regression lines and their 95% confidence bands.

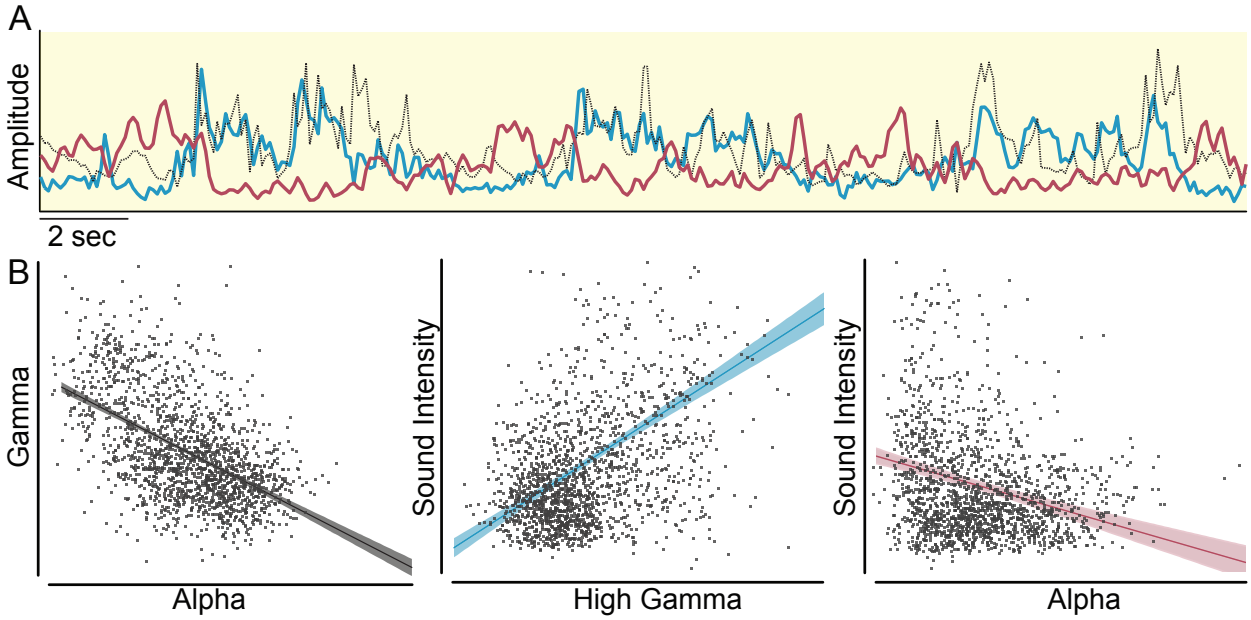

Figure 6.5: **Relationship between anatomy of auditory processing, current understanding of ECoG physiology, and results of this study.** (A) Auditory pathways between the medial geniculate nucleus of the thalamus and primary auditory cortex. Thalamic neurons (i.e., thalamo-cortical (TC) and reticular (R) neurons) are shown in gray, auditory cortex (AC) neurons are shown in blue, and their interactions are shown in red. (B) Top: Exemplary illustration of typical power spectral density of ECoG signals. Activity in the alpha (8-12 Hz) band, indicated by the red band, reflects thalamocortical interactions. Activity in the gamma (70-110 Hz) band, indicated by the blue band, indexes activity of local populations of neurons. Bottom: Average time course of the first 120 sec of ECoG activity. The blue trace gives gamma activity — the red trace gives alpha activity. (C) Outline of areas with significant ISC values in the alpha and gamma ECoG amplitudes given by the results in Fig. 6.3. Taken together, the results of this study are consistent with the hypothesis that auditory information reaches the cortex in areas close to auditory cortex, from where they are communicated to peri-sylvian and distinct frontal cortical locations (see illustrative yellow arrows).

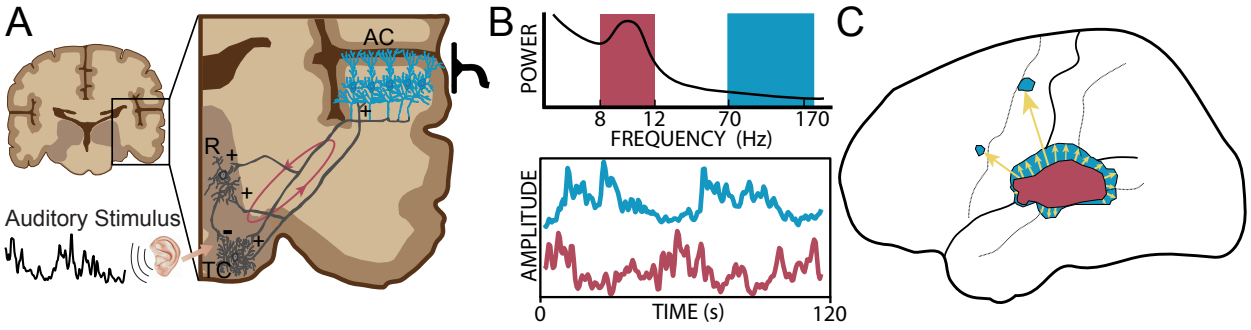

Figure 6.6: **Intersubject Granger causality analysis.** Causal relationships of activity in the high gamma band recorded during listening to music and between different pairs of electrode locations. Across all possible 630800 electrode combinations, only 68 connections were significant at $\alpha = 1.58e^{-8}$ after Bonferroni correction (A). These connections were further reduced to the ten most salient 10 connections (B). See text for details.

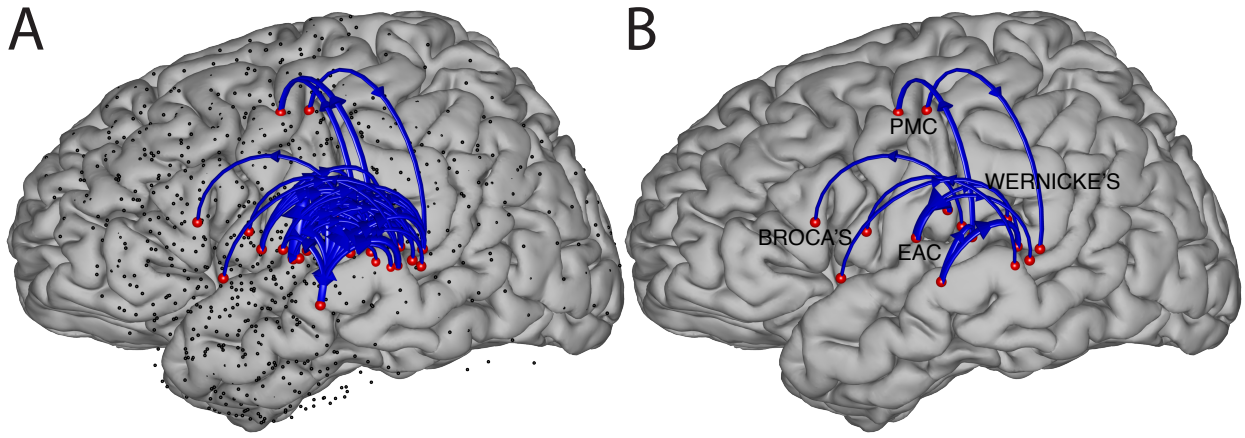

Figure 6.7: Intersubject Granger causality analysis during the task (left panels) and rest (right panels) conditions for ECoG activity in the alpha (8-12 Hz), beta (12-30 Hz), low gamma (35-50 Hz), and high gamma (70-110 Hz) frequency bands.

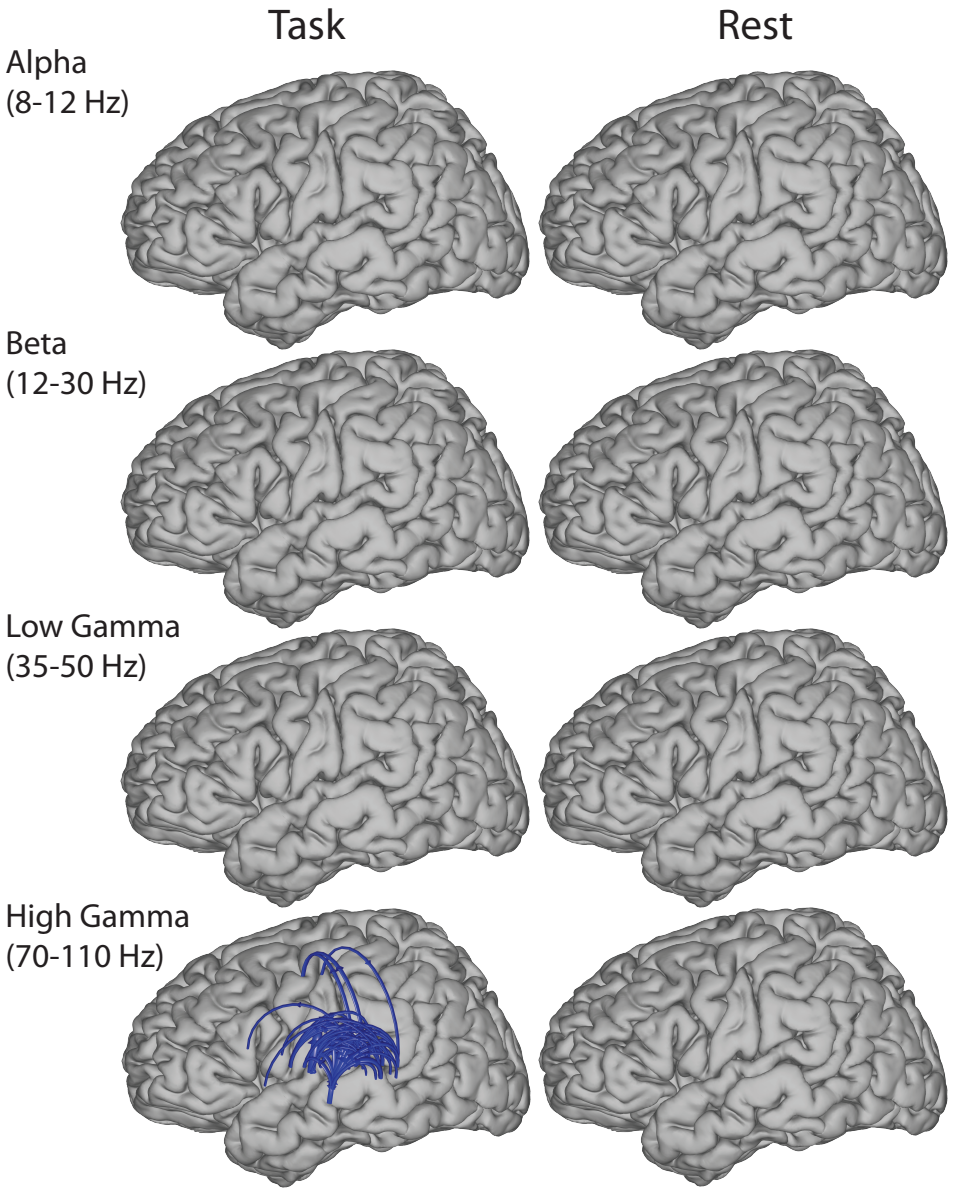

7

Conclusion and Future Work

In this dissertation, a general neuroimaging framework to identify the cortical areas and networks associated with specific functions of the brain was presented. This framework was applied to and validated in a specific auditory task. It can also be easily extended to other type of experiments. This framework includes novel methods to identify the most common aspects of task-related activity. These methods do not depend on prior knowledge of the stimulus or on recordings from the baseline period and are less susceptible to inclusion of brain activity that is unrelated to the task. To validate the methods proposed in this framework, electrical activity from the surface of the brain (ECoG) was recorded from ten patients with epilepsy while they were attentively listening to a continuous piece of music. The results presented here are not only consistent with previous auditory studies but also provide new information about the neural mechanisms engaged in music processing. The main points are summarized here:

- ✗ Unlike other neuroimaging techniques, ECoG can continuously track the temporal and spectral dynamics of the stimulus. Particularly, ECoG signals can encode the time-frequency characteristics of a continuous piece of music, as demonstrated in Chapter 5.

- ✗ ECoG can capture the underlying neurophysiological processes involved in auditory processing. In Chapter 6, experimental evidence was provided relating ECoG

activity in the alpha band with neural interactions between the thalamus and cortex, a process by which the auditory cortex is enabled to further process auditory information. Likewise, experimental evidence was provided, relating ECoG activity in the gamma band with neural interactions in the cortex.

- ✗ The music-related brain network identified with ECoG gamma activity is consistent with current functional models of auditory processing, and also points out an important and previously unrecognized cortical area (e.g.,the superior premotor cortex) involved in music processing.

7.1 Limitations

The present results are encouraging, and could not have been readily derived using other imaging techniques. At the same time, there will ultimately be limits to what can be achieved using the current subject population.

- ✗ The present results are derived from patients with epilepsy and cannot be easily generalized to non-epileptic individuals. Patients with epilepsy may have some degree of functional reorganization different from non-epileptic individuals.

- ✗ The placement of the electrode grids is based on the clinical needs of the patients for the localization of epileptic foci. These grids are usually placed only over one brain hemisphere. Most of the subjects in this study had coverage over the left hemisphere. Therefore, investigation of brain lateralization of auditory processing cannot be addressed with the current subject population.

- ✗ This study depends on the physical and cognitive conditions, and level of cooperation of each subject. These factors, in addition to the subject's specific neuroanatomy and grid location, might partially explain the variations in the functional mapping results across subjects.

✗ Access to patients with ECoG grids and the time with such subjects is very limited. Therefore, Recording of ECoG signals from a significant number of subjects could take one or two years.

7.2 Future Work

Despite these limitations, the results presented in this dissertation are consistent with expectations based on the neuroanatomy or on results from other imaging modalities. Based on these results, ECoG appears to be a powerful recording technique for capturing the high dynamics of neural activity. ECoG promises to have further clinical and research applications.

Clinical Applications

✗ To define whether a specific place in the cerebral cortex is eloquent (i.e., functional) or not depends on the patient's behavioral response after electrical cortical stimulation (ECS). The neurologist arbitrarily selects a pair of electrodes from the implanted grid and delivers mild electrical current. If there is a behavioral response (e.g., involuntary movement of the hand), it could be that any or both cortical sites under these two electrodes are eloquent. The same procedure is performed over and over again across all possible electrode pairs to identify the eloquent cortex. This is a very long and complex procedure since stimulation of all possible electrode pairs of the grid can take several (up to eight) hours and can even induce seizures. In addition of being extenuating and inefficient, this procedure completely overlooks the brain networks involved in a particular function. Also, the neurologist must constantly inspect the time traces of the electrical recordings to discern the responses of the brain to the electrical stimulation. The framework proposed in this dissertation can be used to resolve these issues and to complement

the mapping results. Use of ECoG would allow clinicians to map not only the cortical areas but also the cortical networks that are engaged when the patient executes a motor task, or perceives a sensory stimulus, or receives ECS. Identification of these cortical areas and networks could provide the clinician with the starting cortical sites for ECS and therefore expedite the mapping procedure. It could provide more insights into what is happening in the brain during ECS. Finally, and more importantly, it could reduce the rate of neurological deficits after brain resection.

✗ Another clinical application of the framework proposed in this dissertation could be in the field of auditory prosthetics. Cochlear implants are auditory prosthetics that convert sounds into electrical impulses to stimulate the cochlear nerve. Although cochlear implants can enhance hearing for the deaf, the sound information that is sent from the cochlear implant to the brain is limited. The decoding of different aspects of the acoustic signal (e.g., sound intensity, pitch, timbre) from brain signals could provide better understanding for the design of artificial cochlear devices.

Research Applications

✗ In this dissertation, a data-driven approach was proposed to extract the underlying cortical networks related to the processing of music. These cortical networks were not only consistent with current models of auditory function, but also highlighted an important area (premotor cortex) during listening to music. More experiments are needed to investigate the interactions between superior temporal gyrus (STG) and premotor cortex in auditory function. For example, to what extent could the functional connection between posterior STG and inferior frontal cortex be related to the processing of lyrics in the music.? Future studies could extend these methods to unveil the cortical networks related to other mental functions (e.g., language).

With further validation, the method described here may allow for a more direct verification and extension of the existing models of brain function.

✗ The results presented here show a negative correlation between high gamma and alpha activity. They also show that high gamma activity predicts alpha activity and precedes it by 280 ms. Hence, it is logical to think that higher gamma amplitudes, which have been shown to be related to higher stimulus intensity (Potes et al., 2012), lead to decrease in alpha amplitudes presumably related to an increase in cortical excitability. This evidence provides a link between higher stimulus intensity and higher cortical excitability. Thus, it may suggest a general mechanism for prioritizing different competing sensory streams, and could also be useful in explaining different types of stimulus-driven or internally-generated (covert or overt) forms of attention. Future studies could be designed to test whether alpha activity may be the mechanism by which the brain facilitates transfer of information to the cortex.

✗ Typical neuroscience studies begin with a very specific hypothesis followed by the design of an experiment and collection of data. This scientific approach, known as hypothesis-driven analysis, has led to highly controlled experiments using artificial stimuli (e.g., responses of the brain to tones at different intensities or frequencies). This is unfortunate, because cortical processing of artificial stimuli may differ in important ways from the processing of complex natural stimuli (such as music), and because evidence suggests that the brain employs additional principles that govern the processing of complex natural stimuli (Hasson, 2010; Hasson et al., 2004). Hypothesis-driven analysis also leads to ignoring variables rather than reduction of variables. On the other hand, data-driven analysis leads to identifying questions and variables that could not be identified if it were merely driven by the hypothesis. The results presented here advocate for analyses that are driven not

only by the hypothesis but also by the data. In addition, the results point to the need for more natural paradigms rather than artificial stimuli. (See Fig. 7.1)

✗ A brain computer interface (BCI) is technology that translates brain signals into commands for controlling an external device. To accurately decode the user's intention, a BCI must be able to extract the appropriate features from the brain signals. Currently, the only features that are incorporated in a BCI rely on the time (P300-based BCIs) or frequency (motor imagery-based BCIs) profiles of the brain signal. With the methods explained here, additional features such as dynamic changes across different regions of the brain could improve the performance of the BCIs.

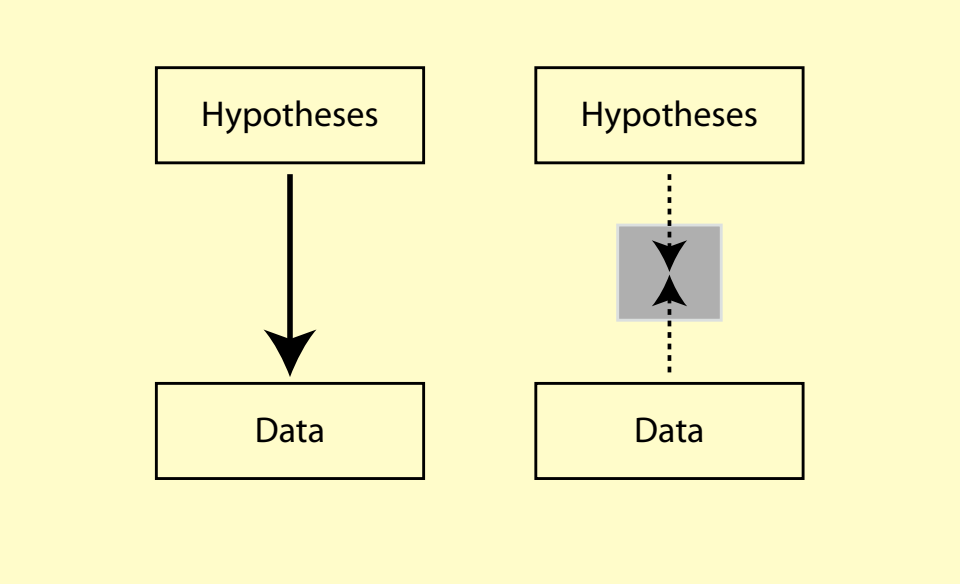

Figure 7.1: **Hypothesis-driven analysis vs. Data-driven analysis.** The results shown in this dissertation advocate for the use of hypothesis-driven and data-driven analyses in further neuroscience studies.

Bibliography

Aine, C. J. (1995). A conceptual overview and critique of functional neuroimaging techniques in humans: I. MRI/fMRI and PET. *Crit Rev Neurobiol*, 9(2-3):229–309. (cited on pages 17 and 67)

Aldrich, J. (1995). Correlations Genuine and Spurious in Pearson and Yule. *Statistical Science*, 10(4):364–376. (cited on page 48)

Anderson, J. R. (2004). *Cognitive Psychology and Its Implications*. Worth Publishers, seventh edition edition. (cited on pages 2 and 19)

Baars, B. J. and Cage, N. M. (2010). *Cognition, Brain, and Consciousness. Introduction to Cognitive Neuroscience*. Academic Press. (cited on pages 1 and 15)

Ball, T., Kern, M., Mutschler, I., Aertsen, A., and Schulze-Bonhage, A. (2009). Signal quality of simultaneously recorded invasive and non-invasive EEG. *NeuroImage*, 46(3):708–716. (cited on page 14)

Belin, P., McAdams, S., Smith, B., Savel, S., Thivard, L., Samson, S., and Samson, Y. (1998). The functional anatomy of sound intensity discrimination. *J Neurosci*, 18(16):6388–6394. (cited on page 78)

Bendor, D. and Wang, X. (2005). The neuronal representation of pitch in primate auditory cortex. *Nature*, 436(7054):1161–1165. (cited on pages 58 and 60)

Bendor, D. and Wang, X. (2006). Cortical representations of pitch in monkeys and humans. *Current opinion in neurobiology*, 16(4):391–9. (cited on pages 58 and 60)

Berger, H. (1929). Ueber das Electroenkephalogramm des Menschen. *Arch Psychiat Nervenkr*, 87:527–570. (cited on page 14)

Bilecen, D., Scheffler, K., Schmid, N., Tschopp, K., and Seelig, J. (1998). Tonotopic organization of the human auditory cortex as detected by BOLD-fMRI. *Hear Res*, 126(1-2):19–27. (cited on page 3)

Bilecen, D., Seifritz, E., Scheffler, K., Henning, J., and Schulte, A.-C. (2002). Amplitopicity of the human auditory cortex: an fMRI study. *Neuroimage*, 17(2):710–8. (cited on pages 58 and 60)

Binder, J. R., Frost, J. A., Hammeke, T. A., Bellgowan, P. S., Springer, J. A., Kaufman, J. N., and Possing, E. T. (2000). Human temporal lobe activation by speech and nonspeech sounds. *Cereb Cortex*, 10(5):512–28. (cited on page 3)

Boatman-Reich, D., Franaszczuk, P. J., Korzeniewska, A., Caffo, B., Ritzl, E. K., Colwell, S., and Crone, N. E. (2010). Quantifying auditory event-related responses in multichannel human intracranial recordings. *Front Comput Neurosci*, 4:4. (cited on page 67)

Brechmann, A., Baumgart, F., and Scheich, H. (2002). Sound-level-dependent representation of frequency modulations in human auditory cortex: a low-noise fMRI study. *J Neurophysiol*, 87(1):423–33. (cited on pages 66, 75, and 83)

Brix, G., Nekolla, E. A., Nosske, D., and Griebel, J. (2009). Risks and safety aspects related to PET/MR examinations. *European Journal of Nuclear Medicine and Molecular Imaging*, 36 Suppl 1(Suppl 1):S131–S138. (cited on page 21)

Broca, P. (1861). Remarques sur le siège de la faculté du langage articule suivies d'une observation d'aphemie. *Bull Soc Anat Paris*, 6:330–357. (cited on page 1)

Brunner, P. (2013). *Improved Methods for the Application of Brain Signals to Communication and Diagnosis*. PhD thesis, Graz University of Technology, Graz. (cited on pages 16, 27, and 45)

Brunner, P., Ritaccio, A. L., Emrich, J. F., Bischof, H., and Schalk, G. (2011). Rapid communication with a "P300" matrix speller using electrocorticographic signals (ECoG). *Frontiers in Neuroscience*, 5(February):5. (cited on page 53)

Brunner, P., Ritaccio, A. L., Lynch, T. M., Emrich, J. F., Wilson, J. A., Williams, J. C., Aarnoutse, E. J., Ramsey, N. F., Leuthardt, E. C., Bischof, H., and Schalk, G. (2009). A practical procedure for real-time functional mapping of eloquent cortex using electrocorticographic signals in humans. *Epilepsy and Behavior*, 15:278–286. (cited on pages 14, 36, 42, 52, 76, and 82)

Calford, M. B. and Aitkin, L. M. (1983). Ascending projections to the medial geniculate body of the cat: evidence for multiple, parallel auditory pathways through thalamus. *Journal of Neuroscience*, 3(11):2365–2380. (cited on page 63)

Canolty, R. T., Edwards, E., Dalal, S. S., Soltani, M., Nagarajan, S. S., Kirsch, H. E., Berger, M. S., Barbaro, N. M., and Knight, R. T. (2006). High gamma power is phase-locked to theta oscillations in human neocortex. *Science*, 313(5793):1626–1628. (cited on pages 26 and 30)

Canolty, R. T. and Knight, R. T. (2010). The functional role of cross-frequency coupling. *Trends in Cognitive Sciences*, 14(11):506–515. (cited on pages 26, 30, and 33)

Cardin, J. A., Carlén, M., Meletis, K., Knoblich, U., Zhang, F., Deisseroth, K., Tsai, L.-H., and Moore, C. I. (2009). Driving fast-spiking cells induces gamma rhythm and controls sensory responses. *Nature*, 459(7247):663–667. (cited on page 96)

Caton, R. (1875). The electric currents of the brain. *British Medical Journal*, 2(1):278. (cited on page 9)

Chen, J. L., Penhune, V. B., and Zatorre, R. J. (2008). Listening to musical rhythms recruits motor regions of the brain. *Cerebral Cortex*, 18(12):2844–54. (cited on page 3)

Chen, J. L., Penhune, V. B., and Zatorre, R. J. (2009). The role of auditory and premotor cortex in sensorimotor transformations. *Ann N Y Acad Sci*, 1169:15–34. (cited on pages 75 and 76)

Chittka, L. and Brockmann, A. (2005). Perception Space—The Final Frontier. *PLoS Biology*, 3(4):e137. (cited on page 61)

Cohen, D. (1972). Magnetoencephalography: detection of the brain's electrical activity with a superconducting magnetometer. *Science (New York, N.Y.)*, 175(22):664–666. (cited on page 2)

Cohen, D. and Cuffin, B. N. (1983). Demonstration of useful differences between magnetoencephalogram and electroencephalogram. *Electroencephalography and Clinical Neurophysiology*, 56(1):38–51. (cited on page 15)

Colin, C. and Frank, W. (1997). An r-squared measure of goodness of fit for some common nonlinear regression models. *Journal of Econometrics*, 77:329–42. (cited on page 90)

Crone, N. E., Boatman, D., Gordon, B., and Hao, L. (2001). Induced electrocorticographic gamma activity during auditory perception. *Clin Neurophysiol*, 112(4):565–82. (cited on pages 44, 67, 84, 93, and 96)

Crone, N. E., Miglioretti, D. L., Gordon, B., and Lesser, R. P. (1998a). Functional mapping of human sensorimotor cortex with electrocorticographic spectral analysis ii. event-

related synchronization in the gamma band. *Brain*, 121(2301–15). (cited on pages 25, 30, 44, 84, and 96)

Crone, N. E., Miglioretti, D. L., Gordon, B., Sieracki, J. M., Wilson, M. T., Uematsu, S., and Lesser, R. P. (1998b). Functional mapping of human sensorimotor cortex with electrocorticographic spectral analysis. I. Alpha and beta event-related desynchronization. *Brain*, 121 (Pt 12):2271–2299. (cited on pages 25 and 44)

da Silva, F. H. L., van Lierop, T. H. M. T., Schrijer, C. F., and van Leeuven, W. S. (1973). Organization of thalamic and cortical alpha rythms: Spectra and coherences. *Electroencephalography and Clinical Neurophysiology*, 35:627–39. (cited on pages 29 and 96)

da Silva, F. L. (1991). Neural mechanisms underlying brain waves: from neural membranes to networks. *Electroencephalography and Neurophysiology*, 79:81–93. (cited on pages 84 and 96)

Desmedt, J. E., Chalklin, V., and Tomberg, C. (1990). Emulation of somatosensory evoked potential (SEP) components with the 3-shell head model and the problem of 'ghost potential fields' when using an average reference in brain mapping. *Electroencephalography and Clinical Neurophysiology*, 77(4):243–258. (cited on page 43)

Durbin, J. and Watson, G. S. (1950). Testing for serial correlation in least squares regression. II. *Biometrika*, 37(3-4):409–428. (cited on page 90)

Edwards, E., Nagarajan, S., Dalal, S., Canolty, R., Kirsch, H., Barbaro, N., and Knight, R. (2010). Spatiotemporal imaging of cortical activation during verb generation and picture naming. *Neuroimage*, 50(1):291–301. (cited on pages 14, 75, and 76)

Edwards, E., Soltani, M., Deouell, L. Y., Berger, M. S., and Knight, R. T. (2005). High gamma activity in response to deviant auditory stimuli recorded directly from human cortex. *J Neurophysiol*, 94(6):4269–4280. (cited on page 67)

Edwards, E., Soltani, M., Kim, W., Dalal, S. S., Nagarajan, S. S., Berger, M. S., and Knight, R. T. (2009). Comparison of time-frequency responses and the event-related potential to auditory speech stimuli in human cortex. *J Neurophysiol*, 102(1):377–386. (cited on pages 67 and 84)

Ferrea, E., Maccione, A., Medrihan, L., Nieus, T., Ghezzi, D., Baldelli, P., Benfenati, F., and Berdondini, L. (2012). Large-scale, high-resolution electrophysiological imaging of field potentials in brain slices with microelectronic multielectrode arrays. *Frontiers in Neural Circuits*, 6(80). (cited on page 13)

Florian, G. and Pfurtscheller, G. (1995). Dynamic spectral analysis of event-related EEG data. *Electroencephalography and Clinical Neurophysiology*, 95(5):393–396. (cited on page 47)

Freeman, W. J. (2004). Origin, structure, and role of background EEG activity. Part 1. Analytic amplitude. *Clinical Neurophysiology*, 115(9):2077–2088. (cited on page 14)

Fries, P., Reynolds, J. H., Rorie, A. E., and Desimone, R. (2001). Modulation of oscillatory neuronal synchronization by selective visual attention. *Science*, 291(5508):1560–1563. (cited on page 32)

Fritsch, G. T. and Hitzig, E. (1870). Ueber die elektrische Erregbarkeit des Grosshirns. *Archiv fuer Anatomie, Physiologie und wissenschaftliche Medicin*, pages 300–332. (cited on page 1)

Gaona, C. M., Sharma, M., Freudenburg, Z. V., Breshears, J. D., Bundy, D. T., Roland, J., Barbour, D. L., Schalk, G., and Leuthardt, E. C. (2011). Nonuniform High-Gamma (60-500 Hz) Power Changes Dissociate Cognitive Task and Anatomy in Human Cortex. *J. Neurosci.*, 31(6):2091–2100. (cited on page 25)

Givens, B., Williams, J., and Gill, T. M. (1998). Cognitive correlates of single neuron ac-

tivity in task-performing animals: Application to ethanol research. *Alcoholism: Clinical and Experimental Research*, 22(1):23–31. (cited on page 13)

Gourévitch, B., Le Bouquin Jeannès, R., Faucon, G., and Liégeois-Chauvel, C. (2008). Temporal envelope processing in the human auditory cortex: response and interconnections of auditory cortical areas. *Hear Res*, 237(1-2):1–18. (cited on page 78)

Granger, C. W. J. (1969). Investigating causal relations by econometric models and cross-spectral methods. *Econometrica*, 37(3):424–38. (cited on pages 51, 52, and 89)

Greenblatt, R. E., Pflieger, M. E., and Ossadtchi, A. E. (2012). Connectivity measures applied to human brain electrophysiological data. *Journal of Neuroscience Methods*, 207(1):1–16. (cited on page 51)

Griffiths, T. D. and Warren, J. D. (2002). The planum temporale as a computational hub. *Trends Neurosci*, 25(7):348–353. (cited on pages 62, 75, 77, 94, and 97)

Griffiths, T. D. and Warren, J. D. (2004). What is an auditory object? *Nat Rev Neurosci*, 5(11):887–92. (cited on page 66)

Gunduz, A., Brunner, P., Daitch, A., Leuthardt, E., Ritaccio, A., Pesaran, B., and Schalk, G. (2011). Neural correlates of visual–spatial attention in electrocorticographic signals in humans. *Frontiers in Human Neuroscience*, 5:1–11. (cited on pages 30 and 73)

Hackett, T. A. (2008). Anatomical organization of the auditory cortex. *J Am Acad Audiol*, 19:774–779. (cited on pages 94 and 97)

Hackett, T. A. (2011). Information flow in the auditory cortical network. *Hearing Research*, 271(1-2):133–146. (cited on page 60)

Haegens, S., Nacher, V., Luna, R., Romo, R., and Jensen, O. (2011). Alpha-oscillations in the monkey sensorimotor network influence discrimination performance by rhythmi-

cal inhibition of neuronal spiking. *Proc Natl Acad Sci USA*, 108(48):19377–19382. (cited on page 96)

Haley, H., Dana, B., and Brian, C. (2010). Estimating temporal associations in electrocorticographic (ecog) time series with first order pruning. *Johns Hopkins University, Dept. of Biostatistics Working Papers*. (cited on page 90)

Hämäläinen, M., Hari, R., Ilmoniemi, R. J., Knuutila, J., and Lounasmaa, O. V. (1993). Magnetoencephalography—theory, instrumentation, and applications to noninvasive studies of the working human brain. *Reviews of Modern Physics*, 65(2):413–497. (cited on page 21)

Hart, H. C., Hall, D. A., and Palmer, A. R. (2003). The sound-level-dependent growth in the extent of fMRI activation in Heschl's gyrus is different for low- and high-frequency tones. *Hear Res*, 179(1-2):104–12. (cited on pages 67, 75, and 83)

Hasson, U. (2010). I can make your brain look like mine. http://www.hbr.org. (cited on page 107)

Hasson, U., Malach, R., and Heeger, D. J. (2010). Reliability of cortical activity during natural stimulation. *Trends Cogn Sci*, 1:40–8. (cited on pages 84 and 88)

Hasson, U., Nir, Y., Levy, I., Fuhrmann, G., and Malach, R. (2004). Intersubject synchronization of cortical activity during natural vision. *Science*, 303:1634–1640. (cited on pages 84, 88, and 107)

He, B. J., Zempel, J. M., Snyder, A. Z., and Raichle, M. E. (2010). The temporal structures and functional significance of scale-free brain activity. *Neuron*, 66(3):353–369. (cited on pages 26 and 30)

Hennig, J., Speck, O., Koch, M. A., and Weiller, C. (2003). Functional magnetic reso-

nance imaging: a review of methodological aspects and clinical applications. *Journal of Magnetic Resonance Imaging*, 18(1):1–15. (cited on page 21)

Hermes, D., Miller, K. J., Vansteensel, M. J., Aarnoutse, E. J., Leijten, F. S. S., and Ramsey, N. F. (2011). Neurophysiologic correlates of fMRI in human motor cortex. *Human Brain Mapping*. (cited on pages 77 and 84)

Hill, N. J., Gupta, D., Brunner, P., Gunduz, A., Adamo, M. A., Ritaccio, A., and Schalk, G. (2012). Recording human electrocorticographic (ECoG) signals for neuroscientific research and real-time functional cortical mapping. *Journal of visualized experiments JoVE*, 1(64). (cited on page 14)

Huetel, S. A., Song, A. W., and McCarthy, G. (2009). *Functional Magnetic Resonance Imaging*. Sinauer. (cited on page 15)

Hughes, S. W. and Crunelli, V. (2005). Thalamic mechanisms of EEG alpha rhythms and their pathological implications. *The Neuroscientist a review journal bringing neurobiology neurology and psychiatry*, 11(4):357–372. (cited on page 96)

Humphrey, D. R. and Schmidt, E. M. (1991). *Neurophysiological Techniques*, volume 15 of *Neuromethods*. Humana Press. (cited on page 13)

Hwang, H.-J., Kim, K.-H., Jung, Y.-J., Kim, D.-W., Lee, Y.-H., and Im, C.-H. (2011). An EEG-based real-time cortical functional connectivity imaging system. *Medical & Biological Engineering & Computing*, 49(9):985–995. (cited on page 3)

Ioannides, A. A. (2006). Magnetoencephalography as a research tool in neuroscience: state of the art. *The Neuroscientist a review journal bringing neurobiology neurology and psychiatry*, 12(6):524–544. (cited on pages 15 and 21)

Jäncke, L., Shah, N. J., Posse, S., Grosse-Ryuken, M., and Müller-Gärtner, H. W. (1998).

Intensity coding of auditory stimuli: an fMRI study. *Neuropsychologia*, 36(9):875–883. (cited on pages 58, 66, 75, and 77)

Jensen, O. and Mazaheri, A. (2010). Shaping functional architecture by oscillatory alpha activity: gating by inhibition. *Frontiers in Human Neuroscience*, 4(186):1–8. (cited on pages 30 and 84)

Johnsrude, I. S., Penhune, V. B., and Zatorre, R. J. (2000). Functional specificity in the right human auditory cortex for perceiving pitch direction. *Brain: A journal of neurology*, 123 (Pt 1(1):155–163. (cited on pages 58 and 60)

Kaas, J. H. and Hackett, T. A. (1999). "What" and "Where" processing in auditory cortex. *Nat Neurosci*, 2(12):1045–7. (cited on page 97)

Katzner, S., Nauhaus, I., Benucci, A., Bonin, V., Ringach, D. L., and Carandini, M. (2009). Local origin of field potentials in visual cortex. *Neuron*, 61(1):35–41. (cited on page 13)

Kellis, S. S., House, P. A., Thomson, K. E., Brown, R., and Greger, B. (2009). Human neocortical electrical activity recorded on nonpenetrating microwire arrays: applicability for neuroprostheses. *Neurosurg Focus*, 27(1):E9. (cited on page 78)

Kimberley, T. J. and Lewis, S. M. (2007). Understanding neuroimaging. *Physical Therapy*, 87(6):670–683. (cited on pages 16, 19, and 20)

Korzeniewska, A., Franaszczuk, P. J., Crainiceanu, C. M., Kuś, R., and Crone, N. E. (2011). Dynamics of large-scale cortical interactions at high gamma frequencies during word production: event related causality (ERC) analysis of human electrocorticography (ECoG). *NeuroImage*, 56(4):2218–2237. (cited on page 4)

Krusienski, D. J., McFarland, D. J., and Wolpaw, J. R. (2006). An Evaluation of Autoregressive Spectral Estimation Model Order for Brain-Computer Interface Applications.

Conference Proceedings of the International Conference of IEEE Engineering in Medicine and Biology Society, 1:1323–1326. (cited on page 47)

Kubánek, J., Miller, K. J., Ojemann, J. G., Wolpaw, J. R., and Schalk, G. (2009). Decoding flexion of individual fingers using electrocorticographic signals in humans. *J Neural Eng*, 6(6):066001. (cited on pages 3, 14, 19, 26, 30, 73, and 96)

Kumar, S., Stephan, K. E., Warren, J. D., Friston, K. J., and Griffiths, T. D. (2007). Hierarchical processing of auditory objects in humans. *PLoS Comput Biol*, 3(6):e100. (cited on pages 66 and 97)

Lachaux, J.-P., Fonlupt, P., Kahane, P., Minotti, L., Hoffmann, D., Bertrand, O., and Baciu, M. (2007a). Relationship between task-related gamma oscillations and BOLD signal: new insights from combined fMRI and intracranial EEG. *Hum Brain Mapp*, 28(12):1368–75. (cited on pages 26, 67, and 77)

Lachaux, J.-P., Jerbi, K., Bertrand, O., Minotti, L., Hoffmann, D., Schoendorff, B., and Kahane, P. (2007b). A blueprint for real-time functional mapping via human intracranial recordings. *PLoS ONE*, 2(10):e1094. (cited on page 84)

Lancaster, J. L., Woldorff, M. G., Parsons, L. M., Liotti, M., Freitas, C. S., Rainey, L., Kochunov, P. V., Nickerson, D., Mikiten, S. A., and Fox, P. T. (2000). Automated Talairach atlas labels for functional brain mapping. *Hum Brain Mapp*, 10(3):120–31. (cited on page 70)

Langers, D. R. M., van Dijk, P., Schoenmaker, E. S., and Backes, W. H. (2007). fMRI activation in relation to sound intensity and loudness. *Neuroimage*, 35(2):709–18. (cited on pages 58, 66, 75, and 77)

Lauren, S., von Kriegstein Katharina, Jason, W. D., and Timothy, G. (2006). Music and the brain: disorders of musical listening. *Brain*, 129:2533–53. (cited on page 83)

Leaver, A. M. and Rauschecker, J. P. (2010). Cortical representation of natural complex sounds: effects of acoustic features and auditory object category. *J Neurosci*, 30(22):7604–12. (cited on page 66)

Lee, C. C. (2012). Thalamic and cortical pathways supporting auditory processing. *Brain and Language*. (cited on pages 62, 63, and 64)

Lee, C. C. and Sherman, S. M. (2008). Synaptic properties of thalamic and intracortical inputs to layer 4 of the first- and higher-order cortical areas in the auditory and somatosensory systems. *Journal of Neurophysiology*, 100(1):317–326. (cited on pages 62 and 63)

Lee, C. C. and Sherman, S. M. (2009). Modulator Property of the Intrinsic Cortical Projection from Layer 6 to Layer 4. *Frontiers in systems neuroscience*, 3(February):5. (cited on pages 62 and 63)

Leuthardt, E. C., Schalk, G., Wolpaw, J. R., Ojemann, J. G., and Moran, D. W. (2004). A brain–computer interface using electrocorticographic signals in humans. *Journal of Neural Engineering*, 1(2):63. (cited on page 14)

Little, A. S., Smith, K. A., Lekovic, G. P., Triman, D. M., Porter, R. W., and Shetter, A. G. (2008). Functional cortical mapping using subdural grid electrodes in patients with low-grade gliomas presenting with seizure. *Barrow Quarterly*, 24(1):4–8. (cited on page 6)

Llinás, R. (2003). Consciousness and the thalamocortical loop. *International Congress Series*, 1250:409–416. (cited on pages 28 and 31)

Llinás, R. R. and Ribary, U. (1998). Temporal conjunction in thalamocortical transactions. *Adv Neurol*, 77(95–102). (cited on page 28)

Llinás, R. R., Ribary, U., Jeanmonod, D., Kronberg, E., and Mitra, P. P. (1999). Thalamocortical dysrhythmia: A neurological and neuropsychiatric syndrome characterized by magnetoencephalography. *Proc Natl Acad Sci USA*, 96(26):15222–27. (cited on pages 28 and 94)

Logothetis, N. K. (2008). What we can do and what we cannot do with fMRI. *Nature*, 453(7197):869–878. (cited on pages 13, 17, and 67)

Logothetis, N. K., Pauls, J., Augath, M., Trinath, T., and Oeltermann, A. (2001). Neurophysiological investigation of the basis of the fMRI signal. *Nature*, 412(6843):150–7. (cited on pages 13, 17, and 77)

Lopes Da Silva, F. H. and Storm Van Leeuwen, W. (1977). The cortical source of the alpha rhythm. (cited on pages 29 and 30)

Ludwig, K. A., Miriani, R. M., Langhals, N. B., Joseph, M. D., Anderson, D. J., and Kipke, D. R. (2009). Using a Common Average Reference to Improve Cortical Neuron Recordings From Microelectrode Arrays. *Journal of Neurophysiology*, 101(3):1679–1689. (cited on page 43)

Manning, J. R., Jacobs, J., Fried, I., and Kahana, M. J. (2009). Broadband shifts in local field potential power spectra are correlated with single-neuron spiking in humans. *J Neurosci*, 29(43):13613–20. (cited on pages 32, 33, and 77)

Mantini, D., Hasson, U., Betti, V., Perrucci, M. G., Romani, G. L., Corbetta, M., Orban, G. A., and Vanduffel, W. (2012). Interspecies activity correlations reveal functional correspondence between monkey and human brain areas. *Nature Methods*, 9(3):277–82. (cited on page 97)

Margalit, E., Weiland, J. D., Clatterbuck, R. E., Fujii, G. Y., Maia, M., Tameesh, M., Torres, G., D'Anna, S. A., Desai, S., Piyathaisere, D. V., Olivi, A., De Juan, E., and Humayun,

M. S. (2003). Visual and electrical evoked response recorded from subdural electrodes implanted above the visual cortex in normal dogs under two methods of anesthesia. *Journal of Neuroscience Methods*, 123(2):129–37. (cited on pages 14 and 24)

Miller, K., Leuthardt, E., Schalk, G., Rao, R., Anderson, N., Moran, D., Miller, J., and Ojemann, J. (2007). Spectral changes in cortical surface potentials during motor movement. *The Journal of neuroscience*, 27(9):2424. (cited on pages 6, 26, 30, 71, and 84)

Miller, K. J. (2010). Broadband spectral change: evidence for a macroscale correlate of population firing rate? *J Neurosci*, 30(19):6477–9. (cited on pages 32, 33, 34, 77, 94, and 96)

Miller, K. J., Sorensen, L. B., Ojemann, J. G., and den Nijs, M. (2009). Power-law scaling in the brain surface electric potential. *PLoS Comput Biol*, 5:1–10. (cited on pages 30, 84, 94, and 96)

Mingzhou, D., Steven, B., Weiming, Y., and Hualou, L. (2000). Short-window spectral analysis of cortical event-related potentials by adaptive multivariate autoregressive modeling: data preprocessing, model validation, and variability assessment. *Biol. Cybern*, 83:35–45. (cited on page 90)

Mulert, C., Jäger, L., Propp, S., Karch, S., Störmann, S., Pogarell, O., Möller, H., Juckel, G., and Hegerl, U. (2005). Sound level dependence of the primary auditory cortex: Simultaneous measurement with 61-channel EEG and fMRI. *Neuroimage*, 28(1):49–58. (cited on pages 66, 75, and 83)

Myers, J. L. and Well, A. D. (2003). *Research Design and Statistical Analysis*. Lawrence Erlbaum Associates. (cited on page 49)

Nicolelis, M. A. (2001). Actions from thoughts. *Nature*, 409(6818):403–7. (cited on page 13)

Niedermeyer, E. and Lopes da Silva, F. H. (2005). *Electroencephalography: Basic Principles, Clinical Applications and Related Fields.* Williams and Wilkins, Baltimore, MD. (cited on page 25)

Niessing, J., Ebisch, B., Schmidt, K. E., Niessing, M., Singer, W., and Galuske, R. A. W. (2005). Hemodynamic signals correlate tightly with synchronized gamma oscillations. *Science*, 309(5736):948–951. (cited on page 26)

Nunez, P. L., Silberstein, R. B., Cadusch, P. J., Wijesinghe, R. S., Westdorp, A. F., and Srinivasan, R. (1994). A theoretical and experimental study of high resolution EEG based on surface Laplacians and cortical imaging. *Electroencephalography and Clinical Neurophysiology*, 90(1):40–57. (cited on page 43)

Nunez, P. L. and Srinivasan, R. (2005). *Electric fields of the brain: The neurophysics of EEG*. Oxford University Press. (cited on page 67)

Ogawa, S., Lee, T. M., Kay, A. R., and Tank, D. W. (1990). Brain magnetic resonance imaging with contrast dependent on blood oxygenation. *Proceedings of the National Academy of Sciences of the United States of America*, 87(24):9868–9872. (cited on page 2)

Pasley, B. N., David, S. V., Mesgarani, N., Flinker, A., Shamma, S. A., Crone, N. E., Knight, R. T., and Chang, E. F. (2012). Reconstructing speech from human auditory cortex. *PLoS Biol*, 10(1):e1001251. (cited on pages 14, 67, 71, and 84)

Pei, X., Barbour, D., Leuthardt, E., and Schalk, G. (2011). Decoding vowels and consonants in spoken and imagined words using electrocorticographic signals in humans. *Journal of Neural Engineering*, 8:046028. (cited on pages 14, 30, and 71)

Pei, X., Leuthardt, E. C., Gaona, C. M., Brunner, P., Wolpaw, J. R., and Schalk, G. (2010). Spatiotemporal dynamics of electrocorticographic high gamma activity during overt and covert word repetition. *Neuroimage*. (cited on page 30)

Penagos, H., Melcher, J. R., and Oxenham, A. J. (2004). A neural representation of pitch salience in nonprimary human auditory cortex revealed with functional magnetic resonance imaging. *Journal of Neuroscience*, 24(30):6810–6815. (cited on pages 58 and 60)

Penfield, W. and Boldrey, E. (1937). Somatic motor and sensory representation in the cerebral cortex of man as studied by electrical stimulation. *Brain*, 60:389–443. (cited on page 23)

Penfield, W., Erickson, T., and Thomas, C. (1942). Epilepsy and cerebral localization: a study of the mechanism, treatment and prevention of epileptic seizures. *Arch Intern Med*, 70:916–917. (cited on page 23)

Penfield, W. and Rasmussen, T., editors (1950). *The Cerebral Cortex of Man*. MacMillan, New York. (cited on page 23)

Pesaran, B., Pezaris, J. S., Sahani, M., Mitra, P. P., and Andersen, R. A. (2002). Temporal structure in neuronal activity during working memory in macaque parietal cortex. *Nature Neuroscience*, 5(8):805–811. (cited on page 32)

Pfurtscheller, G. and Aranibar, A. (1977). Event-related cortical desynchronization detected by power measurements of scalp EEG. *Electroencephalography and Clinical Neurophysiology*, 42(5):817–826. (cited on page 25)

Pfurtscheller, G. and Lopes da Silva, F. (1999). *Event-related desynchronization.*, volume 5. Elsevier, Amsterdam. (cited on page 25)

Pfurtscheller, G. and Lopes Da Silva, F. H. (1999). Event-related EEG/MEG synchronization and desynchronization: basic principles. *Clinical Neurophysiology*, 110(11):1842–1857. (cited on page 25)

Pilcher, W. H. and Rusyniak, W. G. (1993). Complications of epilepsy surgery. *Neurosurgery Clinics Of North America*, 4(2):311–325. (cited on pages 14 and 24)

Platel, H., Price, C., Baron, J. C., Wise, R., Lambert, J., Frackowiak, R. S., Lechevalier, B., and Eustache, F. (1997). The structural components of music perception. A functional anatomical study. *Brain*, 120 (Pt 2):229–43. (cited on pages 66 and 78)

Popescu, M., Otsuka, A., and Ioannides, A. (2004). Dynamics of brain activity in motor and frontal cortical areas during music listening: a magnetoencephalographic study. *Neuroimage*, 21(4):1622–1638. (cited on pages 3, 75, and 77)

Potes, C., Brunner, P., Gunduz, A., Knight, R. T., and Schalk, G. (2013). Spatial and temporal relationships of electrocorticography alpha and gamma activity during music processing. *Neuroimage*. (cited on pages 3, 4, 8, and 48)

Potes, C., Gunduz, A., Brunner, P., and Schalk, G. (2012). Dynamics of electrocorticographic (ECoG) activity in human temporal and frontal cortical areas during music listening. *Neuroimage*, 61(4):841–48. (cited on pages 3, 8, 19, 26, 48, 58, 60, 61, 88, 93, 96, 97, and 107)

Rauschecker, J. P. (1998). Cortical processing of complex sounds Josef P Rauschecker. *Current*, 8(4):516–521. (cited on pages 6 and 62)

Rauschecker, J. P. and Scott, S. K. (2009). Maps and streams in the auditory cortex: non human primates illuminate human speech processing. *Nature Neuroscience*, 12(6):718–24. (cited on page 62)

Rauschecker, J. P. and Tian, B. (2000). Mechanisms and streams for processing of "what" and "where" in auditory cortex. *Proc Natl Acad Sci USA*, 97(22):11800–11806. (cited on page 62)

Ray, S., Jouny, C. C., Crone, N. E., Boatman, D., Thakor, N. V., and Franaszczuk, P. J. (2003). Human ECoG analysis during speech perception using matching pursuit: a comparison between stochastic and dyadic dictionaries. *IEEE Trans Biomed Eng*, 50(12):1371–3. (cited on page 67)

Ray, S. and Maunsell, J. H. R. (2011). Different Origins of Gamma Rhythm and High-Gamma Activity in Macaque Visual Cortex. *PLoS Biology*, 9(4):15. (cited on page 96)

Reiterer, S., Erb, M., Grodd, W., and Wildgruber, D. (2008). Cerebral processing of timbre and loudness: fMRI evidence for a contribution of Broca's area to basic auditory discrimination. *Brain Imaging and Behavior*, 2(1):1–10. (cited on page 66)

Ryugo, D. K. and Weinberger, N. M. (1976). Corticofugal modulation of the medial geniculate body. *Experimental Neurology*, 51(2):377–391. (cited on page 62)

Saalmann, Y. B., Pinsk, M. A., Wang, L., Li, X., and Kastner, S. (2012). The pulvinar regulates information transmission between cortical areas based on attention demands. *Science*, 337(6095):753–756. (cited on pages 29, 33, 94, and 96)

Schaefer, R. S., Desain, P., and Suppes, P. (2009). Structural decomposition of EEG signatures of melodic processing. *Biological Psychology*, 82:253–9. (cited on page 83)

Schaefer, R. S., Farquhar, J., Blokland, Y., Sadakata, M., and Desain, P. (2010). Name that tune: Decoding music from the listening brain. *Neuroimage*, 56(2):843–849. (cited on page 67)

Schalk, G., Kubánek, J., Miller, K. J., Anderson, N. R., Leuthardt, E. C., Ojemann, J. G., Limbrick, D., Moran, D., Gerhardt, L. A., and Wolpaw, J. R. (2007). Decoding two-dimensional movement trajectories using electrocorticographic signals in humans. *J. Neural Eng.*, 4:264–75. (cited on pages 3, 14, 30, 71, 73, 84, and 96)

Schalk, G., McFarland, D. J., Hinterberger, T., Birbaumer, N., and Wolpaw, J. R. (2004). BCI2000: a general-purpose brain-computer interface (BCI) system. *IEEE Trans Biomed Eng*, 51(6):1034–1043. (cited on pages 39, 69, and 85)

Schalk, G. and Mellinger, J. (2010). *A Practical Guide to Brain-Computer Interfacing with BCI2000*. Springer, London, UK, 1st edition. (cited on pages 39, 69, and 85)

Schwarz, G. (1978). Estimating the dimension of a model. *The annals of statistics*, 6(2):461–464. (cited on pages 89 and 90)

Shenoy, P., Miller, K. J., Ojemann, J. G., and Rao, R. P. N. (2008). Generalized features for electrocorticographic BCIs. *IEEE Transactions on Biomedical Engineering*, 55(1):273–280. (cited on page 14)

Sherman, S. M. and Guillery, R. W. (2002). The role of the thalamus in the flow of information to the cortex. *Philosophical Transactions of the Royal Society of London - Series B: Biological Sciences*, 357(1428):1695–1708. (cited on page 62)

Shibasaki, H. (2008). Human brain mapping: hemodynamic response and electrophysiology. *Clin Neurophysiol*, 119(4):731–743. (cited on page 67)

Shum, J., Hermes, D., Foster, B. L., Dastjerdi, M., Rangarajan, V., Winawer, J., Miller, K. J., and Parvizi, J. (2013). A brain area for visual numerals. *The Journal of neuroscience*, 33(16):6709–15. (cited on page 14)

Sinai, A., Bowers, C. W., Crainiceanu, C. M., Boatman, D., Gordon, B., Lesser, R. P., Lenz, F. A., and Crone, N. E. (2005). Electrocorticographic high gamma activity versus electrical cortical stimulation mapping of naming. *Brain*, 128(Pt 7):1556–1570. (cited on page 30)

Sinai, A., Crone, N. E., Wied, H. M., Franaszczuk, P. J., Miglioretti, D., and Boatman-Reich, D. (2009). Intracranial mapping of auditory perception: event-related responses and electrocortical stimulation. *Clin Neurophysiol*, 120(1):140–9. (cited on pages 67, 71, and 84)

Sitaram, R., Zhang, H., Guan, C., Thulasidas, M., Hoshi, Y., Ishikawa, A., Shimizu, K., and Birbaumer, N. (2007). Temporal classification of multichannel near-infrared spectroscopy signals of motor imagery for developing a brain–computer interface. *NeuroImage*, 34(4):1416 – 1427. (cited on page 19)

Spencer, S. and Huh, L. (2008). Outcomes of epilepsy surgery in adults and children. *The Lancet*, 7(6):525–537. (cited on page 35)

Srinivasan, R. (1999). Methods to improve the spatial resolution of EEG. *International Journal of Bioelectromagnetism*, 1(1):102–111. (cited on page 14)

Staba, R. J., Wilson, C. L., Bragin, A., Fried, I., and Engel, J. (2002). Quantitative analysis of high-frequency oscillations (80-500 Hz) recorded in human epileptic hippocampus and entorhinal cortex. *Journal of Neurophysiology*, 88(4):1743–1752. (cited on page 25)

Stangor, C. (2010). *Introduction to Psychology*. Flatworld. (cited on page 57)

Steriade, M., Gloor, P., Llinás, R., da Silva, F. L., and Mesulam, M. (1990). Basic mechanisms of cerebral rhythmic activities. *Electroencephalography and Neurophysiology*, 76:481–508. (cited on pages 29, 84, and 93)

Steriade, M. and Llinás, R. R. (1988). The functional states of the thalamus and the associated neuronal interplay. *Physiol Rev*, 68(3):649–742. (cited on pages 27 and 28)

Tanji, K., Leopold, D. A., Ye, F. Q., Zhu, C., Malloy, M., Saunders, R. C., and Mishkin, M. (2010). Effect of sound intensity on tonotopic fMRI maps in the unanesthetized monkey. *Neuroimage*, 49(1):150–7. (cited on pages 67 and 83)

Ter-Pogossian, M. M., Phelps, M. E., Hoffman, E. J., and Mullani, N. A. (1975). A positron-emission transaxial tomograph for nuclear imaging (PETT). *Radiology*, 114(1):89–98. (cited on page 2)

Thaerig, S., Behne, N., Schadow, J., Lenz, D., Scheich, H., Brechmann, A., and Herrmann, C. S. (2008). Sound level dependence of auditory evoked potentials: simultaneous EEG recording and low-noise fMRI. *Int J Psychophysiol*, 67(3):235–241. (cited on pages 66 and 83)

Tudor, M., Tudor, L., and Tudor, K. I. (2005). The history of electroencephalography. *Acta medica Croatica : cÌ†asopis Hravatske akademije medicinskih znanosti*, 59(4):307–13. (cited on page 2)

Vinoo, A., Petri, T., Iiro, J., Enrico, G., Mikko, S., and Elvira, B. (2012). Large-scale brain networks emerge from dynamic processing of musical, timbre, key and rhythm. *Neuroimage*, 59:3677–89. (cited on pages 3, 83, and 94)

Wada, J. and Rassmussen, T. (1960). Intracarotid injection of sodium amytal for the lateralization of cerebral speech dominance. *Neurosurgery*, 17:266–82. (cited on page 68)

Warren, J. D., Jennings, A. R., and Griffiths, T. D. (2005). Analysis of the spectral envelope of sounds by the human brain. *Neuroimage*, 24(4):1052–7. (cited on page 62)

Welch, P. (1967). The use of fast Fourier transform for the estimation of power spectra: A method based on time averaging over short, modified periodograms. *IEEE Transactions on Audio and Electroacoustics*, 15(2):70–73. (cited on page 43)

Wernicke, C. and Eggert, G. (1874). Der aphasische symptomenkomplex eine psychologische studie auf anotomomischer basis. In Eggert, G., editor, *Wernicke's work on aphasia*, pages 219–283. Mouton. (cited on page 1)

Wilson, J. A., Felton, E. A., Garell, P. C., Schalk, G., and Williams, J. C. (2006). ECoG factors underlying multimodal control of a brain-computer interface. *IEEE Trans Neural Syst Rehabil Eng*, 14(2):246–250. (cited on page 78)

Winer, J. A. (1984). The human medial geniculate body. *Hearing Research*, 15(3):225–247. (cited on page 63)

Yetkin, F. Z., Roland, P. S., Christensen, W. F., and Purdy, P. D. (2004). Silent functional magnetic resonance imaging (fMRI) of tonotopicity and stimulus intensity coding in

human primary auditory cortex. *Laryngoscope*, 114(3):512–8. (cited on pages 67, 75, and 83)

Yu-Luen, C., Fuk-Tan, T., H, C. W., May-Keun, W., Ying-Ying, S., and Te-Son, K. (1999). The new design of an infrared-controlled human-computer interface for the disabled. (cited on page 18)

Zatorre, R. J. (1988). Pitch perception of complex tones and human temporal-lobe function. *Journal of the Acoustical Society of America*, 84(2):566–572. (cited on pages 58 and 60)

Zatorre, R. J. and Belin, P. (2001). Spectral and temporal processing in human auditory cortex. *Cereb Cortex*, 11(10):946–53. (cited on pages 66, 78, 94, and 97)

Zatorre, R. J., Belin, P., and Penhune, V. B. (2002). Structure and function of auditory cortex: music and speech. *Trends Cogn Sci*, 6(1):37–46. (cited on pages 59, 94, and 97)

Zatorre, R. J., Bouffard, M., and Belin, P. (2004). Sensitivity to auditory object features in human temporal neocortex. *J Neurosci*, 24(14):3637–42. (cited on pages 62, 66, and 94)

Zatorre, R. J., Chen, J. L., and Penhune, V. B. (2007). When the brain plays music: auditory–motor interactions in music perception and production. *Nat Rev Neurosci*, 8:547–558. (cited on pages 6, 62, 75, 76, 77, 94, and 97)

Zhang, Z., Chan, Y.-S., and He, J. (2004). Thalamocortical and corticothalamic interaction in the auditory system. *Neuroembryology and Aging*, 5(239–48). (cited on pages 84 and 97)

Curriculum Vitae

Cristhian M. Potes earned his Bachelor degree in Bioengineering at the Universidad Santiago de Cali in 2001. He then joined the master's program at the University of Texas at El Paso (UTEP) and received his Master of Science degree in Electrical Engineering in 2008. At the same institution, he continued with his doctoral studies and received his Doctor of Philosophy degree in Electrical and Computer Engineering in 2013.

Dr. Potes has been the recipient of numerous honors and awards including the best-student award given by the Colombian Society of Engineers. During his doctoral studies, he was the recipient of the Texas Instruments Endowed Scholarship, the Good Neighborhood Scholarship, the Miner Heroe award, and the Texas Public Education Grant (TPEG) for International Students. From 2006 to 2013, he received funding from the Air Force Research Lab, National Institutes of Health, and the US Army Research Office.

While pursuing his masters and doctoral degrees, Dr. Potes worked as a teaching assistant and lab instructor of different undergraduate courses at UTEP, and as a research associate for the Wadsworth Center, New York State Department of Health. He also worked as a consultant for a medical engineering company (g.tec) in Austria, and interned at a medical device company (Cyberonics, Houston, TX) in 2013.

Dr. Potes has presented his research at national and international conference meetings and workshops including the Society for Neuroscience, Electrocorticography Work-

shop, International Brain Computer Interface, SACNAS National Conference, and the Southern Biomedical Engineering Conference. Dr. Potes' research has been also published in high impact scientific journals such as Neuroimage.

Dr. Potes' dissertation, *Development and Validation of a Novel Framework to Map Brain Function*, was supervised by Dr. Patricia Nava at UTEP and Dr. Gerwin Schalk at Wadsworth Center. His main research interests include statistical digital signal processing, brain computer interface, and brain functional connectivity.

He is currently a full time research staff member at Wadsworth Center and is planning to open a branch office for g.tec in the USA. He can be reached through the email cmpotes@gmail.com